

Modelling of Glucose and Insulin Kinetics to
Facilitate the Development of a Wearable
Artificial Pancreas

by

Malgorzata Elzbieta Wilinska

Thesis submitted in partial fulfilment of the requirements for the
degree of

Doctor of Philosophy

in

Measurement and Information in Medicine

City University

Year 2004

Abstract

A wearable artificial pancreas (AP) has been a research goal for over three decades. The aim of this device is to establish effective closed-loop control of blood glucose in patients with type 1 diabetes mellitus (T1DM) using subcutaneous (SC) glucose measurements and SC insulin delivery. The main difficulties that hamper the successful development of a wearable AP concern the stability and accuracy of SC glucose sensing, the predictability of the absorption kinetics of the injected insulin, and finally the performance of the glucose control algorithm. As clinical tests on humans are costly, time consuming, and demand ethical approval, *in silico* testing of the AP has become a critical feature to facilitate an accelerated development of the AP and, specifically, the control algorithm.

The primary aim of the work reported in this thesis was to explore the use of compartmental modelling techniques with in-built physiological constraints to facilitate the development of a wearable AP.

In particular, the study aimed to extend and evaluate an existing model of whole-body glucose kinetics on a set of data obtained in a clinical trial designed to test the AP algorithm. The model was extended to represent the input-output relationship between the SC insulin and intravenous glucose concentrations. The extended model was re-evaluated in subjects with T1DM under new conditions with the objective to obtain sets of parameters to represent 'virtual' subjects with T1DM in the AP simulator. The parameter estimation was completed, but the 'virtual' subjects for use in the AP simulator could not be generated due to the uncertain validity of the tested model.

Further objectives included the support for *in silico* testing of an AP through investigating insulin lispro and interstitial glucose kinetics.

To explore the kinetics of SC administered insulin lispro, ten competing models were proposed assuming a number of physiological effects. The principle of parsimony was used to select the model, which best represented our data. The best model included slow and fast absorption channels, and the presence of local insulin degradation at the injection site.

In order to establish the relationship between the interstitial glucose (IG) and plasma glucose (PG), nine models of IG kinetics were postulated. The model which best represented the experimental data was selected using the principle of parsimony. Two mechanisms explaining the temporal variation in the IG-PG ratio were identified, a zero-order removal of glucose from the interstitial fluid (ISF) and the stimulatory effect of insulin on glucose transfer from the plasma to the ISF. This best model found its use in the simulator to represent SC glucose measurements.

In conclusion, valuable insights were obtained into the mechanisms involved in the insulin and interstitial glucose kinetics, as well as the whole-body glucose kinetics.

Acknowledgement

I would like to thank my supervisor Dr. Roman Hovorka for his expert advice, ongoing support, and encouragement. I am also very grateful to him for introducing me to the fascinating field of mathematical modelling in physiology.

Many thanks to my colleagues from Graz, Austria, for stimulating discussions, comments, and for supplying the data. A special thank you to Helga Schaller for her prompt replies to my numerous emails.

I am also thankful to my second supervisor Dr. Peter Weller for his input and support and to my colleague Ludovic Chassin for his comments, ideas and for his good sense of humour.

Lastly, I would like to thank my husband Hesham for his understanding and support and my daughter Magda for providing me with the daily boost of energy and determination to move on.

Glossary

ADA	American Diabetes Association
ADICOL	ADvanced Insulin infusion using a COntrol Loop
AIC	Akaike information criterion
AP	Artificial pancreas
CGMS	Continuous glucose monitoring system
CHO	Carbohydrate
CIGMA	Constant infusion of glucose with model assessment
CSII	Continuous subcutaneous insulin infusion
CV	Coefficient of variation
DCCT	Diabetes Control and Complications Trial
HbA _{1c}	Glycated haemoglobin concentration
HOMA	Homeostasis model assessment
IG	Interstitial glucose
IIR	Insulin infusion rate
ISF	Interstitial fluid
ITS	Iterative two-stage
IV	Intravenous
IVGTT	Intravenous glucose tolerance test
MAP	Maximum <i>a posteriori</i> probability
MM	Michaelis Menten
OFM	Open-flow microperfusion
PG	Plasma glucose
PI	Plasma insulin
SC	Subcutaneous
STS	Standard two-stage
T1DM	Type 1 diabetes mellitus
WHO	World Health Organisation
WRSS	Weighted residual sum of squares

Table of Contents

Abstract	i
Acknowledgement	iii
Glossary	iv
Table of Contents	v
Table of Figures	ix
Table of Tables	xii
Table of Tables	xii
Chapter 1 Introduction and Plan of Thesis	1
1.1 Background and Motivation	1
1.2 Plan of Thesis	4
Chapter 2 Aims and Objectives	5
2.1 Aims	5
2.2 Objectives	5
Chapter 3 Review of Literature and Associated Techniques	7
3.1 Glucose Regulatory System	7
3.1.1 Glucose distribution and metabolism	7
3.1.2 Glucose concentration throughout the body	7
3.1.3 Glucose transporters: categories and distribution	9
3.1.4 Insulin and other hormones playing a part in the regulation of glucose ...	9
3.2 Diabetes Mellitus	12
3.2.1 Definition and classification of diabetes mellitus.....	12
3.2.2 Epidemiology and aetiology of diabetes	13
3.2.3 Diagnosis and treatment	14
3.2.4 Glucose monitoring	16
3.2.5 Artificial pancreas.....	17
3.3 Compartmental Modelling Techniques	19
3.3.1 The concept and purpose of modelling	19
3.3.2 The theory of compartmental models	19
3.3.3 Model identification	22
3.3.4 Model validation	24
3.3.5 Model selection process.....	24

3.3.6	Population modelling techniques.....	25
3.4	Review of Existing Techniques to Model Whole-body Glucose Kinetics	28
3.4.1	Knowledge driven models of whole-body glucose kinetics	28
3.4.2	Experimentally driven models of glucose-insulin interactions.....	32
3.5	Review of Existing Techniques to Model Interstitial Glucose Kinetics	37
3.5.1	Indirect measurement of interstitial glucose using a sensor	39
3.5.2	Direct measurement of interstitial glucose by interstitial fluid sampling or ultrafiltration.....	40
3.5.3	Comparison of direct and indirect methods of interstitial glucose measurement.....	41
3.6	Existing Techniques to Model Subcutaneous Insulin Kinetics.	43
3.6.1	Compartmental models.....	43
3.6.2	Noncompartmental models	47
Chapter 4	Modelling Glucose Kinetics over Twenty Eight Hours in Subjects with Type 1 Diabetes.....	51
4.1	Introduction	51
4.2	Subjects and Methods	51
4.2.1	Subjects and experimental protocol	51
4.2.2	Model of glucoregulation.....	53
4.2.3	Gut absorption model.....	55
4.2.4	Insulin absorption model	56
4.2.5	Model constants and parameters	57
4.2.6	Parameter estimation.....	59
4.2.7	Model identification and validation	60
4.2.8	Statistical analysis.....	60
4.3	Results	61
4.3.1	Plasma glucose and insulin.....	61
4.3.2	Model identification and validation	61
4.3.3	Model parameters	65
4.4	Discussion	71
Chapter 5	Modelling Insulin Lispro Kinetics during Continuous Subcutaneous Insulin Infusion in Subjects with Type 1 Diabetes	74
5.1	Introduction	74

5.2	Subjects and Methods	75
5.2.1	Subjects and experimental protocol	75
5.2.2	Modelling insulin lispro kinetics	76
5.2.3	Parameter estimation	82
5.2.4	Model identification and validation	83
5.2.5	Model selection	83
5.3	Results	83
5.3.1	Experimental data	83
5.3.2	Model identification and validation	83
5.3.3	Model selection	84
5.4	Discussion	89
5.5	Conclusion	93
Chapter 6 Modelling Interstitial Glucose Kinetics under		
Physiological Conditions in Type 1 Diabetes		94
6.1	Introduction	94
6.2	Subjects and Methods	96
6.2.1	Subjects and experimental protocol	96
6.2.2	Open-flow microperfusion	97
6.2.3	Assays and determination of interstitial glucose	98
6.2.4	Data analysis	98
6.3	Results	103
6.3.1	Plasma glucose, interstitial glucose and interstitial-to-plasma glucose ratio	103
6.3.2	Model identification and validation	103
6.3.3	Model selection	105
6.4	Discussion	109
6.5	Conclusion	113
Chapter 7 Further Evaluation of the Model of Interstitial Glucose		
Kinetics		114
7.1	Introduction	114
7.2	Methods	114
7.2.1	Subjects and experimental protocol	114
7.2.2	Data analysis	115
7.3	Results	117

7.3.1 Plasma glucose, interstitial glucose, plasma insulin and interstitial to plasma glucose ratio	117
7.3.2 Parameter estimates and model validation	117
7.3.3 Comparison with estimates obtained in Chapter 6	122
7.4 Discussion	123
Chapter 8 Discussion and Conclusion.....	125
8.1 Overall Discussion	125
8.2 Achievement of Objectives	129
8.3 Future Work	130
8.3.1 Generating 'virtual' subjects with type 1 diabetes	130
8.3.2 Insulin lispro kinetics	131
8.3.3 Interstitial glucose kinetics	131
References	132
Personal Bibliography.....	146
Journal Papers	146
Abstracts	146
Appendix	150

Table of Figures

Figure 3.1 Structure of human insulin.	10
Figure 3.2 Model of artificial pancreas used in ADICOL project. MMI stands for Man-Machine Interface.	17
Figure 3.3 Diagram showing the compartment containing quantity of material Q_i with its input and output fluxes.	20
Figure 3.4 Schematic representation of the whole-body glucose kinetics/metabolism.	29
Figure 3.5 The glucose-insulin system. Dotted line arrows indicate insulin control.	32
Figure 3.6 Conceptual model of interstitial glucose kinetics; C_1 and C_1 represent glucose concentration in the plasma and interstitial fluid, respectively; V_1 and V_1 are the plasma and ISF glucose distribution volume, respectively; f_{02} represents glucose flux from ISF into the fat cell, f_{12} and f_{21} represent glucose fluxes from ISF into plasma and from plasma to ISF, respectively.	38
Figure 3.7 Model of insulin absorption kinetics proposed by Kobayashi <i>et al</i> (76); x_1 is the amount of insulin in the SC depot, i is plasma insulin, V_d is the distribution volume, k_a is the absorption rate constant, k_e is the elimination rate constant, τ is the time delay and $u(t)$ is the rate of insulin administration.	45
Figure 3.8 Model of subcutaneous insulin absorption proposed by Kraegen (77); x_1 and x_2 are insulin masses in each of the two SC compartments (accessible and nonaccessible), i is plasma insulin concentration, V_d is the distribution volume of insulin, k_{21} and k_a are the transport rate constants describing transport of insulin between SC compartments and SC compartment and plasma respectively, k_e is the elimination rate constant, and k_d is the degradation rate constant from the respective SC pool.	45
Figure 3.9 Model of subcutaneous insulin absorption proposed by Puckett (78); x_1 and x_2 are insulin masses in SC tissue and interstitial fluid respectively, i is plasma insulin concentration, V_d is the distribution volume of insulin, k_a are the absorption rate constant from SC compartments to	

interstitial fluid and interstitial fluid to plasma respectively, k_e is the elimination rate constant.....	46
Figure 3.10 Mathematical model for SC insulin absorption proposed by Shimoda and colleagues (79); k_d is the degradation rate constant in SC tissue, other symbols as in Figure 3.8.	47
Figure 3.11 Overview of the model by Mosekilde of subcutaneous absorption of soluble insulin.	49
Figure 4.1 Structure of model of glucoregulation from (52).....	53
Figure 4.2 Structure of the gut absorption model for dinner one.....	56
Figure 4.3 Structure of the insulin absorption model.....	57
Figure 4.4 Plasma glucose; values are mean \pm SE, n=12.	62
Figure 4.5 Weighted residuals; values are mean \pm SE, n=12.	62
Figure 4.6 Model fits for individual subjects. Pink dot represents measurement and green line represents model fit.....	67
Figure 4.7 Oscillatory patterns of insulin sensitivities for individual subjects.	69
Figure 5.1 Plasma insulin concentration. Values are mean \pm SE (n=7).	84
Figure 5.2 Mean weighted residuals for Models 1, 2, 3, and 5 (top panel), and for Models 7, 8, 9, and 10 (bottom panel) (n=7).	86
Figure 5.3 Example model fit generated by Model 9.....	89
Figure 6.1 Plasma glucose and interstitial glucose (top panel), interstitial to plasma glucose ratio (middle panel), and plasma insulin concentration (bottom panel)	104
Figure 6.2 Weighted residuals for posteriorly identifiable models. Values are mean (n=9).	107
Figure 6.3 Example model fit generated by Model 9.....	108
Figure 6.4. The Clarke error grid showing relationship between measured plasma glucose and glucose predicted from IG using Model 1 (top panel; 56% in zone A), and Model 7(bottom panel; 60% in zone A).	113
Figure 7.1 Structure of Model 9.	116
Figure 7.2 Plasma glucose, interstitial glucose (top panel), interstitial to plasma glucose ratio (middle panel), and plasma insulin (bottom panel). Values are mean \pm SE, n=11.....	119

Figure 7.3 Individual model fits generated by Model 9. Pink dot represents measurement and continuous line represents the model fit. 120

Figure 7.4 Weighted residuals assuming a nominal value for the ME at 10%. Values are mean \pm SE, n = 11..... 122

Table of Tables

Table 3.1 Summary of findings relating interstitial glucose dynamics to plasma glucose dynamics published by various authors.	42
Table 3.2 Parameter values for models described in this section.	44
Table 4.1 Model constants	58
Table 4.2 Model parameters	59
Table 4.3 Parameters describing time variation of insulin sensitivities	59
Table 4.4 Parameter estimates for individual subjects.	63
Table 4.5 Parameter estimates describing time variation of insulin sensitivities.	65
Table 4.6 Model parameters; values are mean (inter-quartile range), n=12..	66
Table 4.7 Parameters describing the time variation of insulin sensitivities; values are mean (inter-quartile range) or mean \pm SD, n=12.....	66
Table 5.1 Compartment models of insulin lispro kinetics.	78
Table 5.2 Model identification, validation, and selection. Summary results...	85
Table 5.3a Parameter estimates of k_{a1} , k_{a2} , k_e , k , V and MCR for identifiable models. Values are population means (inter-quartile range of individual values) (n=7).	87
Table 5.3b Parameter estimates of $V_{MAX,a}$, $K_{M,a}$, $V_{MAX,LD}$, $K_{M,LD}$, B and a_1 for Models 2, 3, 8, and 9. Values are population means (inter-quartile range of individual values) (n = 7).....	88
Table 5.3c Parameter estimates of a , b , b_i , s , s_i , for Model 10. Values are population means (inter-quartile range of individual values) (n = 7).....	88
Table 6.1 Nine proposed compartment models of interstitial glucose kinetics (see text for details).	101
Table 6.2 Population analysis results for a posteriori identifiable models. Values are means (inter-quartile range) (n=9).....	106
Table 6.3 Summary of validation and model selection results.	107
Table 6.4 Parameter estimates for Model 9.	108
Table 7.1 Parameter estimates and their accuracy.	118
Table 7.2 Population parameter estimates for the two data sets.	122

Chapter 1 Introduction and Plan of Thesis

1.1 Background and Motivation

Diabetes mellitus is a group of metabolic disorders characterised by hyperglycaemia due to defects in insulin secretion, insulin action, or both. The condition is associated with potentially severe long-term complications responsible for high morbidity and mortality rates and, hence, high costs to the National Health Service.

Type 1 diabetes (T1DM) accounts for approximately 20% of all diabetes cases in Europe and North America (1). The condition is caused by autoimmune destruction of pancreatic beta cells, resulting in absolute insulin deficiency. A person with this condition has to rely on exogenous insulin delivery for survival.

The aim of all subjects with T1DM is to achieve a good, near normal, glycaemic control while avoiding hypoglycaemia. The main benefits of good metabolic control, delaying the onset and slowing the progression of long term macrovascular and microvascular complications, has been demonstrated by the Diabetes Control and Complications Trial (DCCT) (2). Intensive insulin therapy with frequent blood glucose monitoring is a clear recommendation coming from this study.

In direct response to the above recommendations, much research has focused on improved methods of glucose monitoring and more physiologic ways of insulin delivery. Continuous subcutaneous (SC) glucose sensing and continuous subcutaneous insulin infusion (CSII) with rapid acting insulin analogues, such as lispro, have since become major advancements in the treatment of diabetes. Combining the two devices in a closed loop with a control algorithm, i.e. creating an artificial pancreas (AP) is now the way forward for researchers around the world.

The artificial pancreas has been a research goal since 1970s. Its aim is to establish effective closed-loop control of blood glucose in patients and to alleviate the burden of frequent treatment decisions. Such a closed-loop control system requires a sensor to provide a blood glucose reading to a controller, an algorithm to calculate an appropriate insulin dosage based on this reading, and a programmable insulin pump to deliver this dose to the patient. The main difficulties that hamper the successful development of AP concern the stability and accuracy of a long term glucose sensing and the predictive powers of control algorithm.

Clinical trials designed to test the AP algorithm were conducted as part of the Advanced Insulin infusion using a Control Loop (ADICOL) project. Several subjects with type 1 diabetes participated in those trials giving rise to a large set of unique data. As a reliable and accurate subcutaneous glucose sensor was not available, the experimental protocol involved subcutaneous insulin infusion and intravenous glucose measurements. The aim of the first study of this thesis was to fully describe the input-output relationship in this experimental set-up, i.e. the relationship between SC administered insulin and intravenous (IV) glucose concentration. For that purpose an existing model of glucoregulatory system was extended and tested. If the model was proven valid, its parameter estimates could be fed into the existing AP simulator to represent 'virtual' patients with type 1 diabetes.

Simulation has obvious advantages in the development of the AP: it reduces costs, limits human resources, and speeds up testing. The present version of AP simulator uses synthetic subjects represented by parameters, some of which were obtained from an overnight tracer study involving normal healthy humans, others were drawn from probability distribution. Bringing the simulation environment closer to reality would constitute a major step in the development of an AP.

A prerequisite of an effective wearable AP control algorithm is detailed understanding of the pharmacokinetic properties of subcutaneously administered insulin. The absorption kinetics of regular insulin is a complex

process with inherent delays and a marked inter-subject variability. The advent of genetically engineered rapid acting insulin analogues, such as insulin lispro, opened new opportunities for the development of a wearable artificial pancreas. This type of insulin is able to mimic closely physiological pattern of insulin secretion and is therefore ideal for use in an AP when administered via CSII. Although the time action profiles of insulin lispro are more predictable than those of the regular insulin, certain issues around the absorption kinetics remain unresolved. Pharmacokinetic properties of insulin lispro have been studied after bolus administration but little is known about those properties during continuous insulin infusion. Hence, the aim of the second study was to investigate the absorption kinetics of insulin lispro during standard insulin pump treatment with bolus and CSII modes of insulin delivery.

An accurate and reliable glucose measurement is yet another prerequisite of an effective AP. As subcutaneous sensing is minimally invasive and avoids the risks associated with a long-term venous access, this type of glucose sensing has become a research goal in recent years. However, the SC glucose sensors measure glucose concentration in the interstitial fluid (ISF) not in the blood. As blood glucose is a commonly used reference for all clinical decision making, the knowledge of exact relationship between interstitial glucose (IG) and plasma glucose (PG) is required. In the currently available continuous glucose monitoring systems (CGMS) this relationship is assumed to be a simple proportion. The aim of this final study was to investigate the IG-PG relationship using compartmental modelling approach with the main objective to be able to estimate plasma glucose concentration from interstitial glucose measured by the SC glucose sensor.

The overall aim of this study was to facilitate the development of AP through validated models and techniques. In particular, this study supports the *in silico* development of an artificial pancreas through investigating interstitial glucose and insulin lispro kinetics, and by generating sets of parameters to represent 'virtual' subjects with T1DM for use in the AP simulator.

1.2 Plan of Thesis

Chapter 1 provides introduction to the thesis.

Chapter 2 sets out the aims and objectives of this study.

Chapter 3 provides literature review including aetiology, physiology and treatment of diabetes, compartmental modelling methods and the iterative two stage technique. The following sections present review of currently available models of the whole body glucose kinetics followed by models of insulin and interstitial glucose kinetics.

Chapter 4 provides the details of a model used to represent the relationship between the subcutaneous insulin infusion and the intravenous glucose concentration. The chapter describes the evaluation and the validation of the model on experimental data and presents the results.

Chapter 5 presents a new model of insulin lispro kinetics. Ten competing models are identified, validated, and compared. The model best representing the experimental data is selected and its parameters summarised.

Chapter 6 proposes a model of interstitial glucose kinetics and examines the interstitial to plasma glucose relationship. This time nine compartmental models are postulated, their parameters estimated, and the validation and selection processes described. The results of the best model are presented and the clinical implications discussed.

Chapter 7 is dedicated to re-evaluation of the model of interstitial glucose kinetics, presented in Chapter 6, on an independent data set. The results are summarised and compared with those obtained in the previous chapter.

Chapter 8 presents the final conclusions, meeting of the objectives, and the recommendations for future work.

Chapter 2 Aims and Objectives

2.1 Aims

The general aim of this research is to explore the use of compartmental modelling with physiological considerations to assist in the development of a wearable artificial pancreas.

In particular, this study aims to support *in silico* development of an artificial pancreas by developing and validating models to represent 'virtual' subjects with type 1 diabetes.

2.2 Objectives

The specific objectives are divided into three main categories.

- A. Objectives in relation to modelling of the input-output relationship between subcutaneously administered insulin and intravenously measured plasma glucose:
 - To extend and validate an existing model of glucoregulatory system on a set of clinical data recorded over 28 hours in trials involving subjects with type 1 diabetes treated by CSII;
 - To estimate model parameters for individual subjects with the aim of providing the AP simulator with a set of 'virtual' subjects with type 1 diabetes.
- B. Objectives in relation to modelling of subcutaneously administered insulin lispro kinetics:
 - To develop and validate a model of absorption kinetics of subcutaneously administered insulin lispro in type 1 diabetes during standard insulin pump treatment with bolus and CSII modes of delivery.

C. Objectives in relation to modelling of interstitial glucose kinetics:

- To investigate relationship between plasma glucose and interstitial glucose;
- To develop and validate a model of interstitial glucose kinetics under physiological conditions in subjects with type 1 diabetes.

Chapter 3 Review of Literature and Associated Techniques

3.1 Glucose Regulatory System

Glucose is the primary source of energy necessary to sustain our body functions. It is the major fuel for the central nervous system. The brain, for instance, consumes about 80% of the glucose utilised under fasting conditions (1), and critically depends on the maintenance of normal glucose levels. In healthy human subjects, blood glucose levels are maintained within relatively narrow limits between 4mmol/L and 7mmol/L (3). Such a tight control of plasma glucose concentrations is achieved by a balance between actions of various hormones, enzymes, and substrates.

3.1.1 Glucose distribution and metabolism

Plasma glucose concentrations are determined by the net balance between glucose released into the circulation and glucose uptake from the plasma. The two main sources of glucose are the food intake and glucose produced in the liver (hepatic glucose production). In the fed conditions, glucose is absorbed from the gastrointestinal tract into the plasma but, during post absorptive conditions, plasma glucose is primarily derived from the liver (3). Glucose uptake from the plasma can be divided into those tissues where glucose utilisation is regulated by insulin, such as the muscle, the adipose tissue and the liver, and those in which insulin has no apparent role in stimulating glucose uptake, such as the brain and the kidney.

3.1.2 Glucose concentration throughout the body

Glucose absorbed from the gastrointestinal tract as well as glucose produced in the liver appears first in the blood stream. Blood delivers glucose to different parts of the body, for it to be utilised. Before glucose enters the cells it needs to cross the capillary wall barrier and enter the extracellular space filled with interstitial fluid (ISF). Hence, the three major compartments of glucose distribution in the body are blood, interstitial or extracellular space and intracellular space.

- ◇ Blood. Blood glucose is distributed between red blood cells and plasma. In adult humans, glucose concentration in plasma water is nearly the same as in red blood cell water over a wide range of blood glucose concentration, until plasma glucose becomes extremely high when erythrocyte glucose transporters are saturated (4). Erythrocyte glucose serves as a buffer to damp the amplitude of variations in plasma glucose concentrations.

- ◇ Interstitial space. Although details of glucose movements across capillaries are unknown, it is assumed that the process is a simple diffusion driven by the concentration gradient (4). Glucose is not distributed instantly across the capillaries into the ISF, as the initial response to the concentration gradient is water movement from the ISF to the plasma. Water crosses the capillaries faster than glucose (bigger particles). The process of passive movement of molecules down its concentration gradient can be described by Fick's Law (5):
$$\text{Flux} = (C_1 - C_2) \times (\text{Area} \times \text{Permeability coefficient}) / \text{Thickness}$$
where C_1 is the higher concentration and C_2 is the lower concentration, Area is the area across which diffusion occurs, and thickness is the length of the diffusion path.
The glucose concentration in the ISF must be less than that in plasma for glucose to diffuse out of the plasma.

- ◇ Intracellular space. The current evidence suggests that there is very little or no free intracellular glucose in the skeletal muscle at normal plasma glucose concentrations (4). This implies that glucose is phosphorylated in the muscle as rapidly as it is translocated into the cell.

At any moment, the change in concentration of glucose in any small volume element of the plasma depends on (i) the rate at which glucose is introduced into the circulating blood, (ii) the rate at which it is apportioned between the red blood cells and the plasma, and (iii) the rate at which it is removed from

the circulation. The limiting event on the rate of glucose removal from the circulation is its rate of entry into the cells. This rate of entry into the cells may be limited by transmembrane transport.

3.1.3 Glucose transporters: categories and distribution

Glucose is carried into the cells across the cell membrane by specialised transporter proteins called GLUTs. There are four main categories of GLUT transporters:

- ◇ GLUT-1 is involved in basal and non-insulin mediated glucose uptake in many cells including pancreatic beta cells;
- ◇ GLUT-2 is important in intestinal absorption and renal reabsorption and for releasing glucose from and translocating it into hepatocytes;
- ◇ GLUT-3 is involved in non-insulin-mediated uptake of glucose in the brain;
- ◇ GLUT-4 is responsible for insulin-stimulated glucose uptake in the muscle and the adipose tissue.

GLUT isoforms vary in their transport efficiency. The lowest Michaelis-Menten constant K_M is 1-5mmol/L for GLUT-3 (the brain GLUT), the highest 20-40mmol/L for GLUT-2. K_M for GLUT-1 and GLUT-4 falls within middle-to-upper range of blood glucose concentrations (4). Kozka and colleagues reported K_M of 4.7 ± 1.1 mmol/L and V_{MAX} of 3.3 ± 0.8 mmol/L min⁻¹ for GLUT-4 in the adipose tissue (6).

3.1.4 Insulin and other hormones playing a part in the regulation of glucose

3.1.4.1 Insulin molecule

The insulin molecule consists of two polypeptide chains linked by disulphide bridges, the **A** chain containing 21 amino acids and the **B** chain 30 amino

acids (see Figure 3.1). Human insulin differs from pig insulin at only one amino acid position (**B30**), and from beef insulin at three amino acid positions (**B30**, **A8** and **A10**) (1). In dilute solution such as in the blood stream, insulin exists as the 6000Da molecular weight monomer (1). In concentrated solution and crystals, the form of insulin found in vials supplied by the pharmaceutical companies for insulin injection, six monomers self-associate with two zinc ions to form a hexamer.

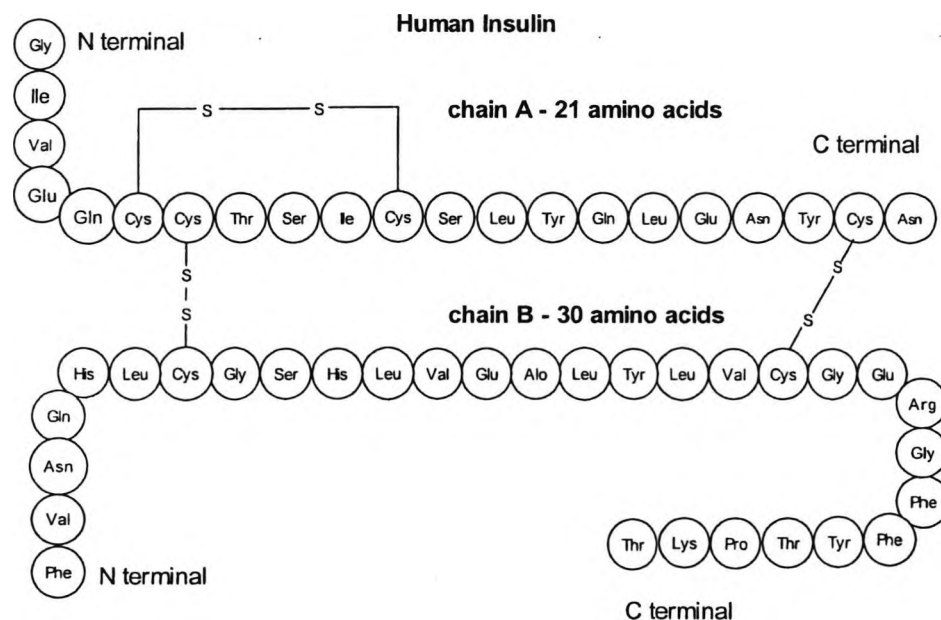


Figure 3.1 Structure of human insulin.

This is of therapeutic importance, as the slow absorption of insulin from the subcutaneous tissue is partly due to the time taken for hexameric insulin to disperse and dissociate into the smaller monomeric form.

3.1.4.2 Insulin secretion and action

The hormone insulin is formed in the beta cells of the pancreatic islets of Langerhans from a single amino acid chain precursor molecule called *proinsulin*. Proinsulin is packaged into vesicles in the Golgi apparatus of the cell, and is then converted by enzymes into insulin and the connecting peptide (C-peptide) (3).

3.1.4.3 Glucagon secretion and action

Another pancreatic hormone involved in the glucoregulatory system and a product of pancreatic alpha cells is glucagon. Its principal physiological activity is to increase the blood glucose levels by accelerating the glycogenolysis and glyconeogenesis in the liver. Glucagon and insulin secretion is inhibited by the growth hormone inhibiting factor or somatostatin, a product of delta cells.

3.1.4.4 Negative feedback control of glucose

The secretion of both glucagon and insulin hormones is directly controlled by the level of blood sugar via a negative feedback system. When the blood sugar level falls below normal, chemical sensors in the alpha cells of the islets stimulate the cells to secrete glucagons, the beta cells are not stimulated. When blood sugar rises, the alpha cells are no longer stimulated and their production slows down; the stimulatory effect is now on the beta cells, which begin to secrete insulin.

Other hormones can indirectly affect insulin production. For instance, growth hormone raises blood glucose level, and the rise in glucose level triggers insulin secretion. Adrenal cortical hormones, by stimulating the secretion of glucocorticoids, bring about hyperglycaemia and also indirectly stimulate the release of insulin. Gastrointestinal hormones, like gastrin, secretin, glucagon-like peptide-1 (GLP-1), glucose-dependent insulintropic polypeptide (GIP), cholecystokinin, and gastric inhibitory peptide also stimulate insulin secretion (3).

3.2 Diabetes Mellitus

3.2.1 Definition and classification of diabetes mellitus

“Diabetes mellitus is a group of metabolic disorders characterised by hyperglycaemia resulting from defects in insulin secretion, insulin action, or both” (7).

The World Health Organisation (WHO) gives a slightly different definition of *“a metabolic disorder of multiple aetiology characterised by chronic hyperglycaemia with disturbances of carbohydrate, fat and protein metabolism resulting from defects in insulin secretion, insulin action, or both” (8).*

The classification of diabetes mellitus includes four clinical classes (7):

- ◇ Type 1 diabetes, in the past referred to as *insulin-dependent diabetes mellitus* or *juvenile onset diabetes*, results from an absolute deficiency of insulin due to an auto-immunological destruction of the insulin producing pancreatic beta cells;
- ◇ Type 2 diabetes, previously referred to as *non-insulin –dependent diabetes mellitus* or *maturity onset diabetes*, results from a progressive insulin secretory defect on the background of insulin resistance (the muscle and the fat cells become 'resistant' to the action of insulin and compensatory mechanisms that are activated in the beta cells to secrete more insulin are not sufficient to maintain blood glucose levels within a normal physiological range (9));
- ◇ Other specific types of diabetes due to other causes, e.g. genetic defects of beta cell function, genetic defects in insulin action, diseases of the exocrine pancreas, drug or chemical induced;
- ◇ Gestational diabetes mellitus diagnosed during pregnancy.

3.2.2 Epidemiology and aetiology of diabetes

3.2.2.1 Type 1 diabetes mellitus

Although type 1 diabetes can, theoretically, occur at any age, it predominantly arises in children and young adults with peak incidence before school age and at around puberty (1).

There is a marked geographical difference in the incidence of type 1 diabetes. Scandinavian countries like Finland and Sweden have a very high incidence (30-35 cases per year per 100,000 of the population), whereas Oriental countries like Japan, China and Korea show a very low incidence (approximately 0.5 – 2.0 cases per year per 100,000 of the population) (1). The difference in the incidences of type 1 diabetes in genetically similar countries like, for example, Finland (high incidence) and Estonia (low incidence), suggest that environmental factors may predominate over the genetic susceptibility in the disease aetiology. The seasonal differences, i.e. a high incidence over the winter and early spring months, and a low incidence over the summer months supports this theory and points to precipitating agents such as common viruses which may trigger the onset of the disease. Other possible determinants of T1DM are foods containing nitrosamines and cow's milk protein.

The commonest cause of the disease is autoimmune destruction of the islet beta cells but the exact aetiology is complex and still not well understood. Research efforts concentrate lately on showing the inherited susceptibility of type 1 diabetes (10).

3.2.2.2 Type 2 diabetes mellitus

This is the commonest type of diabetes with various predisposing factors such as obesity, low level of exercise, older age and family history of diabetes. Similarly to T1DM, there is also a large variation in the prevalence of type 2 diabetes in different countries. The highest prevalence were found in Pima Indians of Arizona and in the South Pacific island of Nauru (>50%) (1). The

most likely cause of this high prevalence is a change in lifestyle due to the rapid westernisation of those previously typically agricultural communities. A low prevalence (<1%) is found in poorly developed rural communities such as parts of Chile or China (1).

Ethnic effects can be observed in multicultural societies such as the UK or the USA. The prevalence of type 2 diabetes in Asians from Southall in West London, for instance, is four times as high as in the local Caucasian population (1). African Caribbean people in the UK also have high frequency of type 2 diabetes (1). The two main pathophysiological defects in type 2 diabetes are impaired insulin secretion and insulin resistance. The main abnormality in the islet beta cells of type 2 diabetic patients is the presence of insoluble fibrils distorting the cell membrane (1). Although insulin resistance is generally high in type 2 diabetic patients, it also varies widely in the non-diabetic population. Hence, this defect alone cannot account for diabetes.

3.2.3 Diagnosis and treatment

Diabetes is diagnosed by identifying chronic hyperglycaemia. The latest WHO recommendations (8) specify diagnostic criteria and the blood glucose values representing the diagnostic cut-off points. WHO defines diabetes as fasting plasma glucose of 7 millimoles per litre and after 2 hour oral glucose tolerance test 11.2 millimoles per litre. The clinical diagnosis of diabetes is often prompted by symptoms such as increased thirst and urine volume, recurrent infections and unexplained weight loss and, in severe cases, drowsiness and coma. In the absence of clear symptoms of diabetes, diagnosis of diabetes should be based on at least two laboratory blood glucose measurements, as hyperglycaemia, even severe, could be only transitory caused by trauma or metabolic stress (11). If in doubt the oral glucose tolerance test should be performed.

Generally, people with T1DM present with acute symptoms and markedly elevated blood glucose levels (7). Type 2 diabetes, on the other hand, is

frequently not diagnosed until complications appear (7). It is suspected that as much as half of all people with diabetes may be undiagnosed (12).

Diabetes management is based on blood glucose monitoring and adjustments of treatment dose/type in response to the blood glucose levels, anticipated meal composition, and planned activities. The blood glucose self-monitoring record as well as two indices, HbA_{1c} and fasting plasma glucose, are commonly used to assess diabetic control – the extent to which metabolism in a patient differs from normal (1).

Treatments vary depending on the type and severity of the disease. Diet and lifestyle, however, always constitute an integral component of diabetes management.

The recent diabetes clinical trials (2,13) have shown the need for an intensive diabetes treatment and tight glycaemic control in order to prevent/delay the onset of the micro- and macro-vascular diabetes complications.

3.2.3.1 Management of type 1 diabetes

People with type 1 diabetes do not produce enough insulin to sustain life and, therefore, depend on exogenous insulin to survive. They often require regular, one to four times daily, insulin injections. The aim of insulin therapy in people with type 1 diabetes is to mimic the pattern of endogenous insulin secretion present in healthy subjects. This is, however, very difficult to achieve due to a high inter-subject variability in the absorption rate of SC administered insulin.

Various types of insulin preparations are currently available differing in their length of action and pharmacological properties. Long acting insulin, usually given once daily, serves to provide a basal level of insulin. Intermediate, short, and rapid acting insulin types are given post-prandially to counteract the effect of the meals. Recently developed by DNA-recombinant technique insulin analogues, both rapid acting (lispro, aspart) and long acting (glargine), proved more effective in mimicking physiological insulin patterns (14). Rapid acting

insulin analogues are quickly absorbed with virtually no delay in their onset of action. This property makes them suitable for use in CSII.

3.2.3.2 Management of type 2 diabetes mellitus

The first line treatment for type 2 diabetes is usually based on dietary and lifestyle changes. Patients are advised to cut out or restrict foods with high sugar/saturated fat contents and to increase their level of activity. These recommendations are essentially the same for type 1 and type 2 diabetes and indeed follow a healthy eating pattern suitable for the entire population (1).

In the event of failure to achieve satisfactory control of blood glucose through diet alone, oral hypoglycaemic agents are introduced. The most common types include sulphonylureas, biguanides and glitazones. As the diabetes progresses and the glycaemic control deteriorates, treatments become more complex and a combination of two or more types of drugs may be used. Eventually, a number of individuals with type 2 diabetes may even require supplemental insulin for adequate blood glucose control (7).

3.2.4 Glucose monitoring

Glucose monitoring is an essential part of diabetes management. While people with type 2 diabetes may get away with urine glucose testing and an occasional blood glucose test, those with type 1 diabetes require frequent self-monitoring using finger stick blood sampling and an analysis with a portable glucose meter device. This is due to the wide fluctuation and unpredictability of blood glucose levels in type 1 diabetes (1). Hence, single blood glucose measurements give little information about overall control. Even when the measurements are done more frequently, typically before and after meals, clinically significant glucose fluctuations and hypos may not be detected. To overcome this problem, methods for continuous glucose monitoring have been introduced in recent years. The ideal method would be a non-invasive technique, such as spectroscopy (15). However, there are considerable problems with these systems due to overlapping spectral features from other substances and optical changes with varying blood volume and temperature (16). Other possible techniques involve

subcutaneous implantation of a glucose sensor, which measure glucose in the interstitial fluid of adipose tissue. Research is still ongoing to produce an accurate and long lasting continuous glucose monitoring device. The products currently on the market are only able to give historical data and their accuracy has been questioned (17,18).

3.2.5 Artificial pancreas

The concept of an artificial endocrine pancreas was introduced as early as 1959 by an endocrinologist Prof. E. Perry McCullagh (19). The aim was to substitute the function of intact beta cells, which recognise the changes in blood glucose, then transmit the information inside the cell and secrete an appropriate amount of insulin to maintain glucose homeostasis.

The ultimate goal of the development of an artificial pancreas is a long-term strict glycaemic control and, subsequently, prevention or delay of the onset of macro- and microvascular complications of diabetes. Hence, in order to create an artificial pancreas one needs a glucose sensor for glucose monitoring, a processor system with control algorithms and insulin delivery system in the form of an insulin pump (see Figure 3.2). These three components are then connected to form a closed loop feedback control system.

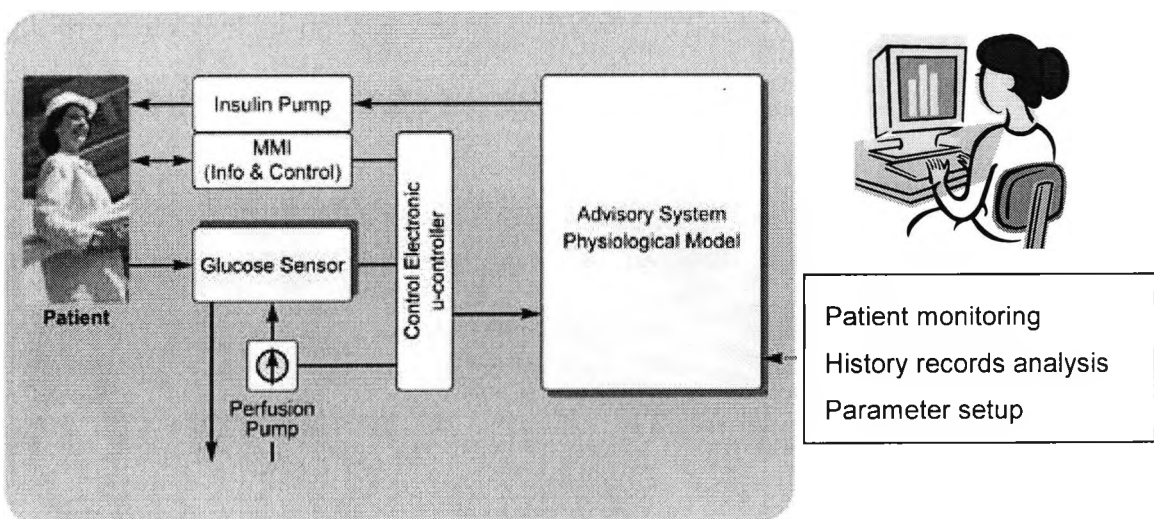


Figure 3.2 Model of artificial pancreas used in ADICOL project. MMI stands for Man-Machine Interface.

The first prototype of an artificial pancreas was created by Prof. A.M. Albisser from the University of Toronto in 1974. It was based on intravenous glucose measurements and intravenous insulin delivery (i.e. IV-IV approach) and consisted of an auto-analyser for blood glucose monitoring, a minicomputer for computing insulin requirement in response to measured blood glucose concentrations and an insulin pump (20). As the next step, to make the device smaller, the auto-analyser was replaced with a continuous glucose sensor (19). This bed-site type artificial endocrine pancreas is still widely used on a short-term basis in a clinical environment (i.e. during clinical trials under glucose clamp conditions).

Since then the work concentrated on the miniaturisation of the device and on long-term clinical applications. A French team of researchers led by Eric Renard have developed an implantable artificial pancreas claiming good, long-term control of blood glucose, low failure and complication rates (21).

Current research efforts, however, concentrate mostly on developing an extra-corporal wearable AP with SC glucose sensing and SC insulin delivery, this way avoiding long-term complications and trauma related to the implantation of the device. Thanks to the recent technical progress we now have small needle type glucose sensors, which measure glucose in the interstitial fluid and miniature programmable insulin pumps. More work is required in the field of sensor stability and reliability. Another goal is to develop an efficient and adaptable control algorithm. The aim of a European Project ADICOL was to accomplish these two goals and to develop a long-term wearable artificial pancreas. Although the project has ended with successful preliminary trials, the efforts are ongoing thanks to the commitment of its collaborators. A prototype AP device should become available in approximately 2-3 years time.

3.3 Compartmental Modelling Techniques

3.3.1 The concept and purpose of modelling

Modelling is a process of mapping or transforming a system into a model - a representation of reality involving some degree of approximation. Any kind of system, i.e. biological, mechanical, organisational, can be transformed into a model. Modelling biological systems, known for their complexity, becomes a necessity in our attempts to understand their structure and their functionality.

When postulating a model of a system one is required to make some assumptions on how the system works and to describe these assumptions mathematically. Models of systems can have different characteristics depending on the system properties. They can be deterministic or stochastic, dynamic or static, with lumped or distributed parameters. Metabolic systems are dynamic systems and we focus here on the most widely used class of dynamic models: compartmental models (22).

Compartmental models are lumped parameter models, in that the events in the system are described by a finite number of changing variables, and are thus described by ordinary differential equations (22). The models which are considered here are deterministic in nature, i.e. they are formulated using exact relationships between model variables.

3.3.2 The theory of compartmental models

A *compartment* is an amount of material that acts as though it is well mixed and kinetically homogenous (22). Well-mixed means that any two samples taken from a compartment at the same time would have the same concentration of the substance being studied. Kinetic homogeneity means that every particle in a compartment has the same probability of taking any pathways leaving the compartment.

The concept is purely theoretical. One compartment may combine material from several different physical spaces. Hence, it can be sometimes difficult to assign a particular physical space to it. Compartments can be divided into accessible and nonaccessible for measurement.

A compartmental model consists of a finite number of compartments with interconnections among them. These connections represent a flux of material, which physiologically represents transport from one location to another, or a chemical transformation or both (22). The function of the compartment can be described by mass balance equations of the following general form. If Q_i is the quantity of a substance in compartment i that interchanges matter with other compartments (see Figure 3.3), then

$$\frac{dQ_i}{dt} = \sum R_{ij} - \sum R_{ji}$$

where $\sum R_{ij}$ represents the summation of the rates of mass transfer (fluxes) into i from all relevant compartments and $\sum R_{ji}$ the summation of the rates of mass transfer from i to other compartments of the system (23).

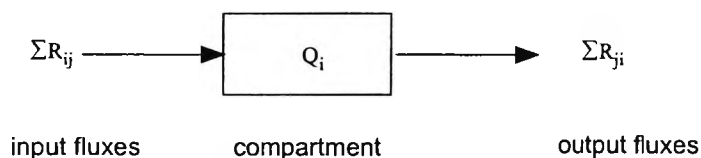


Figure 3.3 Diagram showing the compartment containing quantity of material Q_i with its input and output fluxes.

The functional dependencies of each flux need to be specified. The dependencies can be either linear or nonlinear. The linear dependence can be described as follows:

$$R_{ij} = k_{ij}Q_j$$

where k_{ij} is a constant defining the fractional rate of transfer of material into compartment i from compartment j .

In biological systems one of the most commonly occurring nonlinear dependencies is the Michaelis-Menten form:

$$R_{ij} = \frac{V_{MAX} Q_j}{k_M + Q_j}$$

where V_{MAX} is the saturation value of flux R_{ij} and K_M is the value of Q_j at which R_{ij} is equal to half of its maximal value.

The number of required compartments depends both on the system being studied and on the richness of the experimental design. A model is unique for each system, as it represents known and hypothesised physiology and biochemistry specific to that system. It provides the investigator with insights into the system's structure and is only as good as the assumptions that are incorporated into its structure.

The essential steps of the modelling process are model formulation and model identification, the latter including parameter estimation and model validation (23).

3.3.2.1 Model formulation

Model formulation can be subdivided into three distinct components, the formulation of the conceptual model, the mathematical realisation of that conceptual model, and finally the solution of the model to give the required relations between the variables of interest (23).

The formulation of the conceptual model is based on the validated *a priori* physiological knowledge. It requires a functional description of the relevant physiological processes, and their interdependence in the form of a final model.

Mathematical realisation comprises constructing the mathematical equations to provide a detailed description of the physical processes and to describe the overall relations contained within the functional model. For each compartment

a mass balance equation is formulated. The complete set of those equations together with the initial conditions constitute the mathematical model of the particular metabolic system (23).

Obtaining the required explicit relations between the model variables, usually done through the implementation of the model on the computer, is called the solution.

3.3.3 Model identification

Model identification is concerned both with determining the structure of a mathematical model and with estimating the model's unknown parameters on the basis of a suitable set of experimental data (23).

3.3.3.1 *A priori* identifiability

A mismatch between the complexity of the model and the richness of the experimental data is known as the identifiability problem.

Before proceeding to estimate the model parameters, one must decide whether the data obtained in the course of the experiment contain enough information to estimate the unknown parameters of the postulated model structure. If the model structure is too complex for the particular data set, e.g. if certain parameters are not identifiable from the ideal noise-free data, it is unlikely that parameters could be identified in a real situation with a possible error in the model structure and the noisy data. This problem is usually referred to as the *a priori* identifiability problem.

In summary, *a priori* identifiability examines whether, given ideal noise-free data and assuming an error-free model structure, it is possible to make unique estimates of all the unknown model parameters. A model can be *uniquely* (each of the parameters has only one possible solution) or *nonuniquely identifiable* (one or more parameters has one or more but a finite number of possible solutions), or *nonidentifiable* (one or more of the parameters has an infinite number of solutions) (22).

If a model is *a priori* nonidentifiable, the incorporation of additional knowledge, the reparametrisation (parameter aggregation), or even the design of a more informative experiment may be required.

3.3.3.2 Parameter estimation and a posteriori identifiability

If a model is *a priori* uniquely or nonuniquely identifiable, then identification techniques can be used to estimate the numerical values of the unknown parameters from the noisy data. As the parameters do not appear in the model linearly as a straight line or a polynomial model, the parameter estimation problem is nonlinear (22).

Weighted nonlinear least squares is the most commonly used parameter estimation technique. In this method the weighted residual sum of squares (WRSS) is defined as a cost function:

$$WRSS = \sum_{i=1}^N \frac{1}{w_i} (y_i^{obs}(t_i) - y(t_i, p_1 \dots p_M))^2$$

where $y_i^{obs}(t_i)$ is the measurement at time t_i , $y(t_i, p_1 \dots p_M)$ is the model prediction at time t_i for a given set of parameters from p_1 to p_M , and w_i is the assigned weight (equal to the inverse of the variance of the measurement error)

The desired parameter estimates are those, which minimise this function. As there is no closed form analytical solution to the WRSS minimisation, an iterative solution is required. Iteration can be thought of as a series of steps where the nonlinear problem is handled in a linear fashion at each step (22). The covariance matrix of the parameter estimates, the Fisher Information Matrix, can be used to evaluate their precision, or in other words, their *a posteriori* identifiability (23).

Other techniques of parameter estimation include Maximum Likelihood and Bayesian Estimation.

3.3.4 Model validation

Once the model has been identified in terms of both structure and parameter estimates it still needs to undergo further validation. Validation is a procedure of examining whether the model is good enough for its intended purpose.

The basic approach in validating a model is to compare the model and system behaviour, based on appropriate output features.

Once the parameter estimation procedure has been completed, the following quantitative tools become available:

- ◇ plausibility of the estimated parameters: if one or more estimated parameters take on values that are absurd in the physical or physiological sense, the model is deemed invalid and is rejected;
- ◇ statistics of the residual errors: it has been assumed *a priori* that the measurement error is normally distributed and with a zero mean; hence, residual errors which are nonrandomly distributed or contain trends put validity of the model in question;
- ◇ precision of parameter estimates expressed as a coefficient of variation (CV) or *a posteriori* (practical) identifiability: this is an arbitrary measure, a commonly agreed level of acceptability is a CV of 100%, good precision of parameter estimates refers usually to a CV of less than 25%.

The validity of a model is only applicable in a specific domain. A model that is valid is not necessarily a true one (22).

3.3.5 Model selection process

When one deals with a number of competing models, comparison between them should be made on the basis of their ability to fit the data. This, so called, goodness of fit can be evaluated through WRSS as a measure of the mismatch between the model prediction and the data. However, goodness of fit on its own does not reflect solely the accuracy of representing the data by

the model. The known effect of an improvement in model fit with increased model complexity (increased number of parameters) is a confounding effect. In order to correct for this effect a different measure needs to be applied. This new measure, also called the parsimony criterion, corrects the goodness of fit for the increase in the number of degrees of freedom. The Akaike information criterion (AIC) is one such measure used for comparing linear models. It takes into account both goodness of fit and the number of parameters when comparing models (24). The Akaike criterion is calculated as follows:

$$AIC = N \ln WRSS + 2P$$

where N is the number of data points, $WRSS$ is the residual sum of squares and P is the number of parameters. The best model, based on the principle of parsimony, is than which achieves the lowest value of AIC.

Other similar criteria are available such as the Schwarz Bayesian information criterion (25). With small-size data sets, both the Akaike and the Schwarz give similar results (26).

3.3.6 Population modelling techniques

In the course of individual modelling analysis a unique set of parameter estimates is assigned to each individual subject. Those parameter estimates will most probably vary among subjects, and hence the interindividual variability will be observed. In other words we will be dealing with a population of individuals. The purpose of population kinetic analysis is to focus on such a population and estimate the population distribution of the model parameters based on a collection of individual data.

Given a specific population of individuals an experiment carried out on each individual with similar modalities and an appropriate system model, population kinetic analysis can be defined as the study of the intersubject variability of the parameters of a kinetic model (27).

Depending on the nature of prior knowledge available on the population distribution, two approaches can be used to facilitate its estimation. In the

parametric approach, the distribution is assumed to be known except for a certain number of unknown parameters, whereas in the *nonparametric* approach no functional form of the distribution is assumed.

The two basic methods for obtaining estimates and their variability are the maximum likelihood method based on the maximisation of the likelihood function and Bayesian methods which use the Bayesian inference approaches to estimate the full conditional population distribution.

3.3.6.1 Standard two-stage analysis

Standard two-stage analysis (STS) is the most common way of determining the distribution of parameter estimates within a population of subjects. From the individual parameter estimates, the empirical sample mean a , and the empirical sample covariance D , are calculated as follows:

$$a = \frac{1}{M} \sum_{i=1}^M p_i$$
$$D = \frac{1}{M-1} \sum_{i=1}^M (p_i - a)(p_i - a)^T$$

where M is a number of individuals in the population and p is an estimate of the parameter vector. The covariance matrix D gives an estimate of the interindividual variability. As no functional form of the population distribution is assumed, the STS belongs to the class of nonparametric estimators.

A clear advantage of this method of population analysis is its simplicity. There are, however, three major shortcomings of this method. One of the main ones is that no knowledge is gained from the fact that the subjects belong to the same population. The second disadvantage is that the intraindividual variability given by the subject-specific covariance matrix is not taken into account. Thirdly, no measure of the precision of the estimates of a and D is available.

3.3.6.2 Iterative two-stage analysis

The Iterative two-stage (ITS) approach is a parametric iterative population analysis method based on the concepts of population prior knowledge and maximum *a posteriori* probability (MAP) empirical Bayes estimator (27). There are three steps of the ITS: step 1 initialisation, step 2 expectation, and step 3 minimisation. In the initialisation step the population mean for each parameter is calculated as the sample mean of all individual parameter estimates. Population variance is also calculated as the corresponding sample variance. In step 2, the expectation step, the parameter estimation for each individual subject j is performed again, this time minimising the following extended MAP Bayesian objective function with respect to p_j (28)

$$MAP(p_j) = \sum_{i=1}^{N_j} \frac{[G_{i,j}^D - G^M(p_j, t_{i,j})]^2}{\sigma_{i,j}^2} + \sum_{i=1}^{N_p} \frac{[\mu_i(k) - p_{j,i}]^2}{\sum_{i,i}^2(k)}$$

where the distance of the current parameter estimate from the population mean is also penalised; we denote with $p_{j,i}$ the i^{th} element of the parameter vector p_j for subject j , $\mu_i(k)$ is the value of the population mean at the k^{th} iteration, N_j is the number of data points available for the j^{th} subject, $t_{i,j}$ and $G_{i,j}^D$ are the i^{th} time point and data point, respectively, for the j^{th} subject, $\sigma_{i,j}^2$ is the variance of the measurement error of the i^{th} data point, $G^M(p_j, t_i)$ is the model prediction for a given p_j , and $\sum_{i,i}(k)$ is the i^{th} diagonal element of the population covariance matrix at the k^{th} iteration. The estimate obtained by minimising this objective function is called *post hoc*, or empirical Bayes, estimate. The updated population mean of the parameter vector and the covariance are calculated. In the final step 3, the check for convergence of the population mean, the population variance, and the individual parameter estimates is carried out. This is done by determining whether or not the current and the previous estimate differ by <1%. If so, the algorithm is stopped, if not, it returns to step 2. Hence, steps 2 and 3 are performed iteratively until convergence is achieved.

3.4 Review of Existing Techniques to Model Whole-body Glucose Kinetics

The whole-body glucose kinetics and its control by insulin is complex. Understanding this system requires the quantification of various fluxes and control effects that are not directly measurable as they take place in nonaccessible compartments. This can only be accomplished with mathematical modelling methods (29).

Mathematical models of the whole-body glucose kinetics and metabolism have been the subject of research for over four decades. The models can be classified according to their specific purpose, i.e. explanatory models, models for measurement or control (29), or, alternatively, according to the way they were derived. This review follows the latter classification, whereby models are placed into two main categories: those derived from existing knowledge and literature, and those derived directly from experimental data. The emphasis will be on models, which have the potential to be used or to provide important information when representing the whole-body glucose kinetics in type 1 diabetes during normal physiological conditions. For this reason, models dealing with insulin secretion will not be considered here.

3.4.1 Knowledge driven models of whole-body glucose kinetics

Knowledge driven models rely on independent knowledge of the metabolic and kinetic processes. If they are to be valid explanatory means of the system, they should mirror structurally and parametrically the component processes. Such models, typically explanatory in nature, promote insight and understanding, and possibly define quantitative interactions, which are not normally measurable. The structure and the kinetic/metabolic processes involved in the glucose regulatory system are illustrated in Figure 3.4.

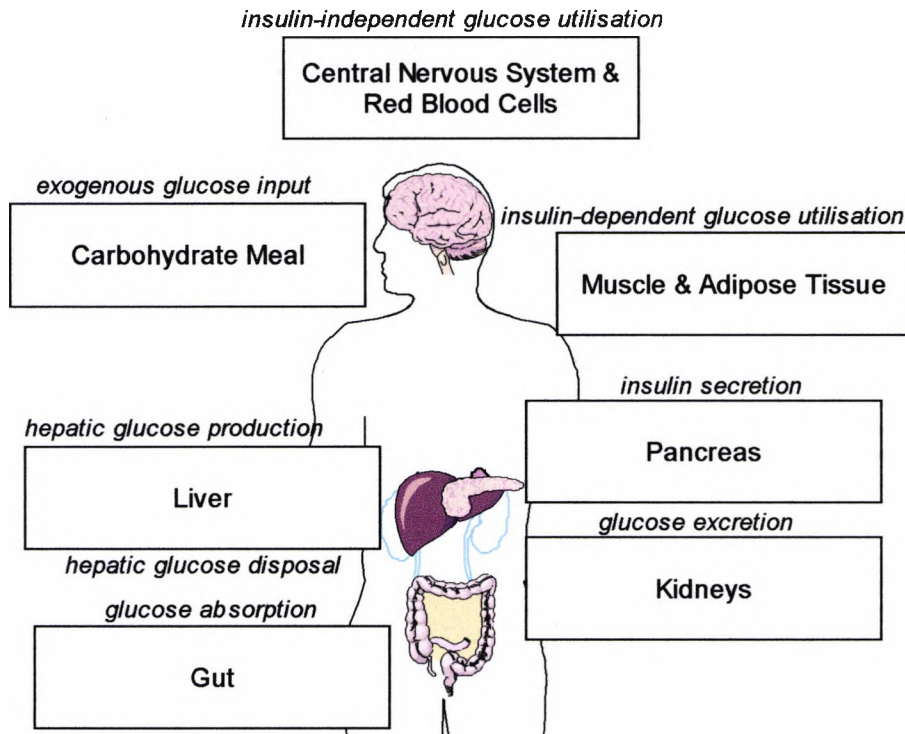


Figure 3.4 Schematic representation of the whole-body glucose kinetics/metabolism.

The very first models of the whole-body glucose kinetics were linear and represented glucose and insulin pools with single compartments (30,31). This was a clear oversimplification of the glucose regulatory system. In the next stage, nonlinear kinetics was introduced while maintaining the two-compartment structure (32).

The following models (33,34), although expanding on the number of compartments to represent insulin kinetics, still could not claim to be a good physiologic representation of a widespread applicability. For instance, insulin-dependent glucose disposal was not partitioned between the periphery and the liver at this stage, and insulin sensitivity was not taken into consideration.

An increased understanding of glucose metabolism and its regulation by insulin led to a number of more accurate explanatory physiologic model formulations. The model presented by Guyton *et al* (35) employed a high degree of body compartmentalisation to an organ level. It was described by 32 ordinary differential equations, 16 of which were nonlinear. The model by Sorensen (36) expanded on the model by Guyton by adding a model of

glucagon counterregulation, an additional compartment for the gut, and an additional parameter for the transcapillary diffusion time. Sorensen's model was described by 22 simultaneous nonlinear ordinary differential equations.

Cramp and Carson (37), and then Cobelli *et al* (38) managed to reduce the mathematical complexity to 9 and 7 differential equations, respectively, by proposing lumped compartmental models. The model by Cramp and Carson represented glucose metabolism in the liver in terms of the major contributing biochemical pathways, i.e. glycolysis, gluconeogenesis, glycogen synthesis and breakdown, and included hepatic glucose 6-phosphate and hepatic glycogen compartments. However, inadequacies of this model include the following: no provision was made for the renal glucose extraction, the pancreatic insulin release was described by a simplified linear function, and the distribution volumes of glucose, insulin, and glucagon were all assigned the same value.

The model by Cobelli *et al* (38) represented a metabolic plant, that is, glucose kinetics and its two controllers, hormones insulin and glucagon. The glucose subsystem, described by a single compartment, considered a net hepatic glucose balance, the renal excretion of glucose, and an insulin-dependent as well as insulin-independent glucose utilisation. The insulin subsystem was described by a five-compartment model representing pancreatic insulin release, portal plasma insulin, plasma insulin, and insulin in the interstitial fluid. The glucagon subsystem was represented by a one-compartment model. The three subsystems interacted via control signals. This model was further improved by the authors by means of experimental testing (see the next section for details).

A number of simulation models were developed in the 1980s and early 1990s with the aim to help optimise insulin therapy in type 1 diabetes. Salzsieder *et al* based their simulation model (39) on the optimal control theory adopted from engineering and used a state-variable technique to model the glucoregulatory system. Four state variables proved sufficient for complete description of the controlled metabolic plant's behaviour: the circulating

concentration of insulin and glucose, the overall endogenous glucose balance, and the peripheral insulin-dependent glucose utilisation. A black-box analysis of transfer functions was employed to estimate parameters of glucose metabolism such as rate constants and sensitivity ratios.

Berger and Rodbard developed a computer program for the simulation of plasma insulin and glucose dynamics after subcutaneous insulin injection (40). They followed the parsimony principle associated with the minimal model approach (41) to find the mathematical formulation to represent the major physiological systems with the fewest parameters. The program incorporated a pharmacokinetic model of insulin absorption to calculate the time courses of plasma insulin for various insulin preparations. The parameter values of the complete model employed by Berger and Rodbard were obtained by analysing data from studies reported in the literature.

The above model was utilised by Lehman and Deutsch in the development of AIDA (42), diabetes simulation program designed specifically for subjects with type 1 diabetes, i.e. assuming a complete lack of endogenous insulin secretion. The model contains a single glucose pool representing extracellular glucose. Glucose enters this pool via both intestinal absorption and hepatic glucose production, and is removed by an insulin-independent glucose utilisation in the red blood cells and the central nervous system as well as by an insulin-dependent glucose utilisation in the liver and the periphery. Hepatic and peripheral handling of glucose is treated separately making it possible to assign patient-specific insulin sensitivity parameters to glucose-insulin interactions in the liver and the periphery. Glucose excretion takes place above the renal threshold of glucose as a function of the creatinine clearance.

The simulation model by Boroujerdi *et al* (43) expands on the previous model by Cobelli *et al* (44) and represents glucose distribution by means of glucose transporters.

3.4.2 Experimentally driven models of glucose-insulin interactions

The conceptual paradigm of models representing glucose-insulin interactions is illustrated in Figure 3.5. The glucose regulation system is commonly represented by a model of insulin action linked to a model of glucose kinetics. Glucose and insulin concentrations are the measured variables. The model of insulin action typically includes a remote compartment to represent a delay in insulin action. The glucose model describes the distribution, production and utilisation of glucose, and their control by insulin. Model parameters are determined by the least squares fitting of the model to the experimental data.

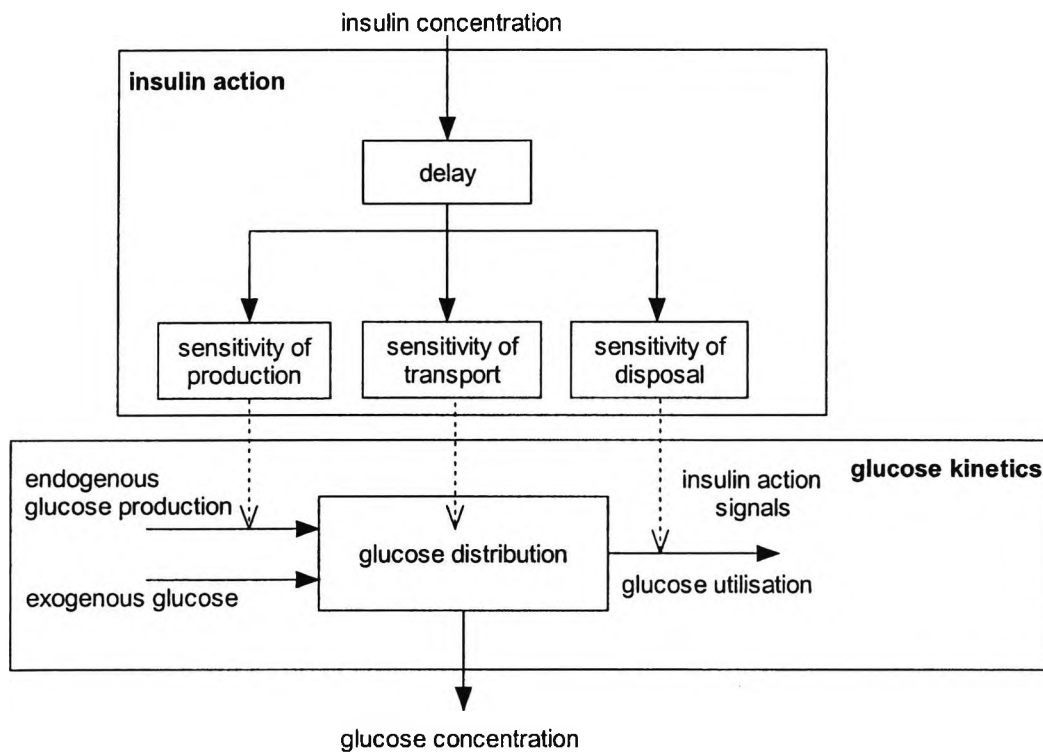


Figure 3.5 The glucose-insulin system; dotted line arrows indicate insulin control; adapted from (45).

The main driving force in the development of these models was the need for easily applicable tools to quantify indices of insulin sensitivity and insulin secretion. As mentioned previously, models of insulin secretion will not be considered in this review.

There is a general agreement that a euglycaemic clamp is the best available standard for the measurement of insulin effect on glucose kinetics. When a steady state is reached, the exogenous glucose infusion rate equals the amount of glucose disposed of by all tissues in the body and thus provides a measure of overall insulin sensitivity.

Unfortunately, the glucose clamp methodology is technically difficult to perform and is, therefore, not suitable for a routine practice. Other simpler and less invasive methods, usually involving a model representation of the glucose-insulin system, had to be devised. Currently, the two most commonly used methods are the homeostatic model assessment and the minimal model.

The homeostatic model assessment (HOMA) and the constant infusion of glucose with model assessment (CIGMA) were used to determine insulin sensitivity from the fasting plasma glucose and insulin concentrations (HOMA) or after a standardised, 1h intravenous glucose infusion (CIGMA) (46,47). Insulin sensitivity, expressed as an index of relative insulin resistance R ($R=1$ corresponds to normal homeostasis), is calculated as a function of the measured glucose and insulin levels. In practice, R is determined from a contour plot.

The minimal model of glucose kinetics (41) was developed using data collected during the intravenous glucose-tolerance test (IVGTT). The original model has two compartments representing remote insulin and plasma glucose. The measured time course of insulin is regarded as the input and the falling glucose concentration as the output. A nonlinear regression analysis is used to estimate four parameters, with insulin sensitivity (S_I) and glucose effectiveness (S_G) being the indices of interest.

A major limitation of the original minimal model stems from the fact that, since the model was developed using unlabelled IVGTT, it was not possible to separate the glucose production from the disposal. Only the net hepatic glucose balance and glucose disposal in non-hepatic tissues could be

described as a function of plasma glucose and the remote insulin action (48). As a consequence, the metabolic indices S_I and S_G are hybrid parameters, which measure not only the effect of glucose and insulin on glucose disposal but also their inhibitory effects on the hepatic glucose production. Other concerns regarding the minimal model include poor precision of parameter estimates and unsatisfactory reproducibility of the insulin sensitivity parameter S_I (29). The usefulness of S_G , defined as the basal fractional glucose clearance, has also been questioned and found to be in error (49,50).

To overcome these limitations, labelled IVGTT methods have been devised (48,51), i.e. a tracer glucose bolus was injected together with the cold glucose. The tracer minimal models allowed the estimation of the true tissue sensitivity to insulin and the true glucose effectiveness without distortion of glucose and insulin effects on glucose production. In addition, precision and reproducibility of the estimates of insulin sensitivity and glucose effectiveness were also improved (51).

Both cold and tracer glucose minimal models describe the functioning of the glucose system in the non-steady state during an IVGTT. Caumo *et al* (52) observed that the models give a very poor prediction of the hepatic glucose production during an IVGTT. The source of the error is likely to be an inadequate mono-compartmental description of the glucose kinetics (29). A good evidence exists that a reliable description of the glucose kinetics requires at least two compartments (44).

Two-compartment minimal models have been proposed in the last decade (50,52,53) with improved results. Unfortunately, the increase in the number of model parameters to six meant that the parameters could not be uniquely estimated using the standard least squares data fitting. The problem was solved using tracer glucose bolus (50,52) or applying Bayesian estimation methods (53). The first approach simplifies the model by separating the hepatic glucose production from the insulin-dependent glucose utilisation. In the second approach, the uncertainty in the individual parameter values is reduced by assuming a given statistical distribution of the parameters. The

two-compartmental models provided a physiologically plausible profile of the endogenous glucose production during the IVGTT.

The two-compartment minimal model allowed for the separation and quantification of two insulin sensitivities, sensitivity of glucose uptake by the periphery and the sensitivity of hepatic glucose production. The estimation of the third insulin sensitivity of glucose transport/distribution (see Figure 3.4) was first attempted by Ferrannini *et al* (54). They proposed a three-compartment model of glucose kinetics and identified the model on data from a euglycaemic hyperinsulinaemic clamp with the use of labelled [$3\text{-}^3\text{H}$] glucose. Apart from the plasma glucose compartment, the other two compartments were a slowly-equilibrating compartment representing insulin-dependent glucose utilisation by the muscle and the adipose tissue and a rapidly-equilibrating compartment representing the insulin-independent glucose utilisation by the central nervous system and the red blood cells. The model also allowed the estimation of other kinetic parameters, in particular, the mean arterio-venous transit time of both the extracellular and the transport tracer.

The partitioning of the three insulin effects on glucose transport/distribution, disposal and hepatic glucose production was accomplished by Hovorka *et al* using a two-compartment model for the labelled IVGTT (55) based on work by Vicini *et al* (50). The separation of the three insulin sensitivities was made possible by the use of two glucose tracers (a dual-tracer IVGTT). A marker of glucose transport (3-O-methyl-D-glucose), which shares with native glucose the transport system but is not metabolised, and a stable tracer indistinguishable from the native glucose (D-[U- ^{13}C] glucose) were administered simultaneously. The validation of hepatic glucose production was facilitated by administering and reconstructing a variable infusion of D-[6,6- $^2\text{H}_2$] glucose. The model described both the steady state (pre-IVGTT) and dynamic (IVGTT) conditions and was validated in healthy subjects. It was found that in healthy subjects insulin has the strongest effect on the hepatic glucose production (approximately 50%), whereas the other two peripheral insulin effects account for the remaining 50%, each effect contributing equally.

A completely different approach to modelling the whole-body glucose kinetics and insulin sensitivity from a labelled IVGTT was taken by Natali *et al* (56), and then Mari *et al* (57). The authors assumed that compartmental models do not represent the physiological system realistically enough and proposed a circulatory model based on the theory of organ kinetics by Zierler (58). The models still fit the scheme shown in Figure 3.5. However, the glucose kinetics is described by a circulatory loop. When compared with the compartment models, the circulatory model was only fractionally superior to the two-compartment minimal model in its prediction of the rate of appearance of glucose in non-steady-state conditions (57).

In conclusion, modelling glucose kinetics and insulin sensitivity are mature but still active areas. New methods and new models are being constantly developed in attempt to resolve physiological complexities.

3.5 Review of Existing Techniques to Model Interstitial Glucose Kinetics

The subcutaneous tissue is easily accessible and appears to be a perfect site for a long-term continuous glucose monitoring, one of the main components of an artificial pancreas. Glucose measurements can be carried out using minimally invasive techniques (skin inoculation) with a low level of trauma and a low risk of infections. When using SC tissue, however, one assumes that the glucose concentration in the interstitial fluid reflects blood glucose level, both under steady state conditions and during dynamic glucose changes. Several studies have been conducted to quantify the relationship between the ISF and blood glucose (17,59-63), but no definite formula has been obtained so far. Authors have reported a varying ISF-to-plasma glucose ratio and time lag between the two sampling sites. This leads to a conclusion that the relationship in question is more complex than previously thought.

The delay, the gradient, and the dynamic relationship between plasma and ISF glucose can be described in physiological terms assuming that the plasma and the interstitial fluid are separated by a capillary wall barrier as shown in Figure 3.6.

If a capillary is a significant barrier to glucose molecules, then changes in ISF glucose will be directly related to the changes in blood glucose by the rate of glucose diffusion across the capillary and by the rate of glucose removal from the ISF (glucose uptake by the cells). If the glucose uptake in the tissue immediately surrounding the sensor is negligible (i.e., if $f_{02}=0$), then steady state plasma and ISF glucose will be equal and deviations will only exist during transient glucose changes (64). If, however, glucose uptake by the surrounding tissue is not negligible, a steady state gradient will exist. Furthermore, if glucose uptake is sensitive to insulin (see insulin effect on f_{02} in Figure 3.6), then the IG-PG gradient will change with insulin concentration. Similarly, if the area of diffusion surface is increased with the higher insulin concentration (insulin-induced capillary recruitment (65)), then the glucose

distribution volume, and consequently fluxes f_{12} and f_{21} , will also increase (see insulin effect on f_{21} in Figure 3.6).

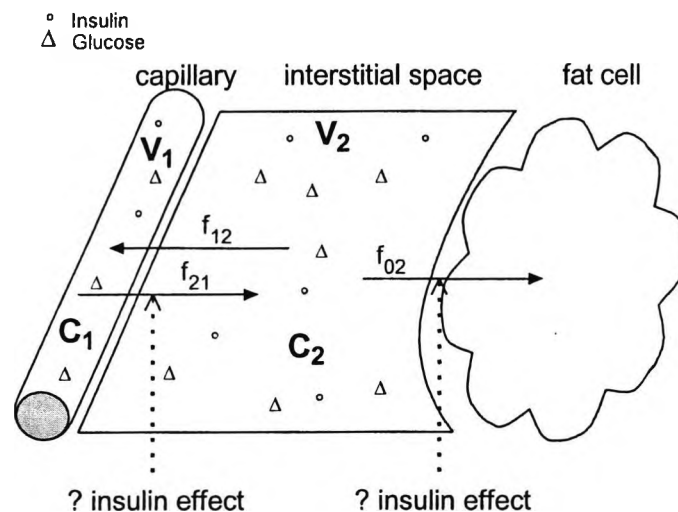


Figure 3.6 Conceptual model of interstitial glucose kinetics; C_1 and C_2 represent glucose concentration in the plasma and the interstitial fluid, respectively; V_1 and V_2 are the plasma and ISF glucose distribution volume, respectively; f_{02} represents glucose flux from the ISF into the fat cell, f_{12} and f_{21} represent glucose fluxes from the ISF into the plasma and from the plasma to the ISF, respectively; adapted from (64).

Dynamically, changes in ISF glucose will lag behind the changes in plasma glucose if this change originates in the plasma space (e.g., a change due to a meal ingestion or a change in the endogenous glucose production). Conversely, if the change in glucose concentration originates in the ISF (glucose uptake by the cells), the changes in ISF glucose should precede the changes in plasma glucose. This effect, often called a push-pull phenomenon, has been discussed widely in the literature and a number of authors claim to have detected it (17,59,60,66).

The studies employed a variety of techniques and sensor types to measure interstitial glucose concentration and attempted to find the ISF versus plasma glucose relationship by comparing these measurements against blood glucose readings taken at calibration points, also called reference values. As a result, any difference in glucose levels between the ISF and capillary blood leads to a “reference” error, which depends on the relationship between the blood and the ISF glucose concentrations. Direct quantification of the ISF to

plasma glucose ratio and the time lag between them cannot be achieved here and the results are difficult, if not impossible, to compare. Values obtained depend on the insertion site, i.e. blood flow, insulin sensitivity, local reaction, device characteristics such as sensitivity, lag time and sampling frequency, also on type of subjects used, i.e. dogs, rats, humans (healthy, with type 1 or type 2 diabetes) and test conditions (physiological, insulin/glucose clamps, fasting, prandial etc.). A wide range of often conflicting results from some of the studies described below can be seen in Table 3.1.

3.5.1 Indirect measurement of interstitial glucose using a sensor

- ◇ Aussedat *et al* (59) studied changes in the ISF and blood glucose concentrations in anaesthetised nondiabetic dogs determined with a miniaturised needle-type enzymatic glucose sensor. Time lag dependent on the plasma glucose gradient and a slower recovery of ISF glucose from hypoglycaemia were observed in this study. The authors also claim to have observed the, so-called, push-pull phenomenon.

- ◇ Rebrin *et al* (64) used an electrochemical enzyme-based glucose sensor to examine the plasma to ISF glucose gradient and the time lag during hyperglycaemic clamps. The study, conducted in nondiabetic dogs also aimed to investigate the effect of insulin on both the gradient and the lag. Although the magnitude of the interstitial to plasma glucose gradient could not be measured with the sensor, the changes in the gradient could be estimated from the changes in sensor sensitivity. These did not prove to be statistically significant. The reported lag was 3-14min, considerably longer than the *in vitro* delay of the sensor (<1.5min). The supposed insulin effect on the gradient or the delay could not be detected in this study.

3.5.2 Direct measurement of interstitial glucose by interstitial fluid sampling or ultrafiltration

- ◇ Thennadil *et al* (67) used the suction blister technique to determine interstitial glucose in six subjects with type 1 diabetes. Scatter plots and linear regression analysis were used to describe the IG-PG relationship. The authors found no time lag between PG and IG even during rapid changes of blood glucose. They also found a considerable inter-subject variability of the ISF and blood glucose bias and a high correlation of the two measurements.
- ◇ Schaupp *et al* (68) employed an open-flow microperfusion (OFM) method with the ionic reference technique (69) to measure interstitial glucose in twenty five healthy volunteers. Their estimated adipose ISF glucose was, on average, 63% of the plasma glucose concentration.
- ◇ Summers *et al* (63) studied seven healthy subjects after an overnight fast under hyperinsulinaemic clamp conditions. A microdialysis technique was used in this study to measure ISF glucose during a rise and a fall of blood glucose. During steady state conditions the IG concentrations were lower than those in the plasma. During the rapid changes from euglycaemia to hyperglycaemia and back, the ISF and plasma glucose concentrations were similar. The authors observed that changes in the ISF concentrations were delayed on average by 20min with a wide inter-subject variation. Summers *et al* noted that the subject with the longest time lag was the most obese, with BMI of 39kg/m^2 , and linked it to the higher insulin resistance in those subjects.
- ◇ Bantle *et al* (70) measured interstitial glucose concentrations in the sampled ISF of seventeen subjects with type 1 diabetes during pre- and post-prandial conditions. Interstitial glucose was measured using a manual hexokinase method. They found IG to be highly correlated with PG. No time lag or gradient was detected.

- ◇ Moberg *et al* (60) employed a microdialysis technique (71) to measure interstitial glucose in ten nondiabetic subjects during hypoglycaemic clamp. Glucose levels in the ISF were observed to be significantly lower during induced hypoglycaemia and a marked protracted glucose fall was also noted. The restoration of the adipose tissue glucose levels following hypoglycaemia was markedly delayed. During euglycaemia, the glucose concentration in the adipose tissue was similar to that in the plasma. The authors concluded that hyperinsulinaemia is a prerequisite for the plasma-ISF differences observed during hypoglycaemia and that an increased glucose extraction is the mechanism whereby this relative glucopenia of the tissue occurs. Apart from the glucose measurement, the authors also measured the local tissue blood flow. An increase in the blood flow was recorded during hypoglycaemia in the adipose tissue.

- ◇ Sternberg *et al* (62) studied the 'real' interstitial glucose concentrations in ten healthy volunteers using a new method based on the recirculation of phosphate-buffered saline in a microdialysis probe. He found the ISF glucose concentration lower both during fasting conditions and during a hyperglycaemic clamp (72 ± 6 and $76 \pm 6\%$, respectively). The mean delay time reported in this study was 12 ± 3 min.

- ◇ Lonroth *et al* (72) measured glucose in the interstitial fluid in ten healthy volunteers with the aid of a microdialysis technique. The reported difference between IG and PG was $12 \pm 3\%$.

3.5.3 Comparison of direct and indirect methods of interstitial glucose measurement

- ◇ Monsod *et al* (17) evaluated the MiniMed[®] CGMS system on eleven healthy volunteers by comparing the system readings to the direct measurement of the ISF glucose through a microdialysis technique. The aim was to examine whether the relationship between interstitial

and plasma glucose is affected by changes in plasma glucose and insulin levels. Applying a hyperinsulinaemic clamp technique, the authors found that insulin induced hypoglycaemia lowers interstitial glucose concentrations, even in the face of unchanged plasma glucose levels. Another finding was that insulin-induced hypoglycaemia increases the interstitial to plasma glucose gradient. During recovery from hypoglycaemia, the sensor reading lagged behind increases in plasma glucose and remained 15% lower than plasma glucose up to the end of the study.

- ◊ Schmidt *et al* (61) compared a microdialysis based enzyme sensor method of measuring the ISF glucose concentration with two reference methods, i.e. the subcutaneous filtrate collection and the equilibration method using ultrafiltration membranes. He found a close agreement between the mean values of interstitial glucose concentrations obtained by these three methods (range of IG-PG ratio of 0.44-0.51).

Table 3.1 Summary of findings relating the interstitial glucose dynamics to the plasma glucose dynamics published by various authors.

Study	Subjects	Test conditions	Method	Delay	Gradient
(59)	Rats (healthy, anaesthetised)	Fasting + glucose injection	Enzymatic sensor	5-10min	N/A
(64)	Dogs (healthy)	Hyperglycaemic clamp	Enzymatic sensor	3-14min	N/A
(67)	Human (diabetic)	Normal	Suction blister	0	100%
(68)	Human (healthy)	Normal	OFM	Not stated	63%
(63)	Human (healthy)	Normal	Microdialysis	0-45min	100%
(70)	Human (diabetic)	Hypoglycaemic clamp	ISF sampling	0	89.4%
(60)	Human (healthy)	Glucose clamp	Microdialysis	25min	100%
(73)	Human (healthy)	Hyperglycaemic clamp + fasting	Recirculation method (PSB)	12min	72-78%
(72)	Human (healthy)	Fasting steady state	Microdialysis	Not stated	100%
(74)	Human (diabetic)	Monitoring	Microdialysis	Not stated	87-101%
(17)	Human (healthy)	Glucose clamp	Microdialysis + MiniMed CGMS	Not stated	65%
(61)	Human (healthy)	Equilibration study	Ultrafiltration + enzyme sensor	Not stated	44-51%

3.6 Existing Techniques to Model Subcutaneous Insulin Kinetics

Subcutaneous insulin absorption is a complex process influenced by many factors including the associated state of insulin, its concentration, injected volume, injection site and depth, and tissue blood flow (75-78). Consequently, the quantitative description of insulin absorption is a difficult task. Several, mostly compartmental, models have been proposed dealing with one or more commercially available insulin preparations (79). Models differ in the description of subcutaneous insulin absorption, hence differing in the number of compartments and the type of processes, which are taken into account. Since plasma insulin is, in all cases, assumed to be a single compartment (79), models differ in the way they consider the SC tissue compartment.

The earliest models consider regular insulin, whereas the more recent ones take the new analogue insulin types into account. Model parameters (except for the model by Mosekilde) estimated for soluble and/or monomeric insulin are shown in Table 3.2.

3.6.1 Compartmental models

- ◇ Kobayashi *et al* (80) proposed a two-compartment (plasma and SC tissue) model with a delay to describe subcutaneous absorption of short acting insulin (see Figure 3.7).

The model is described by the following set of equations:

$$\begin{aligned} dx_1 / dt &= -k_a x_1(t) + u(t - \tau) \\ di / dt &= -k_e i(t) + (k_a / V_d) x_1(t) \end{aligned}$$

where x_1 is the amount of insulin in the SC depot, $i(t)$ is plasma insulin, V_d is the distribution volume, k_a is the absorption rate constant, k_e is the elimination rate constant, τ is the time delay and $u(t)$ is the rate of insulin administration.

The parameter values were obtained by fitting the model to data obtained through the administration of both bolus and infusion of short acting insulin (Actrapid MC, 40U/ml) to 9 subjects with type 1 and 3 subjects with type 2 diabetes. Monomeric insulin was not available at the time of this publication.

Table 3.2 Parameter values for models described in this section.

Model	Parameter	Unit	Value	
			soluble insulin	monomeric insulin
Kobayashi (80)	τ	min	7	
	k_a	min ⁻¹	2.7×10^{-2}	
	k_e	min ⁻¹	1.2×10^{-2}	
	V_d	ml kg ⁻¹	1.5×10^3	
Kraegen (81)	k_{21}	min ⁻¹	3.0×10^{-2}	
	k_d	min ⁻¹	0.0	
	k_a	min ⁻¹	9.7×10^{-2}	
	k_e	min ⁻¹	9.0×10^{-2}	
	V_d	ml	12.0×10^3	
Puckett (82)	k_a	min ⁻¹	1.4×10^{-2}	
	k_e	min ⁻¹	6.3×10^{-2}	
	β	ml	3.5×10^{-2}	
Shimoda (83)	k_{21}	min ⁻¹	1.1×10^{-2}	1.7×10^{-2}
	k_a	min ⁻¹	1.5×10^{-2}	4.8×10^{-2}
	k_d	min ⁻¹	2.1×10^{-2}	2.9×10^{-2}
	k_e	min ⁻¹	9.9×10^{-2}	1.3×10^{-2}
	V_d	ml kg ⁻¹	1.25×10^{-1}	8.0×10^{-2}
Berger (84)	s	unitless	2	
	a	min U ⁻¹	3	
	b	min	102	
	k_e	min ⁻¹	9×10^{-2}	
	V_d	ml	12×10^3	
Trajanoski (85)	Q	ml ² U ²	1.3×10^{-1}	1.3×10^{-1}
	P	min ⁻¹	5×10^{-1}	5×10^{-1}
	D	cm ² min ⁻¹	9×10^{-5}	9×10^{-5}
	B	min ⁻¹	1.3×10^{-2}	1.3×10^{-2}
	k_e	min ⁻¹	9×10^{-2}	9×10^{-2}
	V_d	ml	12×10^3	12×10^3

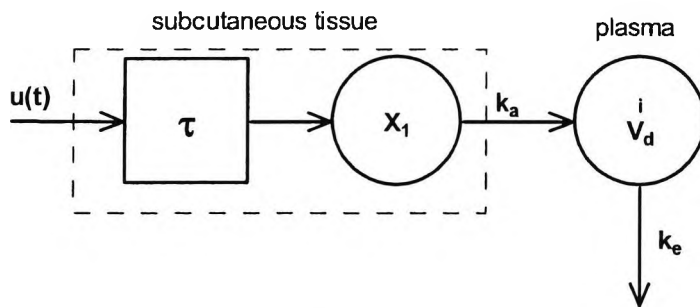


Figure 3.7 A model of insulin absorption kinetics proposed by Kobayashi et al (80); x_1 is the amount of insulin in the SC depot, i is plasma insulin, V_d is the distribution volume, k_a is the absorption rate constant, k_e is the elimination rate constant, τ is the time delay and $u(t)$ is the rate of insulin administration.

◇ Kraegen et al (81) proposed a three-compartment model (see Figure 3.8).

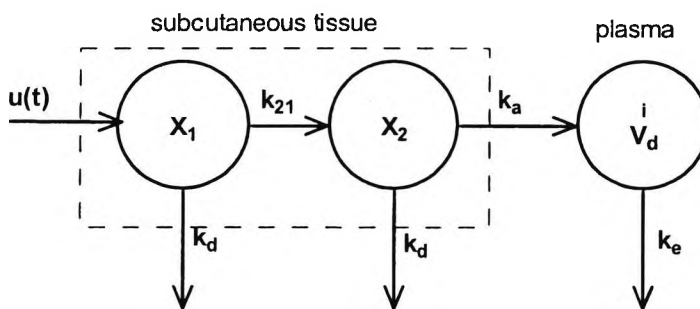


Figure 3.8 Model of subcutaneous insulin absorption proposed by Kraegen (81); x_1 and x_2 are insulin masses in each of the two SC compartments (accessible and nonaccessible), i is plasma insulin concentration, V_d is the distribution volume of insulin, k_{21} and k_a are the transport rate constants describing transport of insulin between SC compartments, and SC compartment and plasma, respectively, k_e is the elimination rate constant, and k_d is the degradation rate constant from the respective SC pool.

The model is described by the following equations:

$$dx_1 / dt = -(k_d + k_{21})x_1(t) + u(t)$$

$$dx_2 / dt = k_{21}x_1 - (k_d + k_a)x_2(t)$$

$$di / dt = \frac{k_a}{V_d} x_2(t) - k_e i(t)$$

The authors fitted the above model to the insulin profiles of normal subjects with a suppressed endogenous insulin secretion. Similarly to Kobayashi, Kraegen also used short acting insulin (Actrapid MC, 40 U/ml). In his conclusion he assessed the model fit as good, and the SC insulin degradation as low (rate constant < 10%/h) regardless of the input profile.

- ◇ Puckett *et al* (82) also proposed a three-compartment model that was identified on diabetic patient data using regular insulin given as a bolus. The SC insulin degradation was assumed to take place at the injection site, not in the SC tissue itself (see Figure 3.9).

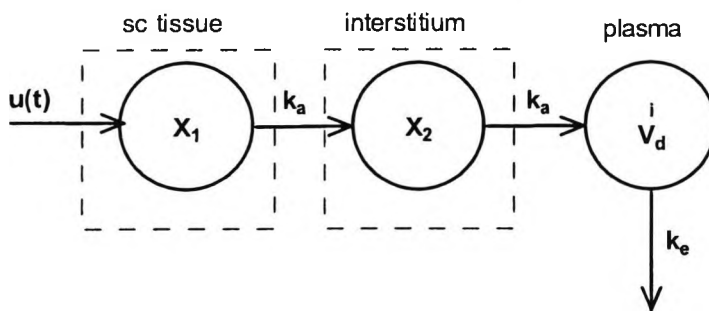


Figure 3.9 Model of subcutaneous insulin absorption proposed by Puckett (82); x_1 and x_2 are insulin masses in the SC tissue and the interstitial fluid, respectively, i is the plasma insulin concentration, V_d is the distribution volume of insulin, k_a are the absorption rate constant from the SC compartments to the interstitial fluid, and the interstitial fluid to plasma, respectively, k_e is the elimination rate constant.

The following equations describe this model:

$$\begin{aligned} dx_1 / dt &= -k_a x_1(t) & x_1(0) &= \alpha D / V_d \\ dx_2 / dt &= -k_a [x_1(t) - x_2(t)] & x_2(0) &= 0 \\ di / dt &= k_a x_2(t) - k_e i(t) \end{aligned}$$

where α is the effectiveness factor which accounts for insulin degradation at the injection site.

To make the model *a priori* uniquely identifiable, the authors lumped α and V_d together in the aggregated parameter $\beta = V_d / \alpha$ and assumed the known plasma insulin removal constant k_e .

- ◇ Shimoda *et al* (83) developed a three-compartment model of a soluble and monomeric insulin analogue, to be used in the artificial pancreas (see Figure 3.10).

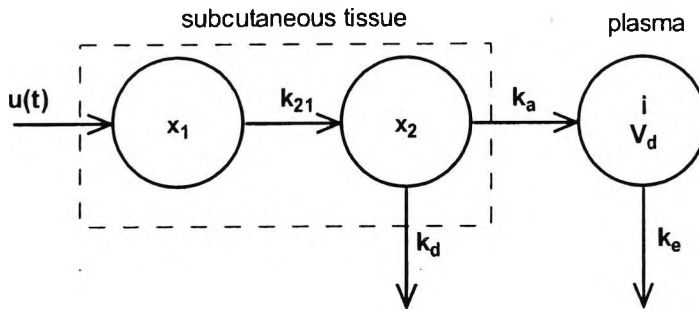


Figure 3.10 A mathematical model for SC insulin absorption proposed by Shimoda and colleagues (83); k_d is the degradation rate constant in the SC tissue, other symbols as in Figure 3.8.

The model is described by the following equations:

$$\begin{aligned} dx_1 / dt &= -k_{21}x_1(t) + u(t) \\ dx_2 / dt &= -k_{21}x_1(t) - (k_d + k_a)x_2(t) \\ di / dt &= \frac{k_a}{V_d}x_2(t) - k_e i(t) \end{aligned}$$

This model was fitted on 3 hour data of ten subjects with T1DM following a subcutaneous injection of 12 U kg^{-1} of regular insulin (Humulin R) or rapid acting insulin analogue (insulin lispro) diluted to the concentration of 4 U ml^{-1} . Contradictory to Kraegen, the degradation rate constant in the subcutaneous tissue estimated from this model is not negligible for either insulin type (see Table 3.2).

3.6.2 Noncompartmental models

- ◇ Berger (86) proposed a model based on an empirically derived logistic equation of insulin absorption for different insulin preparations.

The percentage of injected insulin remaining at the absorption site is expressed as:

$$\begin{aligned} A\%(t) &= 100 - \frac{100t^s}{(T_{50})^s + t^s} \\ T_{50}(D) &= aD + b \end{aligned}$$

where T_{50} is the time interval to reach a 50% absorption of the injected insulin, D is the insulin dose, a and b assume different values for each insulin preparation, and s characterises the absorption rate of various insulin preparations.

The absorption velocity is the time derivative of $A(t)$ multiplied by the dose. It is hence the insulin input flux into plasma:

$$\frac{dA}{dt} D = \frac{t^{s-1} s T_{50}^s D}{(T_{50}^s + t^s)^2}$$

Hence, the plasma insulin concentration can be expressed as:

$$\frac{di}{dt} = -k_e i(t) + \frac{dA}{dt} \frac{D}{V_d} = -k_e i(t) + \frac{t^{s-1} s T_{50}^s D}{V_d (T_{50}^s + t^s)^2}$$

The model was used by authors to describe the dynamics of regular and NPH (neutral protamine Hagedorn) insulin preparations. Parameter values for these two insulin types are shown in Table 3.2.

- ◇ Mosekilde *et al* (87) formulated a mathematical model of SC absorption of soluble insulin in terms of well-established physical and pharmacokinetic principles, i.e. the diffusion, the equilibration between different multimeric (hexameric and dimeric) forms of soluble insulin, and either reversible binding of insulin molecules in the tissue or precipitation in situ of polymerised insulin.

Figure 3.11 gives an overview of this model, which is described by the following set of three coupled partial differential equations:

$$\begin{aligned} \frac{\partial C_H}{\partial t} &= P(QC_D^3 - C_H) + D\nabla^2 C_H \\ \frac{\partial C_D}{\partial t} &= -P(QC_D^3 - C_H) + D\nabla^2 C_D - BC_D - SC_D(C - C_B) + \frac{C_B}{T} \\ \frac{\partial C_B}{\partial t} &= SC_D(C - C_B) - \frac{C_B}{T} \end{aligned}$$

where C_H , C_D , and C_B denote the concentrations of hexameric, dimeric, and bound insulin, respectively, Q is the chemical equilibrium constant, C is the binding capacity per unit tissue volume, P is a rate constant, S is a binding rate constant, and T is an average life time for insulin in its bound state; terms involving the Laplacian operator ∇^2 describe the diffusion of free insulin, terms

involving the rate constant P describe transformations between hexameric and dimeric insulin, terms involving the rate constant S describe the capture of insulin in the tissue, and terms involving the time constant T describe the release of bound insulin.

The above equations are solved numerically by dividing the subcutaneous layer into a number of rings, centred around the injection site.

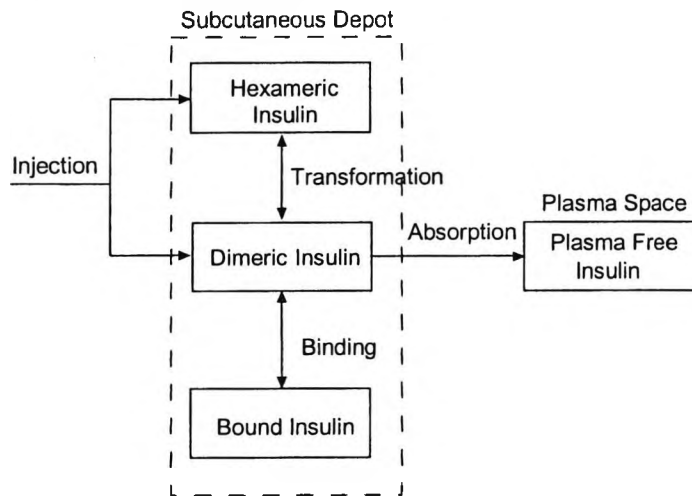


Figure 3.11 An overview of the model by Mosekilde of subcutaneous absorption of soluble insulin; adapted from (87).

- ◇ Trajanoski *et al* (85) developed a simplified and more practical model to one proposed by Mosekilde and colleagues (87) while also taking into account the new monomeric insulin preparations.

The following assumptions were made:

1. insulin binding in the SC tissue is negligible
2. the size of the initial depot equals the injected volume
3. the injected volume builds up a spherical homogenous depot which is symmetrically widened through diffusion of insulin into the tissue
4. at pharmaceutical concentrations of soluble insulin the predominant association state is hexamer
5. only dimers are absorbed from the SC tissue into plasma (88)

6. monomeric insulin analogues have reduced tendency to self-associate and their mean association state is monomer (89)

The model is described by the following equations:

$$\frac{\partial C_H}{\partial t} = P(QC_D^3 - C_H) + D_H \nabla^2 C_H$$

$$\frac{\partial C_D}{\partial t} = -P(QC_D^3 - C_H) + D_H \nabla^2 C_D - B_D C_D$$

$$\frac{\partial C_M}{\partial t} = D_M \nabla^2 C_M - B_M C_M$$

where C_M is the concentration of monomeric insulin in the SC depot, D_H and D_M are diffusion constants for soluble and monomeric insulin, respectively, and B_D and B_M are absorption rate constants for dimeric and monomeric insulin, respectively; other symbols as in the previous model by Mosekilde.

Chapter 4 Modelling Glucose Kinetics over Twenty Eight Hours in Subjects with Type 1 Diabetes

4.1 Introduction

A model of glucose regulatory system was previously developed by Hovorka *et al* (55). The model linked intravenous insulin concentration to the plasma glucose concentration during basal conditions and during an intravenous glucose tolerance test. It was identified using a tracer study in normal subjects.

This model is adopted in the present work and is extended to include models of insulin absorption, insulin kinetics and gut absorption. The aim of this study is to evaluate the model feasibility to represent glucose excursions over 24 hours in subjects with T1DM treated by CSII. The data comes from clinical trials designed to test the AP algorithm. An SC-IV approach, i.e. subcutaneous insulin delivery and intravenous glucose measurements, was adopted in these trials as a reliable and accurate subcutaneous glucose sensor was not available.

The secondary objective of this study is to generate the model parameters for individual subjects, which could be used in the AP simulator to represent a 'virtual' set of simulated subjects.

4.2 Subjects and Methods

4.2.1 Subjects and experimental protocol

Twelve subjects with type 1 diabetes (duration of diabetes 24 ± 11 years), eight men and 4 women aged 21 to 64 years participated in this study. Subjects were all treated by CSII with short acting insulin (basal/prandial insulin requirements $20 \pm 6 / 22 \pm 6$ IU/day; mean \pm SD). All subjects had normal or near normal body weight (BMI 24 ± 2 kg/m²) and their diabetes was well controlled (HbA_{1c} $7.3 \pm 0.9\%$).

The study was a single-centre trial which took place at the University Hospital, University of Graz, Austria. The study was approved by the local ethics committee and all subjects signed an informed consent.

Basal insulin infusion profile was optimised prior to the study and the subjects not using the short acting insulin analogue lispro were switched to this insulin. The subjects were admitted to the clinic at 13:30 and remained there until 22:00 on the following day. At the start of the study the patient's own insulin pump was replaced with the "study day pump" and the infusion of insulin lispro (Humalog®, Eli Lilly) was started according to the subjects optimised insulin infusion profile. A cannula for blood sampling was inserted into the vein of the hand and was kept patent with saline. Another cannula for intravenous administration of insulin and glucose boluses during the normalisation period was inserted into the vein of the other hand.

At the start of the study blood glucose was normalised to a level between 5.5 to 6.6mmol/L using intravenous insulin or glucose as appropriate. During the clamp period blood samples were taken as needed. After 17:00 intravenous glucose and insulin administration was stopped. From then on blood samples for glucose measurement were taken every 15min. Plasma glucose was measured in duplicate with Beckman Glucose Analyser 2 (Beckman Instruments, Fullerton, CA) and a CV < 1.5% of the intra-assay measurement error. The insulin infusion rates were adjusted every 15min in response to the blood glucose values. Blood samples for plasma insulin were collected every 30min from 14:00. In case of hypoglycaemia (PG < 3.3mmol/L) oral glucose consisting of 10g of carbohydrates was given.

Subjects were given their first meal, dinner one, at 18:00. On the second study day they were given breakfast at 8:00, lunch at 14:00 and dinner two at 18:00. Depending on their total daily calorie intake patients were assigned to one of the four menu groups (see Appendix). Prandial boli of insulin lispro were administered immediately before each meal using the insulin pump.

4.2.2 Model of glucoregulation

Data analysis was based on the model of the glucose regulatory system as in (55).

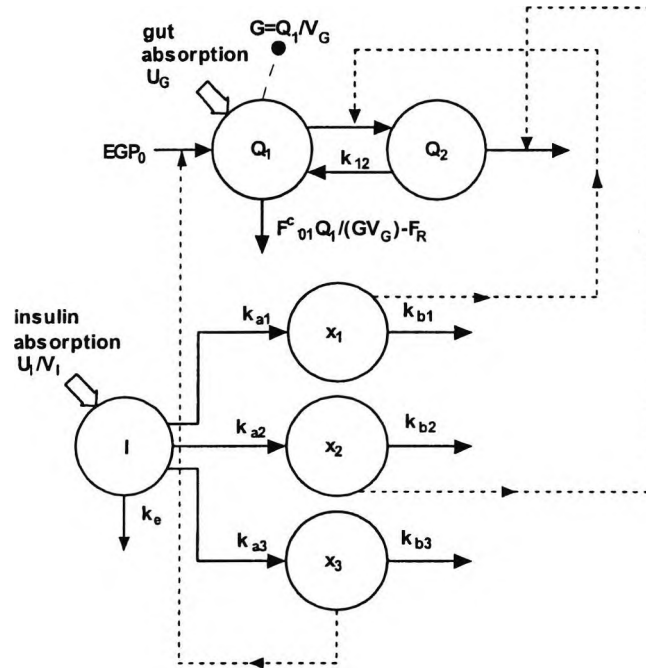


Figure 4.1 Structure of model of glucoregulation from (55).

The model shown in Figure 4.1 represents the input-output relationship between plasma insulin and plasma glucose concentrations. Intravenous glucose infusion and meal ingestion are additional inputs.

The explanation of symbols is as follows: Q_1 and Q_2 represent the masses of glucose in accessible and nonaccessible compartments (mmol), k_{12} represents the transfer rate constant from the nonaccessible to the accessible compartment (min^{-1}), V_G is the distribution volume of glucose in the accessible compartment (L), G is the measured glucose concentration (mmol L^{-1}), EGP_0 represents endogenous glucose production (EGP) extrapolated to the zero insulin concentration (mmol min^{-1}), U_G represents gut absorption rate (mmol min^{-1}), F_{01}^c is the total non-insulin dependent glucose flux corrected for ambient glucose concentration (mmol min^{-1}), F_R is the renal glucose clearance (mmol L^{-1} per min), I is the plasma insulin concentration (mU L^{-1}), x_1 , x_2 and x_3

represent the remote effect of insulin on glucose distribution, disposal and endogenous glucose production, respectively, k_{ai} , $i=1,2,3$, represent activation rate constants (min^{-1}), and k_{bi} , $i=1,2$ represent deactivation rate constants (min^{-2} per mU L^{-1}), k_{b3} represents deactivation rate constant for the insulin effect on endogenous glucose production (min^{-1} per mU L^{-1}), V_I represents the volume of distribution of plasma insulin (L), U_I represents the insulin mass in plasma (mU), k_e is the elimination rate constant for plasma insulin (min^{-1}).

The model consists of a glucose subsystem (glucose absorption, distribution, and disposal) and insulin action subsystem (insulin action on glucose transport/distribution, disposal and endogenous production). For the sake of clarity, the differential equations describing the above model are given separately for each of its subsystems.

4.2.2.1 Glucose subsystem

The glucose subsystem is represented by a two-compartment model of glucose kinetics and described by the following equations:

$$\begin{aligned} \frac{dQ_1(t)}{dt} &= - \left[\frac{F_{01}^c}{V_G G(t)} + x_1(t) \right] Q_1(t) + k_{12} Q_2(t) - F_R + U_G(t) + EGP_0 [1 - x_3(t)] \quad Q_1(0) = Q_{1,0} \\ \frac{dQ_2(t)}{dt} &= x_1(t) Q_1(t) - [k_{12} + x_2(t)] Q_2(t) \quad Q_2(0) = Q_{2,0} \\ y(t) &= G(t) = Q_1(t) / V_G \end{aligned}$$

where $Q_{1,0}$ and $Q_{2,0}$ are masses of glucose in the accessible and nonaccessible glucose compartments, respectively; other terms as defined in Figure 4.1.

The total non-insulin dependent glucose flux represented by F_{01}^c is defined as follows:

$$F_{01}^c = \begin{cases} F_{01}, & \text{if } G \geq 4.5 \text{ mmol/L} \\ F_{01} G (9 - G) / (4.5)^2, & \text{otherwise} \end{cases}$$

F_R is the renal glucose clearance above the glucose threshold of 9mmol/L:

$$F_R = \begin{cases} 0.003(G-9)V_G, & \text{if } G \geq 9\text{mmol/L} \\ 0, & \text{otherwise} \end{cases}$$

4.2.2.2 Insulin action subsystem

The model represents three actions of insulin on glucose kinetics. These are the remote effects on glucose distribution/transport, glucose disposal and endogenous glucose production:

$$\begin{aligned} \frac{dx_1}{dt} &= -k_{b1}x_1(t) + S_{IT}k_{b1}k_{osc}I(t) & x_1(0) &= 0 \\ \frac{dx_2}{dt} &= -k_{b2}x_2(t) + S_{ID}k_{b2}k_{osc}I(t) & x_2(0) &= 0 \\ \frac{dx_3}{dt} &= -k_{b3}x_3(t) + S_{IE}k_{b3}k_{osc}I(t) & x_3(0) &= 0 \end{aligned}$$

where $S_{IT}=k_{a1}/k_{b1}$, $S_{ID}=k_{a2}/k_{b2}$, $S_{IE}=k_{a3}/k_{b3}$ are insulin sensitivities for transport, distribution and endogenous glucose production, k_{osc} represents the oscillatory component defined in section 4.2.5.2, the remaining symbols are described in section 4.2.2.

4.2.3 Gut absorption model

Postprandial glucose excursions are determined by the rate of glucose absorption from the alimentary canal represented in Figure 4.1 by U_G . The physiology of the gut absorption model is represented here by a simple two-compartment model with identical transfer rates (see Figure 4.2). This model was shown to be adequate in representing the glucose rate of appearance in plasma from the gut (90). For dinner one the model is described by the following equations:

$$\begin{aligned} \frac{dG_{1,D1}(t)}{dt} &= -\frac{1}{t_{max,D1}}G_{1,D1}(t) + \delta(t_{D1})B_{\infty,D1}D_{D1} \\ \frac{dG_{2,D1}(t)}{dt} &= \frac{1}{t_{max,D1}}G_{1,D1}(t) - \frac{1}{t_{max,D1}}G_{2,D1}(t) \\ G_{1,D1}(0) &= 0 \end{aligned}$$

where $G_{1,D1}$ and $G_{2,D1}$ are the glucose masses in the accessible and nonaccessible compartments corresponding to the absorption of dinner one (mmol), $t_{max,D1}$ is the time-of-maximum appearance rate of glucose in the accessible compartment (min), δ represents the Dirac function, t_{D1} is time of

dinner one (min), D_{D1} is the amount of carbohydrate ingested at dinner one (g), $B_{io,D1}$ is the carbohydrate bioavailability of dinner one (unitless).

The models representing gut absorption of breakfast, lunch and dinner two are similar giving rise to the corresponding parameters: $G_{1,B}$, $G_{2,B}$, $t_{max,B}$, t_B , D_B , $B_{io,B}$ for breakfast, $G_{1,L}$, $G_{2,L}$, $t_{max,L}$, t_L , D_L , $B_{io,L}$ for lunch, and $G_{1,D2}$, $G_{2,D2}$, $t_{max,D2}$, t_{D2} , D_{D2} , $B_{io,D2}$ for dinner two.

U_G , the total glucose flux entering plasma, is obtained by summing absorption rates due to the four meals.

$$U_G(t) = \frac{G_{2,D1}(t)}{t_{max,D1}} + \frac{G_{2,B}(t)}{t_{max,B}} + \frac{G_{2,L}(t)}{t_{max,L}} + \frac{G_{2,D2}(t)}{t_{max,D2}}$$

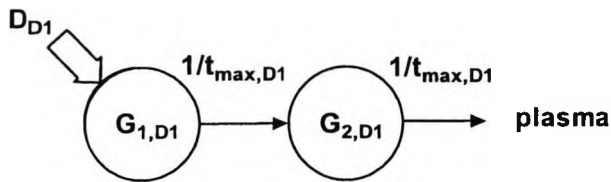


Figure 4.2 Structure of the gut absorption model for dinner one.

4.2.4 Insulin absorption model

To reduce the complexity of the final model we represented insulin lispro SC absorption kinetics as a simple three-compartment model. The previously validated model (see Chapter 5) of structure shown in Figure 4.3 is described by the following equations:

$$\frac{dS_1(t)}{dt} = u(t) - k_a S_1(t)$$

$$\frac{dS_2(t)}{dt} = k_a S_1(t) - k_a S_2(t)$$

$$\frac{dI}{dt} = \frac{k_a S_2(t)}{V_I} - k_e I(t)$$

where S_1 and S_2 represent insulin masses in the accessible and nonaccessible compartments, respectively (mU), u represents administration (bolus and infusion) of insulin lispro, k_a represents insulin lispro absorption

rate constant (min^{-1}), V_I is the volume of distribution of insulin lispro (L), I is the insulin concentration in plasma (mU/L), k_e represents the fractional elimination rate from plasma (min^{-1}).

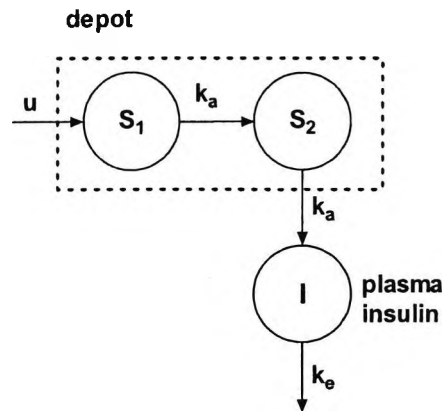


Figure 4.3 Structure of the insulin absorption model.

4.2.5 Model constants and parameters

The model quantities were divided into model constants and model parameters with the objective of reducing the number of parameters while retaining the ability to represent the wide range of glucose excursions seen in subjects with T1DM during physiological conditions.

4.2.5.1 Model constants

The model constants were those quantities which were either *a priori* non-identifiable or were unlikely to be identifiable from the data (*a posteriori* non-identifiability). The model constants with the source their values were taken from are given in Table 4.1 below.

Table 4.1 Model constants

Symbol	Quantity	Value	Source
k_{12}	transfer rate constant	0.065min^{-1}	(55)
k_{a1}	activation rate	0.006min^{-1}	(55)
k_{a2}	activation rate	0.07min^{-1}	(55)
k_{a3}	activation rate	0.03min^{-1}	(55)
k_e	elimination rate from plasma	0.1408min^{-1}	(91)
V_I	Insulin distribution volume	0.12L kg^{-1}	(91)

4.2.5.2 Model parameters

The model parameters are listed in Table 4.2.

Initial investigations with time invariant parameters were not successful and the analysis of the results (data not shown) and physiological considerations suggested the adoption of time variant insulin sensitivities. Sinusoidal oscillations were superimposed on the three insulin sensitivities S_{IT} , S_{ID} and S_{IE} . A combination of two sinusoids was chosen with the following parameterisation:

$$k_{acc} = 1 + amp_1 \sin 2\pi \left(\frac{t}{cycle} - phase_1 \times cycle \right) + amp_2 \sin 2\pi \left(\frac{t}{cycle + \Delta cycle} - phase_2 \times (cycle + \Delta cycle) \right)$$

where t represents time (min). The remaining parameters are described in Table 4.3.

Table 4.2 Model parameters

Symbol	Quantity
$B_{io,D1}, B_{io,B}, B_{io,L}, B_{io,D2}$	CHO bioavailability of dinner one, breakfast, lunch and dinner two, respectively
$t_{max,D1}, t_{max,B}, t_{max,L}, t_{max,D2}$	time-to-maximum of CHO absorption for dinner one, breakfast, lunch and dinner two
EGP_0	EGP extrapolated to zero insulin
$*S_{IT}$	insulin sensitivity of glucose transport
$*S_{ID}$	insulin sensitivity of glucose disposal
$*S_{IE}$	insulin sensitivity of EGP
F_{01}	non-insulin dependent glucose flux
V_G	glucose distribution volume
k_a	absorption rate of SC injected insulin lispro
$Q_{1,0}, Q_{2,0}$	glucose masses in accessible and nonaccessible compartments at time zero

*Alternative parameterisation: $S_{IT}=k_{a1}/k_{b1}$, $S_{ID}=k_{a2}/k_{b2}$, and $S_{IE}=k_{a3}/k_{b3}$

Table 4.3 Parameters describing time variation of insulin sensitivities

Symbol	Quantity
cycle	cycle of the first sinusoid
Δ cycle	cycle difference of the second sinusoid
amp ₁	fractional amplitude of the first sinusoid
amp ₂	fractional amplitude of the second sinusoid
phase ₁	phase of the first sinusoid expressed as a fraction of cycle of the first sinusoid
phase ₂	phase of the second sinusoid expressed as a fraction of cycle of the second sinusoid

4.2.6 Parameter estimation

The model parameters were estimated using the ITS technique implemented in SAAM II Population Kinetics v 1.01 software package (SAAM Institute, Seattle, WA, USA). In each iteration, the parameters were estimated employing a nonlinear, weighted, least-squares algorithm with an empirical Bayesian term. Prior to estimation the parameters were log-transformed with

the exception of amp_1 , amp_2 , $phase_1$, $phase_2$ and $\Delta cycle$. The distribution of these parameters was assessed as normal using Blom's proportional estimation formula in preliminary investigations (data not shown). This was done to assure non-negativity and to correct for skewed distribution of the parameters.

Insulin infusion rate, insulin boluses and the carbohydrate intake were the model input. Plasma glucose was the model output. The parameter estimation started at 600min in order to avoid the multiple disturbances during the normalisation period and to achieve initial conditions of the insulin action model.

The measurement error was assumed at 1.5% and the absolute weighting method in SAAM II was adopted. The weight was defined as the reciprocal of the square of the measurement error.

The precision of parameter estimates was obtained from the inverse of the Fisher information matrix (23).

4.2.7 Model identification and validation

The validity of this model was assessed on the basis of physiological feasibility of its parameter estimates, posterior identifiability, and the distribution of weighted residuals. Posterior identifiability was assessed on the basis of the precision of parameter estimates ($CV < 100\%$).

4.2.8 Statistical analysis

The significance of the change of carbohydrate bioavailability and time-to-maximum absorption was established using a two-way analysis of variance (ANOVA) with effects due to time instance and subject. Dinner one (ingestion at 360min) was excluded from this and any further analysis as it is estimated with lower confidence (glucose data were zero weighted up to 600min).

The runs test was used to test for the randomness of the weighted residuals. The Bonferroni correction was applied to the runs test results to correct for multiple comparisons.

4.3 Results

4.3.1 Plasma glucose and insulin

Figure 4.4 shows mean plasma glucose over the course of the experiment. The range of plasma glucose concentration and insulin infusion rate was 3.1 to 18.0mmol/L and 0 to 4.0U/h, respectively. The insulin bolus was $3.5 \pm 2.3U$ (0.3 -10U); mean \pm SD (range).

4.3.2 Model identification and validation

Parameter estimates with their precision expressed as a CV are shown in Table 4.4. The parameters describing time variations of insulin sensitivities are shown in Table 4.5.

The weighted residuals, shown in Figure 4.5, passed the Runs test in 83% of cases.

Figure 4.6 shows model fits for all twelve subjects, whereas Figure 4.7 the oscillation patterns of insulin sensitivities for all subjects.

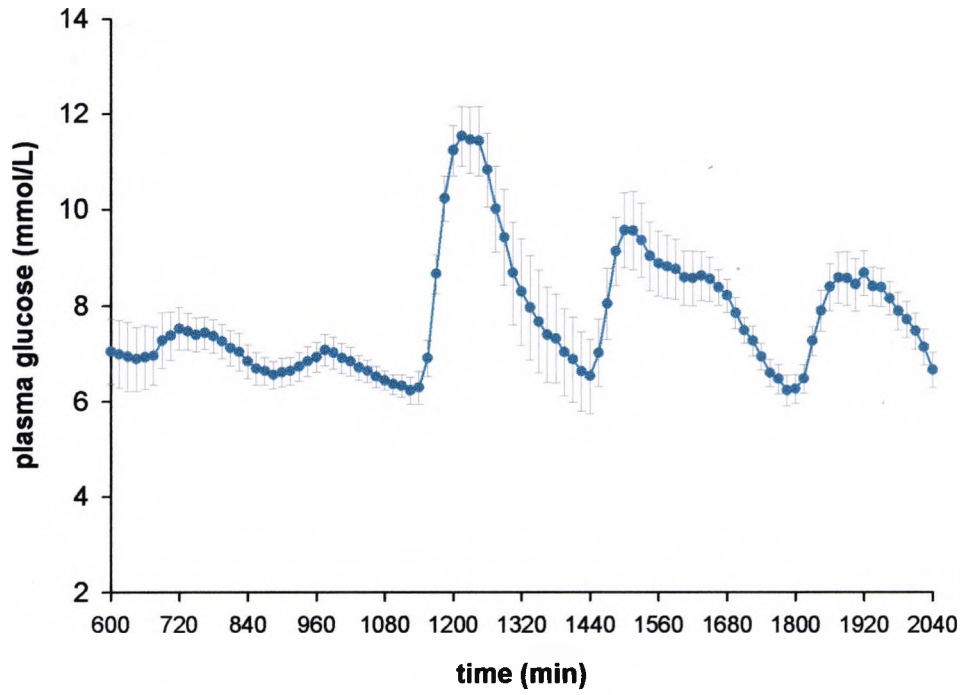


Figure 4.4 Plasma glucose; values are mean \pm SE, $n=12$.

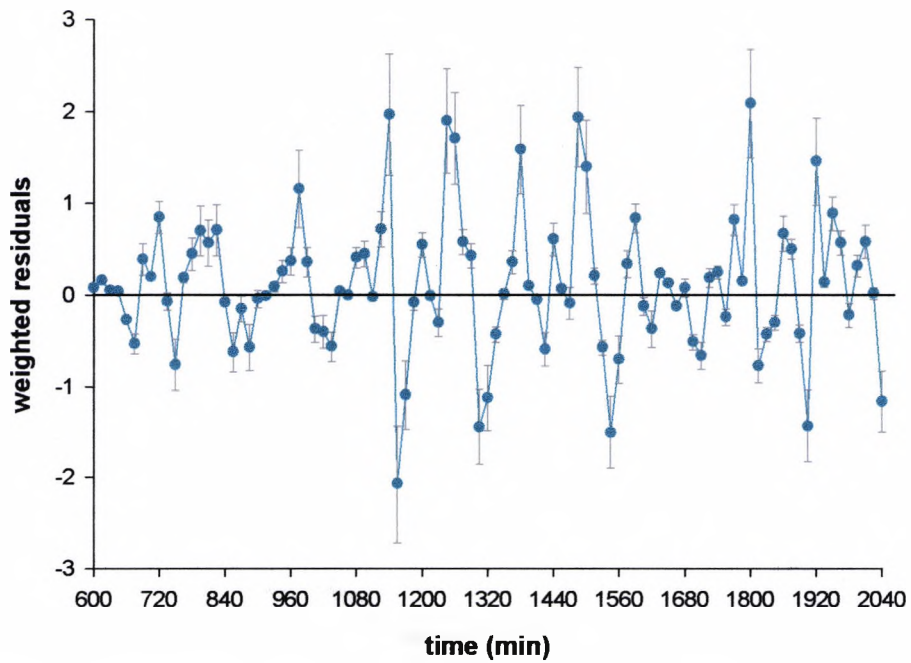


Figure 4.5 Weighted residuals; values are mean \pm SE, $n=12$.

Table 4.4 Parameter estimates for individual subjects.

Subject	$B_{io,D1}$ (unitless)	$B_{io,B}$ (unitless)	$B_{io,L}$ (unitless)	$B_{io,D2}$ (unitless)	$t_{max,D1}$ (min)	$t_{max,B}$ (min)	$t_{max,L}$ (min)	$t_{max,D2}$ (min)
1	0.66 (41)*	0.59 (13)	0.82 (15)	1.14 (15)	64 (15)	32 (10)	40 (8)	71 (10)
2	2.50 (17)	0.70 (9)	0.82 (9)	0.79 (10)	68 (8)	41 (3)	50 (4)	42 (3)
3	0.57 (15)	0.59 (11)	1.15 (11)	0.76 (11)	76 (9)	102 (6)	104 (4)	85 (3)
4	0.66 (16)	0.77 (14)	1.07 (15)	0.98 (14)	110 (10)	64 (12)	65 (9)	76 (9)
5	1.08 (31)	1.87 (16)	0.54 (16)	1.14 (15)	331 (20)	82 (7)	100 (12)	70 (10)
6	0.89 (45)	1.03 (10)	1.13 (11)	0.94 (10)	31 (45)	27 (6)	53 (2)	42 (4)
7	0.54 (17)	0.67 (6)	0.91 (6)	1.25 (9)	215 (10)	33 (4)	60 (3)	55 (5)
8	0.86 (45)	0.85 (11)	0.66 (15)	1.07 (10)	22 (98)	47 (3)	38 (5)	108 (6)
9	0.95 (17)	1.10 (12)	1.05 (10)	0.72 (12)	190 (11)	73 (4)	46 (4)	48 (5)
10	0.54 (13)	0.52 (14)	0.73 (13)	1.72 (15)	23 (6)	69 (6)	63 (3)	194 (14)
11	0.98 (18)	0.57 (11)	0.72 (11)	1.01 (11)	352 (8)	33 (4)	61 (2)	69 (3)
12	1.51 (16)	0.85 (14)	0.85 (14)	0.95 (14)	257 (6)	82 (6)	110 (7)	109 (8)

*Precision of parameter estimate expressed as a fractional standard deviation (%)

Table 4.4 (cont.) Parameter estimates for individual subjects.

Subject	EGP ₀ (10 ⁻² x mmol min ⁻¹)	S _{IT} (10 ⁻⁴ x min ⁻¹ per mU L ⁻¹)	S _{ID}	S _{IE} (10 ⁻⁴ x mU L ⁻¹)	F ₀₁ (10 ⁻² x mmol min ⁻¹)	V _G (L kg ⁻¹)	k _a (10 ⁻² x min ⁻¹)
1	1.73 (11)*	42 (5)	338 (3)	1 (5)	1.4 (13)	0.17 (24)	1.75 (1)
2	1.54 (7)	1 (73)	32 (17)	734 (3)	1.0 (8)	0.11 (12)	4.65 (2)
3	1.96 (10)	611 (42)	42 (7)	206 (12)	0.9 (18)	0.03 (18)	0.99 (1)
4	1.66 (12)	6 (31)	21 (39)	44 (82)	1.5 (13)	0.9 (27)	1.75 (2)
5	1.71 (11)	14 (30)	124 (27)	53 (82)	0.9 (30)	0.04 (28)	1.24 (2)
6	1.69 (10)	2 (17)	21 (22)	494 (4)	0.3 (23)	0.23 (16)	3.11 (2)
7	2.50 (4)	1 (128)	4 (34)	277 (4)	2.0 (4)	0.13 (8)	2.84 (1)
8	1.78 (10)	10 (37)	5 (19)	403 (7)	1.1 (13)	0.15 (12)	3.67 (1)
9	1.78 (10)	267 (24)	5 (9)	156 (6)	0.5 (30)	0.14 (12)	5.41 (1)
10	1.71 (11)	11 (17)	42 (19)	25 (54)	1.3 (14)	0.6 (20)	2.28 (1)
11	1.85 (10)	7 (31)	6 (17)	339 (4)	1.3 (12)	0.20 (10)	4.81 (1)
12	1.73 (12)	93 (41)	12 (13)	70 (32)	1.8 (12)	0.06 (21)	2.27 (1)

*Precision of parameter estimate expressed as a fractional standard deviation (%)

Table 4.5 Parameter estimates describing time variation of insulin sensitivities.

Subject	cycle (min)	Δ cycle (min)	amp ₁ (unitless)	amp ₂ (unitless)	phase ₁ (unitless)	phase ₂ (unitless)
1	231 (1)*	59 (14)	0.27 (15)	0.18 (14)	0.20 (36)	0.58 (14)
2	286 (1)	218 (5)	0.10 (18)	0.31 (5)	0.21 (37)	0.66 (6)
3	223 (0)	103 (3)	0.19 (16)	0.09 (11)	-0.55 (4)	-0.47 (8)
4	191 (1)	172 (2)	0.13 (18)	0.17 (24)	0.35 (23)	0.86 (6)
5	383 (5)	99 (30)	0.08 (38)	0.22 (17)	0.55 (31)	0.32 (24)
6	168 (1)	71 (3)	0.28 (10)	0.22 (11)	-0.31 (12)	0.20 (20)
7	182 (1)	204 (4)	0.18 (9)	0.16 (7)	0.94 (6)	-0.35 (14)
8	247 (0)	368 (6)	0.38 (5)	0.15 (7)	0.61 (4)	0.00 (203)
9	265 (1)	233 (2)	0.19 (8)	0.32 (6)	-0.56 (8)	0.57 (4)
10	336 (1)	192 (4)	0.28 (3)	0.31 (4)	-0.20 (15)	-0.52 (0)
11	185 (1)	11 (20)	0.44 (15)	0.34 (18)	0.53 (9)	0.57 (11)
12	149 (0)	93 (4)	0.24 (10)	0.08 (17)	-1.00 (4)	0.22 (42)

*Precision of parameter estimate expressed as a CV (%)

4.3.3 Model parameters

The population parameters and the parameters describing the oscillatory pattern of insulin sensitivities are summarised in Tables 4.6 and 4.7, respectively.

The normally distributed parameters are expressed as a mean and standard deviation, whereas log-normally distributed parameters are expressed as a mean and the inter-quartile range.

The carbohydrate bio-availability and time-to-maximum absorption were not significantly different for breakfast, lunch and dinner two with p values of 0.94 and 0.096, respectively. Dinner one was not taken into account in this comparison as the parameter estimation begun 4 hours later at 600min.

Table 4.6 Model parameters; values are mean (inter-quartile range), n=12.

Parameter	Population Mean
$B_{io,D1}$ (unitless)	0.88 (0.63 - 1.23)
$B_{io,B}$ (unitless)	0.79 (0.60 - 1.03)
$B_{io,L}$ (unitless)	0.85 (0.72 - 1.01)
$B_{io,D2}$ (unitless)	1.01 (0.85 - 1.21)
$t_{max,D1}$ (min)	97 (46 - 204)
$t_{max,B}$ (min)	52 (37 - 73)
$t_{max,L}$ (min)	62 (48 - 81)
$t_{max,D2}$ (min)	73 (53 - 101)
EGP_0 (10^{-2} x mmol min $^{-1}$)	1.79 (1.64 - 1.96)
S_{IT} (10^{-4} x min $^{-1}$ per mU L $^{-1}$)	17 (7 - 39)
S_{ID} (10^{-4} x min $^{-1}$ per mU L $^{-1}$)	11 (2 - 53)
S_{IE} (10^{-4} x mU L $^{-1}$)	170 (77 - 376)
F_{01} (10^{-2} x mmol min $^{-1}$)	1.04 (0.71 - 1.54)
V_G (L kg $^{-1}$)	0.10 (0.06 - 0.16)
k_a (10^{-2} x min $^{-1}$)	2.55 (1.71 - 3.80)

Table 4.7 Parameters describing the time variation of insulin sensitivities; values are mean (inter-quartile range) or mean \pm SD, n=12.

Parameter	Population Mean
cycle (min)	228 (185 - 282)
Δ cycle (min)	152 \pm 98
amp $_1$ (unitless)	0.23 \pm 0.11
amp $_2$ (unitless)	0.21 \pm 0.09
phase $_1$ (unitless)	0.06 \pm 0.59
phase $_2$ (unitless)	0.22 \pm 0.46

Chapter 4. Modelling Glucose Kinetics over Twenty Eight Hours in Subjects with Type 1 Diabetes

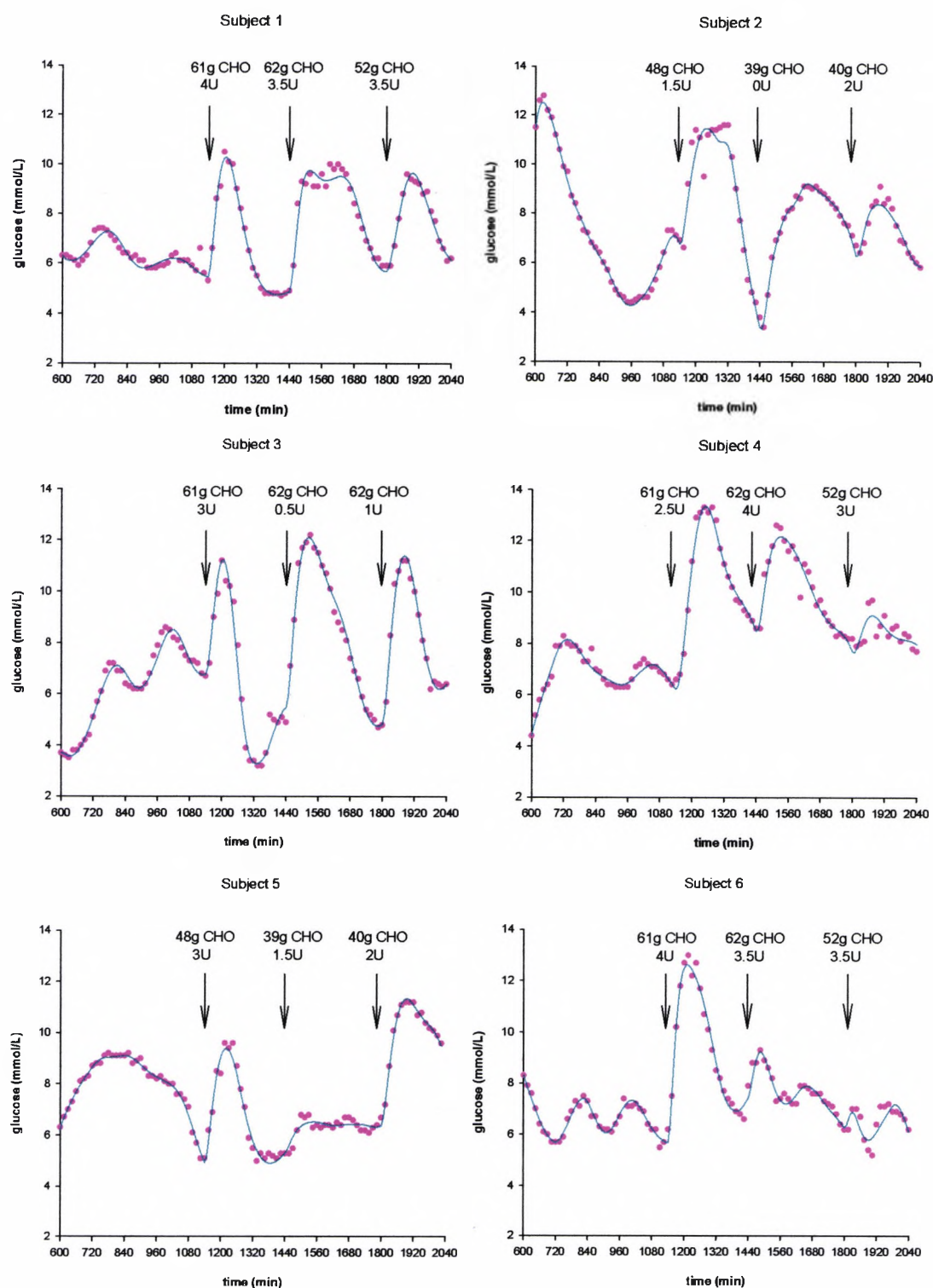


Figure 4.6 Model fits for individual subjects. Pink dot (•) represents measurement and green line (—) represents model fit.

Chapter 4. Modelling Glucose Kinetics over Twenty Eight Hours in Subjects with Type 1 Diabetes

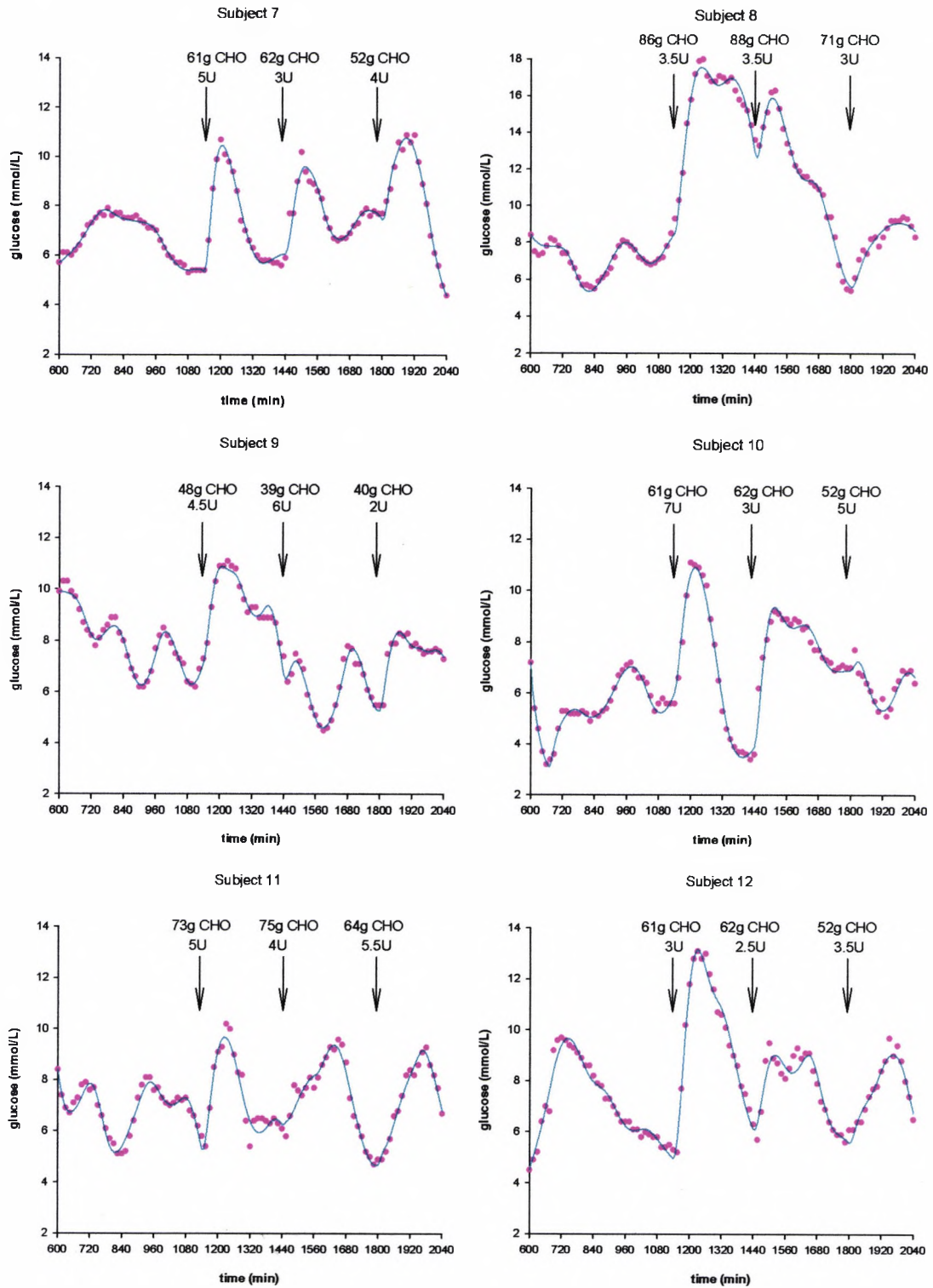


Figure 4.6 (cont.) Model fits for individual subjects. Pink dot (•) represents measurement and green line (—) represents model fit.

Chapter 4. Modelling Glucose Kinetics over Twenty Eight Hours in Subjects with Type 1 Diabetes

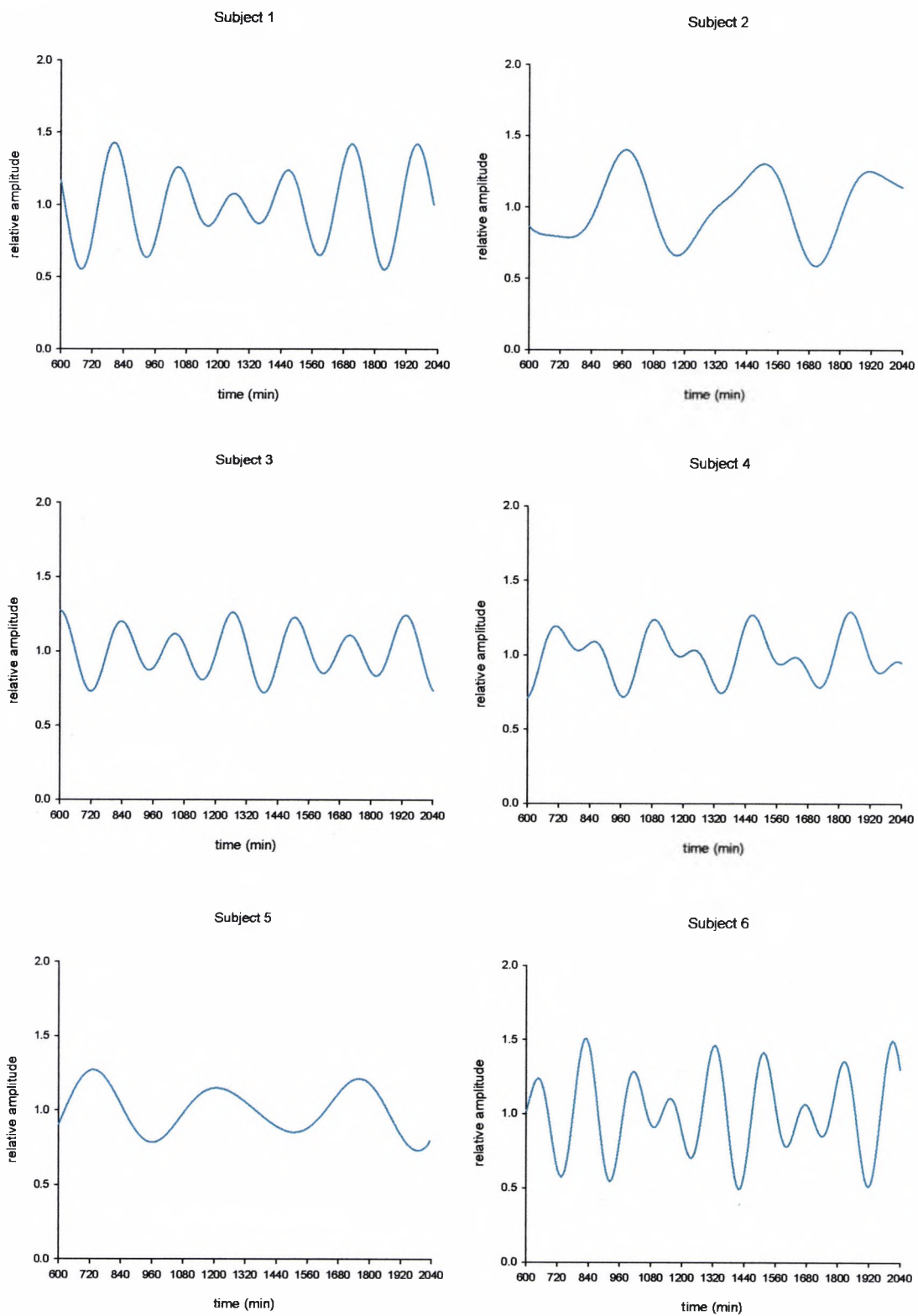


Figure 4.7 Oscillatory patterns of insulin sensitivities for individual subjects.

Chapter 4. Modelling Glucose Kinetics over Twenty Eight Hours in Subjects with Type 1 Diabetes

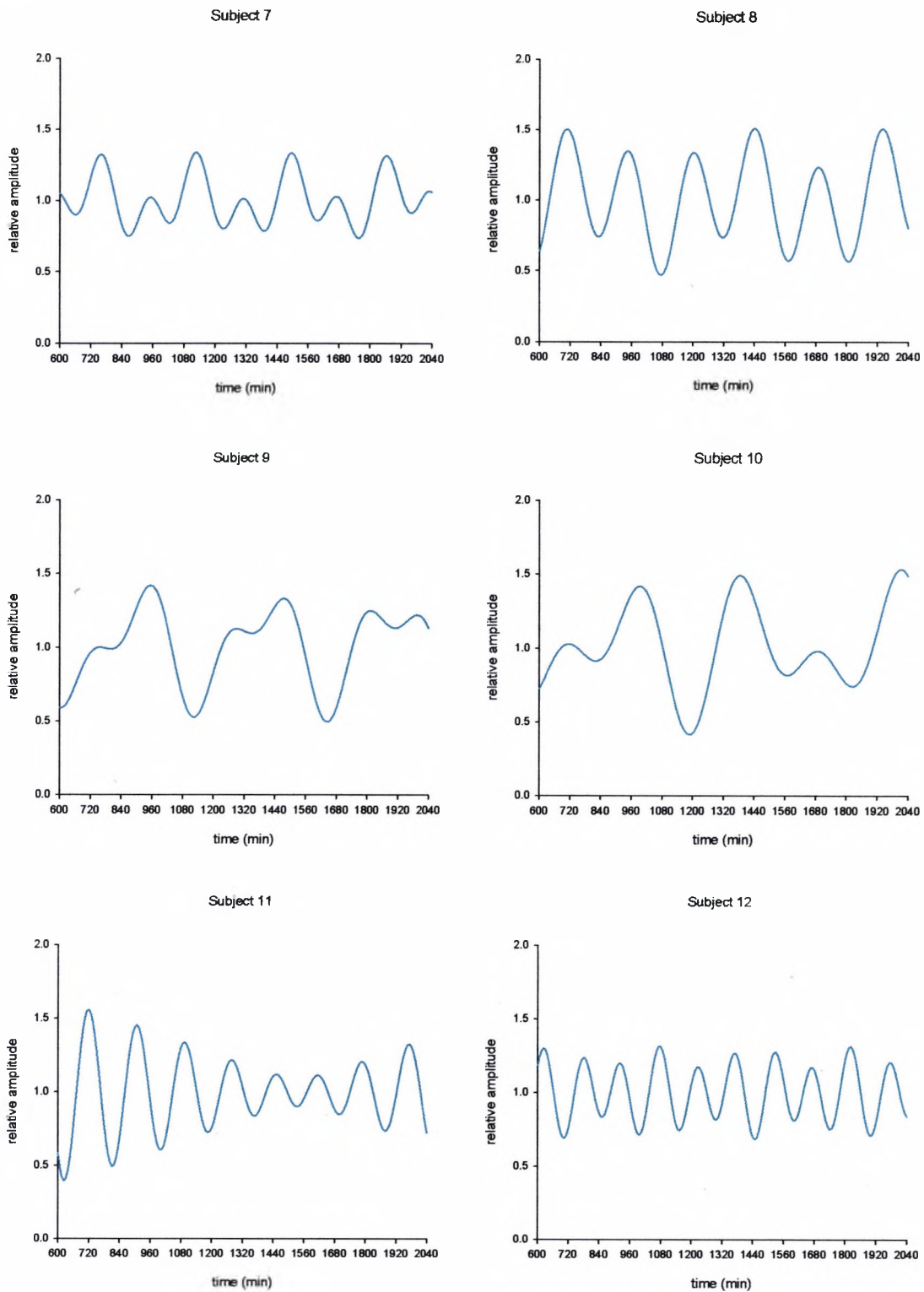


Figure 4.7 (cont.) Oscillatory patterns of insulin sensitivities for individual subjects.

4.4 Discussion

The present results do not fully support the validity of our proposed model. Although population means of parameter estimates are physiologically feasible (see Table 4.6), physiological feasibility of individual parameters is occasionally questionable (see Tables 4.4 and 4.5). This applies to insulin sensitivities, the extent of their oscillations, and to the volume of glucose distribution. The amplitude of oscillations in subject 11 (see Table 4.5), for instance, reached 0.44 for the first sinusoid and 0.34 for the second sinusoid giving the total magnitude of oscillations at 0.78. Oscillations of this size, increasing and decreasing the insulin sensitivities almost two-fold, are very unlikely. The volume of distribution, on the other hand, reached very small, non-physiological values in subjects 3 and 5. The physiological limits were taken from published and validated studies (55,92)

The model validity is also compromised by a high inter-subject variability of the three insulin sensitivities. For example, the values of insulin sensitivity of glucose transport/distribution increase 600-fold from 1 to $611 \times 10^{-4} \text{ min}^{-1} \text{ per } \mu\text{U L}^{-1}$ (see Table 4.4). This is too high when compared with other published studies (55,93,94). The likely cause of this excessive variability is in the nature of the ITS technique itself. In this technique the level of confidence in the individual parameters is disregarded for the calculation of the population mean at the end of each ITS cycle. Hence, parameter values distant from the current population mean, even when estimated with lower confidence, carry the same weight as those lying in a close proximity to the mean. This will have an effect on the next calculated mean and, in our case, will cause an overestimation of the variability in the study population.

Apart from the concerns regarding physiological feasibility and high inter-subject variability of certain model parameters, our model was posteriorly identifiable and provided a very good fit to the experimental data (see Figure 4.6). The precision of parameter estimates was excellent (see Table 4.4) and

the visual inspection of the weighted residuals did not reveal any obvious trends (see Figure 4.5).

Oscillations in plasma glucose under fasting conditions were first discovered in 1923 by Hansen (95) who suggested that the rapid glucose oscillations originating from the rapid insulin pulses were superimposed on larger oscillations of lower frequency. More recent studies in dogs (40,96) and humans (97-100) indeed demonstrated the existence of ultradian oscillations in glucose and insulin with periods of 50-200min. The precise mechanisms that generate these oscillations are not fully understood. Representing oscillations in our model would mean superimposing them on some of the model parameters.

In a preliminary data analysis (data not shown) oscillations in the model parameters were not assumed. Strong evidence coming from the literature (101-103), however, and a poor fit to the data led to the decision to superimpose oscillations on the three insulin sensitivities S_{IT} , S_{ID} , and S_{IE} . Initially only one sinusoid was assumed. However, the best improvement in the model fit was achieved when two sinusoids were used (data not shown).

The mean cycle of faster oscillations in the insulin sensitivities was approximately four hours and the mean cycle of slower oscillations was approximately 6 hours (see Table 4.7). This is longer than 120min reported by (104) but shorter than diurnal changes reported by (105). The spread of meals in our study, which were approximately 6 hours apart, may have influenced our results.

The variability of responses to different meals was not statistically significant ($p=0.096$) in this study. Visual inspection of the results suggests that there is a tendency of breakfast to be absorbed faster than lunch or dinner, but this is not consistent across all individuals (see Tables 4.4 and 4.6). A high inter-subject variability of time-to-maximum absorption of carbohydrates and bioavailability is also evident. It should be emphasised that current modelling knowledge of the glycaemic effect of food is very limited. The fact that we based our

assessment of the effect of food on the carbohydrate content of the meal is a well recognised simplification of a very complex physiological process. Two other inadequacies of a simple two compartment gut absorption model may have played a part here. The time delay caused by meal ingestion and the ceiling in the CHO absorption rate from the gut were two main effects not implemented in our model. To justify this decision it should be mentioned that representing a parameterised delay in meal ingestion is a difficult task. As far as the ceiling of the gut absorption rate is concerned, our preliminary studies have demonstrated (data not shown) that the commonly stated ceiling of $4.5\text{mg per kg min}^{-1}$ (106) was not reached in our experiments. An additional factor when deciding not to implement the above effects was an increase in the complexity of our model. This was an important issue, as the implementation of the complete model in SAAM II software package proved labour intensive and time consuming.

In conclusion, modelling the whole body glucose metabolism during subcutaneous insulin delivery and intravenous glucose measurements in subject with type1 diabetes was an important task contributing to the current knowledge. Only one specific model was evaluated. Although the validity of this model was questioned, the study also produced some important quantitative results. Clearly, more work needs to be done in this field. Other models should be explored. The presented results can be used as a benchmark for further studies in the future.

Chapter 5 Modelling Insulin Lispro Kinetics during Continuous Subcutaneous Insulin Infusion in Subjects with Type 1 Diabetes

5.1 Introduction

Insulin therapy in people with type 1 diabetes aims to mimic the pattern of endogenous insulin secretion present in healthy subjects. This pattern can be achieved to a certain extent by CSII with an insulin pump administering individually titrated basal insulin infusion and prandial insulin boluses.

Despite considerable progress, currently available insulin preparations still do not fully deliver the desired insulin profile, partly due to a delay in insulin appearance in the plasma following subcutaneous injection. In particular, absorption of regular insulin from the subcutaneous depot is impeded by the formation of hexameric macromolecules. The DNA-recombinant technique has contributed to the synthesis of rapid acting human insulin analogues such as lispro, with a reduced formation of higher order hexamers and with binding to the receptors and biological activity preserved (107). As this type of insulin is absorbed faster from the subcutaneous tissue, its ability to mimic the physiological pattern of insulin secretion is improved (14). For that reason lispro and, for that matter, other rapid acting insulin analogues have become the insulin of choice for CSII therapy (107).

A better understanding of the insulin absorption process could lead to further improvements in glycaemic control. However, the pharmacokinetics of subcutaneous insulin is yet to be fully understood. The absorption from the subcutaneous tissue is influenced by many factors including the associated state of insulin, i.e. hexameric, dimeric, or monomeric, concentration, injected volume, injection site and depth, and blood flow (79).

Several models of the subcutaneous insulin kinetics have been proposed (40,80-83,85,87) dealing with different types of commercially available insulin

preparations. Only two of those models (83,85) consider monomeric rapid acting insulin such as lispro.

The pharmacokinetics of insulin lispro was studied extensively after a bolus injection but little is known about its kinetics during CSII. The aim of this study was to investigate the kinetics of insulin lispro during standard insulin pump treatment with bolus and continuous infusion modes of insulin delivery.

5.2 Subjects and Methods

5.2.1 Subjects and experimental protocol

Seven subjects with type 1 diabetes (4/3 F/M, age 31.7 ± 14.1 years, HbA_{1c} $8.5 \pm 1\%$, BMI 26.2 ± 4.9 kg/m², daily basal insulin requirements 23.6 ± 6.4 U/day; means \pm SD) treated by CSII participated in the study. All participants provided written informed consent and the study was approved by the local ethics committee. Six subjects (Subject 1 to 6) were studied after an overnight fast (start of the study at 8:00) and one subject (Subject 7) was studied at postprandial conditions overnight (start of the study at 19:00). The subjects arrived at the University Hospital, University of Graz, Austria one hour prior to the start of the study and remained in a supine position for the 12 hours of the experiment.

On the arrival at the hospital, an intravenous cannula was inserted into a forearm vein to facilitate arterialised venous blood sampling using a thermoregulated (55°C) box. A replacement cannula was inserted into the subcutaneous abdominal tissue for the variable administration of rapid acting insulin analogue (Humalog[®], Eli Lilly, Indiannapolis, USA) by an insulin pump (D-Tron, Disetronic Medical Systems, Burgdorf, Switzerland).

At the start of the study, the subjects ingested a standard meal (40g CHO) with a co-administration of an individually determined prandial insulin bolus. Only water was allowed for the rest of the study. In case of a low plasma

glucose concentration ($< 3.3\text{mmol L}^{-1}$) a 10-20g bolus of intravenous glucose (20% Dextrose solution, Fresenius Kabi, Graz, Austria) was administered. Arterialised venous blood samples were drawn every 30min for the determination of plasma insulin measured using the Iso-Insulin ELISA (Mercodia AB, Uppsala, Sweden) assay with an intra-assay CV $< 6\%$.

5.2.2 Modelling insulin lispro kinetics

Ten alternative compartment models were postulated to represent the insulin kinetics following the administration of a bolus and continuous infusion of insulin lispro (see Table 5.1). The models differed in the description of subcutaneous insulin absorption and its elimination from the plasma. The following effects were identified and assessed:

- (i) the effect of insulin delivery mode, i.e. bolus or basal, on the insulin absorption rate,
- (ii) the effect of insulin dose on the insulin absorption rate,
- (iii) the remote insulin effect on its volume of distribution,
- (iv) the effect of insulin dose on insulin disappearance,
- (v) the presence of insulin degradation at the injection site, and finally
- (vi) the existence of two pathways, fast and slow, for the insulin absorption.

These putative effects were identified from the literature (65,87,108). The structure of the most basic insulin kinetics model was based on an assumption that there is a delay in insulin action. This delay was represented by an additional nonaccessible compartment (see Table 5.1, models 1 to 4). In the consequent models, the basic structure was expanded to account for the additional effects. The only noncompartmental Model 10 was adopted from Berger *et al* (40).

In all models plasma insulin was represented by a single compartment. Insulin in the subcutaneous tissue was represented by two compartments to describe the delay in insulin absorption, or by just one compartment with the aim of representing the faster absorption channel.

Formal definitions of models are shown in Table 5.1. The explanation of symbols is as follows: Q_1 and Q_2 represent the insulin mass (mU) in the two subcutaneous compartments, respectively; Q_{1a} and Q_{2a} represent the mass of insulin (mU) administered as continuous infusion, and Q_{1b} and Q_{2b} represent the mass of insulin (mU) given as a bolus; Q_3 represents the insulin mass (mU) in the plasma compartment; u represents the insulin input (mU min^{-1}), u_i and u_b (mU min^{-1}) represent the continuous insulin infusion and the bolus input, respectively; k_{a1} , k_{a2} , k_{04} , k_{40} and k_e are transfer rates (min^{-1}), a_1 is the slope of the saturable insulin absorption ($\text{min}^{-1} \text{mU L}^{-1}$); V is the insulin distribution volume (L kg^{-1}); W is the body weight (kg); $V_{MAX, a}$ and $V_{MAX, e}$ are the maximal values of the insulin flux (mU min^{-1}) describing the Michaelis-Menten dynamics of the insulin absorption and the insulin disappearance, respectively; $K_{M, a}$ and $K_{M, e}$ are the values of insulin mass (mU) at which the insulin flux is equal to half of its maximal value when describing the Michaelis-Menten dynamics of insulin absorption and disappearance, respectively; X is the remote insulin effect in (mU L^{-1}), K_M is the value of insulin concentration at which the distribution volume attains half of its maximal value (mU L^{-1}), and V_M (unitless) is the maximum proportional increase in the volume of distribution; $V_{MAX, LD}$ is the saturation level (mU min^{-1}) describing the Michaelis-Menten dynamics of insulin degradation for continuous infusion and bolus; $K_{M, LD}$ is the value of insulin mass (mU) at which insulin degradation is equal to half of its maximal value for the continuous infusion and the bolus; B (unitless) is the bioavailability of the insulin bolus relative to the continuous infusion; $L_{D, a}$ and $L_{D, b}$ represent the local degradation at the injection site (mU min^{-1}) for the continuous infusion and the bolus, respectively; k (unitless) is the proportion of the total input flux passing through the slower two compartment channel; s and s_i (unitless) characterise the absorption rate of bolus and continuous infusion, respectively, $T_{50, b}$ (min) is the time to reach 50% absorption of the injected insulin bolus (min) with a (min U^{-1}) and b (min) parameter, and $T_{50, i}$ (equal to b_i) is the time interval (min) to reach 50% absorption of the continuous infusion. All models are *a priori* identifiable.

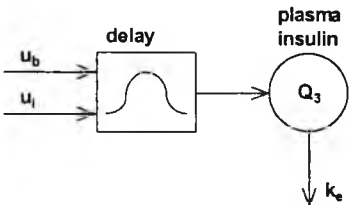
Table 5.1 Compartment models of insulin lispro kinetics.

Compartment Structure	Model	Equations	Comments	Parameters
	1	$\frac{dQ_1}{dt} = u - k_{a1}Q_1 \quad [\text{Eq. 1}]$ $\frac{dQ_2}{dt} = k_{a1}Q_1 - k_{a1}Q_2 \quad [\text{Eq. 2}]$ $\frac{dQ_3}{dt} = k_{a1}Q_2 - k_eQ_3 \quad [\text{Eq. 3}]$	Basic linear model	k_{a1}, k_e
	2	$\frac{dQ_1}{dt} = u - (-a_1Q_1 + k_{a1})Q_1$ $\frac{dQ_2}{dt} = (-a_1Q_1 + k_{a1})Q_1 - (-a_1Q_2 + k_{a1})Q_2$ $\frac{dQ_3}{dt} = (-a_1Q_2 + k_{a1})Q_2 - k_eQ_3$	Saturable insulin absorption rate - simplified MM relation	a_1, k_{a1}, k_e
	3	$\frac{dQ_1}{dt} = u - V_{MAX,a}Q_1 / (K_{M,a} + Q_1)$ $\frac{dQ_2}{dt} = V_{MAX,a}Q_1 / (K_{M,a} + Q_1) - V_{MAX,a}Q_2 / (K_{M,a} + Q_2)$ $\frac{dQ_3}{dt} = V_{MAX,a}Q_2 / (K_{M,a} + Q_2) - k_eQ_3$	Saturable insulin absorption rate - MM relation	$V_{MAX,a}, K_{M,a}, k_e$
	4	Equations 1, 2 and 3 $k_e = V_{MAX,e} / (K_{M,e} + Q_3)$	Saturable insulin disappearance	$V_{MAX,e}, K_{M,e}, k_e$
	5	$\frac{dQ_{1a}}{dt} = u_a - k_{a1}Q_{1a}$ $\frac{dQ_{1b}}{dt} = u_b - k_{a2}Q_{1b}$ $\frac{dQ_{2a}}{dt} = k_{a1}Q_{1a} - k_{a1}Q_{2a}$ $\frac{dQ_{2b}}{dt} = k_{a2}Q_{1b} - k_{a2}Q_{2b}$ $\frac{dQ_3}{dt} = k_{a1}Q_{2a} + k_{a2}Q_{2b} - k_eQ_3$	Delivery mode dependent insulin absorption rate	k_{a1}, k_{a2}, k_e

Table 5.1 (cont.) Compartment models of insulin lispro kinetics.

Compartment Structure	Model	Equations	Comments	Parameters
	6	$\begin{aligned} dQ_1/dt &= u - k_{a1}Q_1 \\ dQ_2/dt &= k_{a1}Q_1 - k_{a1}Q_2 \\ dQ_3/dt &= k_{a1}Q_2 - k_eQ_3 \\ dX/dt &= k_{40}p_i - k_{04}X \end{aligned}$ $k_{40}=1$ $Q_3 = p_i V W \text{ in steady state}$ $V = V(1 + V_{MAX}X/(K_M + X))$	Remote insulin effect on its volume of distribution	$k_{a1}, k_e, k_{04}, V, V_{MAX}, K_M$
	7	$\begin{aligned} dQ_{1a}/dt &= ku - k_{a1}Q_{1a} \\ dQ_{1b}/dt &= (1-k)u - k_{a2}Q_{1b} \\ dQ_2/dt &= k_{a1}Q_{1a} - k_{a1}Q_2 \\ dQ_3/dt &= k_{a1}Q_2 + k_{a2}Q_{1b} - k_eQ_3 \end{aligned}$	Slow and fast insulin absorption channels	k_{a1}, k_{a2}, k_e, k
	8	as above and $u = u_i + Bu_b$	Relative bio-availability of bolus to continuous infusion	$k_{a1}, k_{a2}, k_e, k, B$
	9	$\begin{aligned} dQ_{1a}/dt &= ku - k_{a1}Q_{1a} - LD_a \\ dQ_{1b}/dt &= (1-k)u - k_{a2}Q_{1b} - LD_b \\ dQ_2/dt &= k_{a1}Q_{1a} - k_{a1}Q_2 \\ dQ_3/dt &= k_{a1}Q_2 + k_{a2}Q_{1b} - k_eQ_3 \end{aligned}$ $LD_a = V_{MAX,LD}Q_{1a}/(K_{M,LD} + Q_{1a})$ $LD_b = V_{MAX,LD}Q_{1b}/(K_{M,LD} + Q_{1b})$	Local degradation of insulin at the injection site	$k_{a1}, k_{a2}, k_e, k, V_{MAX,LD}, K_{M,LD}$

Table 5.1 (cont.) Proposed compartment models of insulin lispro kinetics.

Compartment Structure	Model	Equations	Comments	Parameters
	10	$dQ_3 / dt = -k_e Q_3 + A(t)$ $A(t) = u_b \frac{t^{s-1} s T_{50,b}^s}{(T_{50,b}^s + t^s)^2} + \int_0^t u_i(\tau) \frac{(t-\tau)^{s_i-1} s_i T_{50,i}^{s_i}}{(T_{50,i}^{s_i} + (t-\tau)^{s_i})^2} d\tau$ $T_{50,b} = a u_b + b$ $T_{50,i} = b_i$	Empirically derived insulin absorption function	k_e, s, s_i, a, b, b_i

Model 1 was a basic three compartment linear model, in which both the insulin absorption rate and the insulin disappearance rate were unaffected by other factors.

Model 2 assumed a linear relationship between the insulin absorption rate and the amount of insulin infused. Model 2 assumed that the saturation level of the insulin absorption rate was not attained as in Model 3.

Model 3 implemented the Michaelis-Menten relation between the insulin absorption rate and the insulin dose. The two delivery modes, a continuous infusion and a bolus administration, were not discriminated by this model.

Model 4 assumed a saturable, dose-dependent insulin disappearance rate implemented as the Michaelis-Menten relation. The absorption rate was assumed linear and independent of the insulin delivery mode.

Model 5 differentiated among continuous insulin infusion and the bolus administration and assumed that the insulin absorption rate is dependent on the delivery mode with the aim of assessing whether, as frequently discussed in the literature, insulin administered in the form of a bolus is absorbed more slowly than insulin given as a continuous infusion.

Model 6 examined the remote insulin effect on its volume of distribution. The relationship between plasma insulin and the volume of distribution was assumed to be of the Michaelis-Menten form.

Model 7 considered two different pathways of the insulin absorption, one consisting of two compartments, as in the previously described models, and the other with one compartment turning it into a faster channel for the insulin absorption. The proportion of insulin channelled through these two pathways was considered to be the same for both modes of the delivery, the continuous infusion and the bolus. This and the following models were formulated to overcome underestimation of the post-prandial plasma insulin peak encountered by previous models.

Model 8 introduced a relative bioavailability of the insulin bolus to the continuous infusion while maintaining the two pathways of the insulin absorption implemented in Model 7. This relative bioavailability is sometimes referred to in the literature as an effectiveness factor and could be explained by different levels of local insulin degradation for the bolus and infusion delivery.

Model 9 considered a local degradation of insulin at the injection side, also maintaining the two pathways of the insulin absorption (as in Model 7). The degradation process was assumed to be saturable and was implemented as a Michaelis-Menten relation.

Finally, Model 10 was based on that published by Berger *et al* (40) and employed description of the insulin absorption which was derived empirically from published studies (76,109).

5.2.3 Parameter estimation

Prior to the estimation process, all parameters except k and B were log-transformed in order to assure non-negativity and to correct for skewed distributions of parameters. The parameters were estimated using an iterative two stage (ITS) population kinetic analysis method (27,110). In each iteration, model parameters were estimated employing a nonlinear, weighted, least-squares algorithm with an empirical Bayesian term.

The absolute data variance model was adopted, which assigns weights subject to the specified measurement error. The weight was defined as the reciprocal of the square of the measurement error. The accuracy of parameter estimates was obtained from the Fisher information matrix (23). The SAAM II Population Kinetics v1.2 software (SAAM Institute, Seattle, WA) was employed to carry out the calculations.

5.2.4 Model identification and validation

Parameter estimates were checked for physiological feasibility. To validate the models two additional criteria were adopted. These were posterior identifiability and the distribution of residuals (23). Posterior identifiability of each model was assessed on the basis of the accuracy of parameter estimates. A given parameter was considered non-identifiable if the coefficient of variation of the parameter estimate was $> 150\%$. The Runs test evaluated the randomness of the residuals.

5.2.5 Model selection

The best model, i.e. the model, which best represented our experimental data, was selected using the principle of parsimony as implemented by the Akaike criterion.

5.3 Results

5.3.1 Experimental data

Mean plasma insulin concentration is shown in Figure 5.1. The continuous insulin infusion rate, which varied during the experiments, was 0.86 ± 0.27 U/h (mean \pm SD), and the bolus administered prior to the meal was 5.95 ± 2.37 U.

5.3.2 Model identification and validation

Model identification and validation results are summarised in Table 5.2. Models 4 and 6 proved non-identifiable with precision of parameter estimates for K_M , V_{MAX} , $K_{M,e}$, $V_{MAX,e}$, and k_{04} expressed as CV considerably exceeding 150%. The remaining eight models demonstrated physiological feasibility of parameter estimates and posterior identifiability (see Table 5.2). Weighted residuals associated with these models are plotted in Figure 5.2. The results of the Runs test applied to the weighted residuals, i.e. the percentage of cases, which passed this test, is shown in Table 5.2. Weighted residuals of models 2, 8, 9 and 10 passed the Runs test in 100% of cases (Table 5.2).

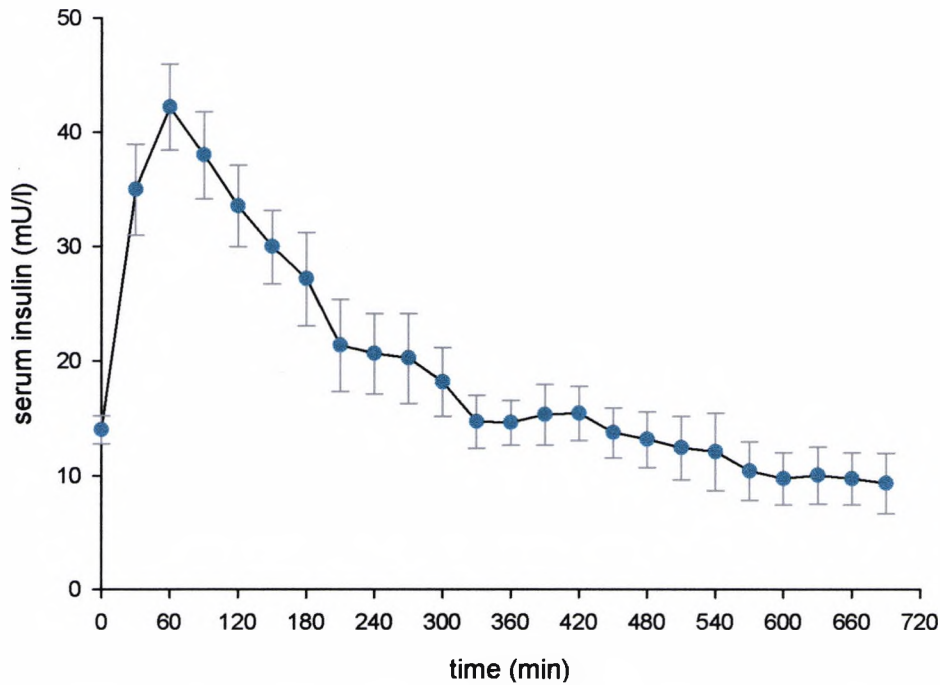


Figure 5.1 Plasma insulin concentration. Values are mean \pm SE ($n=7$).

5.3.3 Model selection

The values of the Akaike criterion for *a posteriori* identifiable models are shown in Table 5.2. On the basis of this criterion, Model 9 was selected as best representing the experimental data. This model is also characterised by 100% of cases passing the Runs test and the tightest range of the weighted residuals. Although parameter estimates for k_e and V were outside the physiological limits, their product, the metabolic clearance rate (MCR), maintained physiological feasibility. The parameter estimates for this model and for all remaining *a posteriori* identifiable models are shown in Tables 5.3a, 5.3b and 5.3c. An example model fit for Model 9 is shown in Figure 5.3.

Table 5.2 Model identification, validation, and selection. Summary results.

Model	Physiological feasibility	Precision of parameter estimates	Runs Test	Akaike criterion
	Yes/No	Good/Acceptable/Unacceptable**	%*	Mean \pm SD
1	Yes	Acceptable	86	8.06 \pm 6.08
2	Yes	Acceptable	100	7.62 \pm 5.85
3	Yes	Good	57	7.78 \pm 5.86
4	Yes	Unacceptable	N/A	N/A
5	Yes	Good	71	7.43 \pm 6.10
6	Yes	Unacceptable	N/A	N/A
7	Yes	Good	86	6.11 \pm 3.41
8	Yes	Good	100	4.32 \pm 2.37
9	Yes	Good	100	4.13 \pm 2.12
10	Yes	Good	100	6.17 \pm 3.59

*Percentage of random cases

** Good (CV<100%), Acceptable (CV<150%), Unacceptable (CV>>150%)

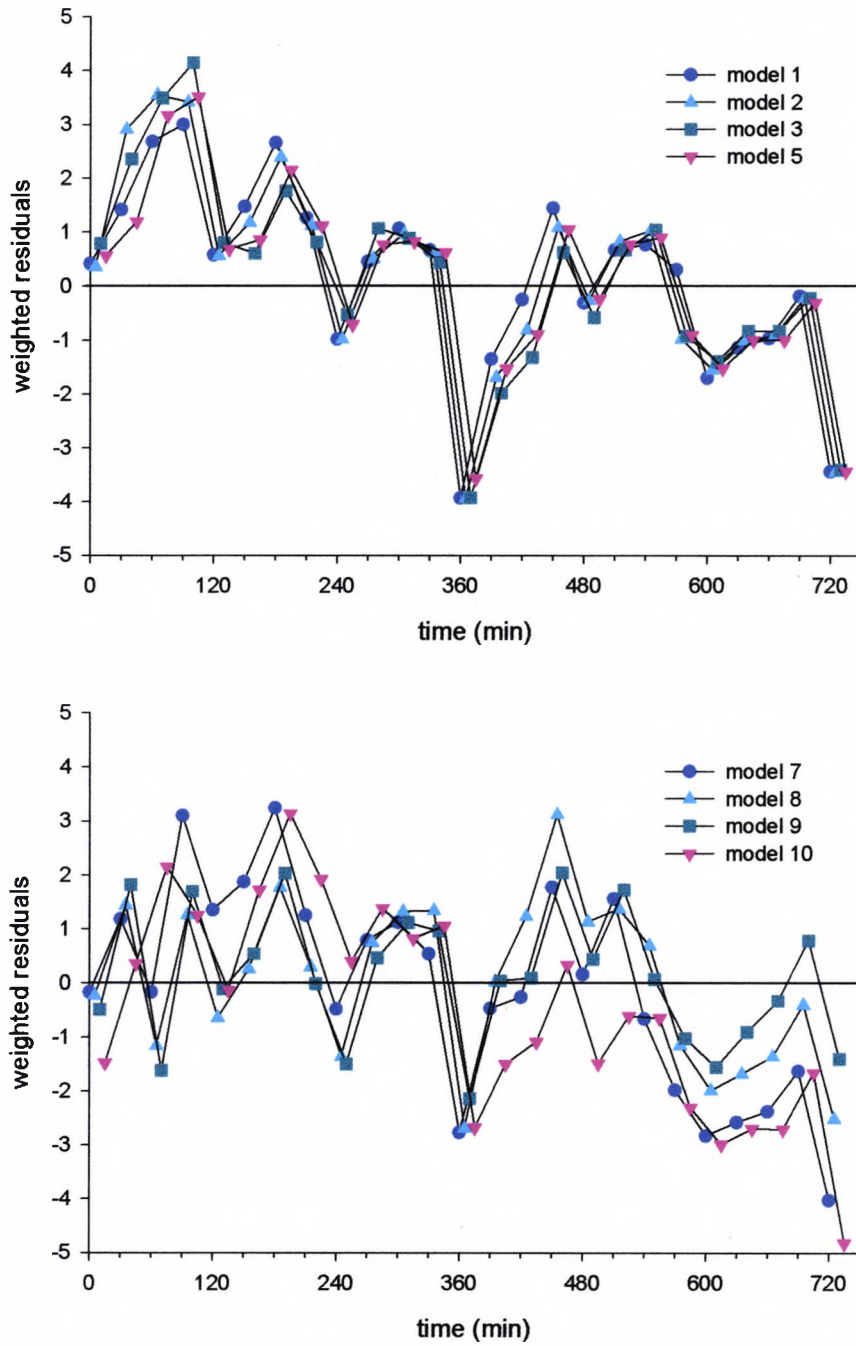


Figure 5.2 Mean weighted residuals for Models 1, 2, 3, and 5 (top panel), and for Models 7, 8, 9, and 10 (bottom panel) ($n=7$).

Table 5.3a Parameter estimates of k_{a1} , k_{a2} , k_e , k , V and MCR for identifiable models. Values are population means (inter-quartile range of individual values) ($n=7$).

Model	k_{a1} ($10^{-2} \times \text{min}^{-1}$)	k_{a2} ($10^{-2} \times \text{min}^{-1}$)	k_e ($10^{-2} \times \text{min}^{-1}$)	k (unitless)	V ($10^{-2} \times \text{L kg}^{-1}$)	MCR ($10^{-3} \times \text{L kg}^{-1} \text{min}^{-1}$)
1	1.66 (1.04 – 2.66)	--	30.22 (6.79 – 134.55)	--	5.38 (1.16 – 25.07)	16.3 (13.1 – 20.1)
2	1.83* (1.05 – 3.19)	--	36.17 (8.57 – 152.70)	--	4.49 (1.03 – 19.68)	16.2 (13.1 – 20.1)
3	--	--	41.50 (15.45 – 111.49)	--	3.90 (1.46 – 10.39)	16.2 (13.1 – 19.9)
5	1.89 (0.97 – 3.66)	1.58 (1.03 – 2.43)	28.58 (7.56 – 108.03)	--	5.62 (1.42 – 22.26)	16.1 (12.9 – 20.0)
7	1.89 (1.00 – 3.57)	2.57 (1.34 – 4.95)	1.91 (1.54 – 2.37)	0.71 (0.60 – 0.82)	84.00**	16.0 (12.9 – 19.9)
8	2.47 (1.69 – 3.61)	0.79 (0.18 – 3.34)	1.98 (1.32 – 2.97)	0.57 (0.44 – 0.70)	86.13 (59.11 – 125.50)	17.1 (12.4 – 23.5)
9	1.12 (0.44 – 2.85)	2.10 (1.12 – 3.96)	1.89 (1.34 – 2.68)	0.67 (0.53 – 0.82)	56.45 (38.79 – 82.16)	10.7 (6.3 – 18.1)
10	--	--	3.68 (1.33 – 10.20)	--	42.01 (16.73 – 105.51)	15.5 (12.5 – 19.1)

*Estimate of k_{a1} at zero insulin concentration

**Individual values converged to an identical estimate

Table 5.3b Parameter estimates of $V_{MAX,a}$, $K_{M,a}$, $V_{MAX,LD}$, $K_{M,LD}$, B and a_1 for Models 2, 3, 8 and 9. Values are population means (inter-quartile range of individual values) ($n=7$).

Model	$V_{MAX,a}$ ($10^3 \times \text{mU min}^{-1}$)	$K_{M,a}$ ($10^3 \times \text{mU}$)	$V_{MAX,LD}$ (mU min^{-1})	$K_{M,LD}$ (mU)	B (unitless)	a_1 ($10^{-8} \times \text{min}^{-1} \text{mmol}^{-1} \text{L}$)
2	--	--	--	--	--	14.8 (2.1 – 105.4)
3	1.14 (0.36 - 3.67)	66.0 (15.1 – 288.8)	--	--	--	--
8	--	--	--	--	1.55 (1.14 – 1.95)	--
9	--	--	1.93 (0.62 – 6.03)	62.6 (62.6 – 62.6)	--	--

*Individual values converged to an identical estimate

Table 5.3c Parameter estimates of a , b , b_i , s , s_i for Model 10. Values are population means (inter-quartile range of individual values) ($n=7$).

a (min U^{-1})	b (min)	b_i (min)	s (unitless)	s_i (unitless)
2.44 (1.66 – 3.59)	53.45 (30.97 – 92.27)	79.19 (36.47 – 171.97)	2.01 (1.74 – 2.32)	2.86 (1.91 – 4.26)

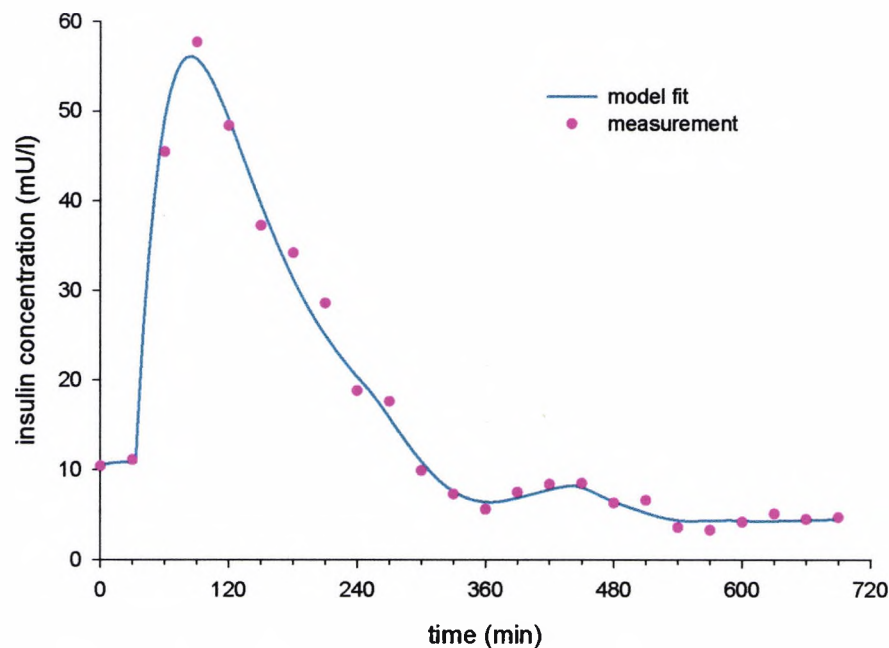


Figure 5.3 Example model fit generated by Model 9.

5.4 Discussion

Mathematical modelling is a common approach to quantify subcutaneous insulin absorption. A number of models have been proposed (40,80-83,85,87) dealing with different insulin types. Two of those models (83,85) consider monomeric rapid acting insulin such as lispro.

Our ten models are partly, or in case of Model 10, entirely based on existing models of the insulin kinetics after the SC insulin injection. Model 1 has an identical structure to the model proposed by Puckett *et al* (82) but with an omitted effectiveness factor to represent the local insulin degradation. The effect of the local insulin degradation was accounted for in Models 8 and 9. In Model 8, instead of Puckett's effectiveness factor, we use relative bioavailability B to account for different levels of the insulin degradation at the injection site for the bolus and continuous infusion. Although this model proved identifiable, it provided marginally worse AIC than best Model 9.

Model 10 is the only noncompartmental model based on an empirical equation describing the subcutaneous insulin absorption derived by Berger *et al* (84).

This model was also identifiable with borderline physiological values of parameter estimates but did not provide the best fit to the data as measured by the Akaike criterion.

All models except Model 1 were nonlinear. Nonlinearity with Michaelis-Menten characteristics was imposed on the insulin absorption (Model 3), the insulin disappearance (Model 4), the remote insulin effect on the volume of distribution (Model 6), and finally on the local insulin degradation (Model 9).

Several authors (81,87,111,112) observed that the insulin absorption rate varies inversely with the concentration of the injected insulin. Trajanoski (85), in his theoretical study, examined this phenomenon in the monomeric insulin and found its absorption rate to be constant regardless of the concentration and the volume. This finding was supported indirectly by Kang (78) in his study of the influence of molecular aggregation on rates of the subcutaneous absorption. Our Models 2 and 3 addressed this issue of the concentration dependent absorption rate by assuming nonlinear dynamics and saturability of the subcutaneous insulin absorption. Model 2 uses a simplified, whereas Model 3 a full form of the Michaelis-Menten relation. Both models proved only borderline identifiable with precision of some parameter estimates exceeding 100%. In particular, the Michaelis-Menten parameters in Model 3, $V_{MAX,a}$ and $K_{M,a}$ achieved borderline precision for some but not all subjects. The highest CV for $V_{MAX,a}$ was 123% and 124% for $K_{M,a}$ indicating a higher degree of uncertainty related to these parameter estimates. In case of Model 2, borderline CVs were recorded for the volume of distribution, and the insulin disappearance rate.

The evidence of a saturable insulin removal in the supraphysiological range of the insulin concentration comes from a number of studies (88,113,114). In the physiological range of insulin concentration, however, existing evidence suggests a linear process (115). Nonlinear kinetics of the insulin removal rate have been represented in Model 4. This model proved non-identifiable with a CV for three of the parameter estimates (V , $V_{MAX,e}$, and $K_{M,e}$) exceeding considerably 150%. An unacceptable uncertainty of Michaelis-Menten

parameters suggests that saturable levels of the plasma insulin concentration were not achieved during the experiment and that the insulin disappearance is most probably linear over the physiological range.

Mosekilde *et al* (87) observed a reverse relationship between the insulin absorption rate and the injected volume. This implies that insulin kinetics depends on the insulin delivery mode, i.e. it is different for the bolus (a large volume) and the continuous subcutaneous infusion (a sequence of small volumes). Other authors (80) did not find such dependence in their studies. In Model 5 it was attempted to examine this finding for insulin lispro. Bolus and continuous infusion inputs were routed via separate absorption channels and the insulin absorption rate constants for bolus and infusion were estimated. Although the population means differed slightly, this difference was not statistically significant ($P = 0.34$, paired t-test). This model, although validated, did not provide the best fit to our data.

It has been suggested that insulin may have a remote effect on its volume of distribution (65). This remote effect of insulin was represented in Model 6. Unfortunately Model 6 proved nonidentifiable with a CV for V_{MAX} and K_M reaching values as high as 400%.

Although some of the above discussed models were identifiable, their representation of our data was not satisfactory, especially around the peak of the plasma insulin curve. In an attempt to achieve a better representation of the experimental data, and the peak region in particular, we introduced two, slow and fast, insulin absorption channels differing in the number of compartments. A marked improvement in the model fit was observed in Models 7, 8, and 9, where the two absorption channels were represented. The best model fit was observed in Models 8 and 9 further assuming the effect of local insulin degradation. Although two parameter estimates, the volume of distribution and the insulin elimination rate, were not physiologically feasible in Models 8 and 9, the insulin metabolic clearance rate (MCR) attained physiological feasibility (see Table 5.3a). For this reason the two models were retained and Model 9, with a slightly lower Akaike criterion, was

selected as best representing our data. The value of the insulin MCR obtained by Model 9 is almost identical to that obtained by Kraegen *et al* (81) with an independent intravenous experiment (10.8 mL min^{-1} for regular insulin) and Shimoda *et al* (83) (10.6 mL min^{-1} for monomeric insulin).

The local insulin degradation seems to be a controversial issue. Some studies confirm its significance (108,116), others discount it as relatively small (81,112,117). In Model 9, we modelled the local degradation as a saturable process with Michaelis-Menten characteristics. The mean precision of the $V_{\text{MAX, LD}}$ parameter estimate was very good ($47 \pm 58\%$; mean \pm SD) with the exception of one subject where it was 150%. On the other hand, the parameter estimate for $K_{\text{M,LD}}$, almost converged to the population mean. The mean precision of each of the parameter estimates in this model was less than 50%. Our best model indicates that the effect of insulin degradation, however small [$V_{\text{MAX,LD}}=1.93(0.62 - 6.03)\text{mU min}^{-1}$, $K_{\text{M,LD}}=62.6(62.6 - 62.6)\text{mU}$], is not, as suggested by Binder *et al* (112), insignificant in the physiological range of insulin concentrations.

As far as the two absorption channels are concerned, Model 9 estimated that 67(53 – 82)% [mean (interquartile range)] of insulin passes through the slow absorption channel [absorption rate $0.011 (0.004 - 0.029)\text{min}^{-1}$] with the remaining 33% passing through the fast channel [absorption rate $0.021(0.011 - 0.040)\text{min}^{-1}$]. The idea of two absorption channels could represent the existence of monomer-dimer equilibrium, as dimers have been shown to be absorbed slower than monomers (78).

A marked inter-subject variability of the insulin absorption rate from the subcutaneous tissue has been observed by many authors (85,87,118). The insulin absorption is thought to be dependent on the injection site (75,119), the injection depth (120), lipodystrophy (121), the low body weight (121), and many other factors such as exercise, smoking, temperature etc. This inter-subject variability can be seen very clearly across all the individual parameter estimates of our best Model 9.

5.5 Conclusion

Ten alternative models of the subcutaneously administered insulin lispro kinetics have been evaluated for posterior identifiability and validated with experimental data collected in subjects with type 1 diabetes. The selection process based on the Akaike criterion identified Model 9 to represent best our data. The model indicates the existence of fast and slow absorption channels and the presence of the local insulin degradation.

Chapter 6 Modelling Interstitial Glucose Kinetics under Physiological Conditions in Type 1 Diabetes

6.1 Introduction

Subcutaneous glucose sensing offers an alternative, minimally invasive approach for long term continuous glucose monitoring in real time. It provides subjects with T1DM and their clinicians with vital information to optimise treatment and to achieve good metabolic control.

Due to difficulties encountered with the long term stability of implantable glucose sensors (122), recent research has explored a wearable subcutaneous glucose measurement using techniques such as ultrafiltration (61), the wick technique (123), microdialysis (124), transdermal extraction (125), and open-flow microperfusion (OFM) (69). Microdialysis and OFM have been shown to be suitable for continuous *ex vivo* on-line glucose monitoring (69,124,126). These techniques have demonstrated the presence of a gradient between plasma and interstitial glucose of a varying magnitude from 20% (127) to 110% (70). An equilibration time delay between plasma and interstitial glucose has been reported in the range from 2.3min (66) to 45min (128).

The understanding of the gradient and the dynamics of the relationship between interstitial and plasma glucose depends on the understanding and quantification of the physiological processes in the ISF compartment surrounding the adipose tissue. Plasma glucose is separated from the interstitial glucose by a capillary wall (see Figure 3.6 in Chapter 3). Hence changes in interstitial glucose are related to changes in plasma glucose by the rate of diffusion across the capillary wall and by the rate of glucose removal from the ISF. The removal represents the uptake by adipose tissue immediately surrounding the sampling probe and transport back to the plasma. Rebrin *et al* (64) argue that if the uptake by adipocytes is negligible, plasma and interstitial glucose should equilibrate in steady-state conditions. If,

however, the uptake is not negligible, then a steady-state gradient will exist between plasma and interstitial glucose concentration. Assuming that glucose uptake by the adipose tissue is sensitive to insulin, an increase in insulin concentration should result in an increased uptake of glucose by adipocytes, and therefore, an increase in the plasma-to-interstitial glucose gradient.

The existence of the so-called “push-pull” phenomenon has been suggested in the literature. When plasma glucose is rising, the changes in interstitial glucose should fall behind the changes in plasma glucose due to glucose being pushed from blood to the ISF. Conversely, with plasma glucose falling, the changes in interstitial glucose should precede the changes in plasma glucose due to glucose being pulled from the ISF as it is assumed that insulin-stimulated glucose uptake from the ISF is primarily responsible for the fall (insulin effect on flux f_{02} in Figure 3.6).

Several authors claim to have detected the push-pull phenomenon (17,59,66). Rebrin *et al* (64) in their study in non-diabetic dogs disputed its existence showing that insulin does not appear to have any effect on glucose removal from the ISF in adipose tissue. The effect of interstitial glucose being pulled out from the ISF surrounding the probe could possibly be counteracted by changes in interstitial glucose originating in the areas distant from the probe/sensor.

Although studies conducted so far provide conflicting results possibly due to differences in techniques and methods as well as subjects/species, most of them have demonstrated not a constant but changing interstitial to plasma glucose gradient (the IG-PG ratio). This implies that the IG-PG relationship is not simple. A more detailed understanding is required if subcutaneous glucose sensing is to become an even more accurate surrogate for plasma glucose measurements.

The majority of previous studies employed glucose clamps achieving non-physiological conditions and/or were carried out in animals or non-diabetic humans. As subcutaneous glucose sensing has its main application in human

subjects with T1DM during normal physiological conditions, the present study aimed to describe the IG-PG relationship during and after meal in T1DM. The OFM technique was employed to measure interstitial glucose. A compartment modelling approach was adopted to postulate competing models and to represent mechanisms explaining temporal variations in the IG-PG ratio. Using selection criteria based on the principle of parsimony, a model was selected which best explained the experimental data while attaining physiological plausibility.

6.2 Subjects and Methods

6.2.1 Subjects and experimental protocol

Nine subjects with T1DM (5/4 M/F, age 33 ± 13 years, body mass index 26.6 ± 4.3 kg m⁻², HbA_{1c} $8.6 \pm 0.9\%$; mean \pm SD) treated by CSII participated in the study. All participants provided written informed consent and the study was approved by the local ethical committee. The subjects followed their standard diet and insulin regimen prior to the study.

Six subjects (Subject 1 to 6) were studied after an overnight fast (start of the study at 8:00) and three subjects (Subject 7 to 9) were studied at postprandial conditions (start of the study at 19:00). The subjects were admitted to the University Hospital, University of Graz, one hour prior to, and remained supine throughout the 12-hour long study.

On arrival at the hospital, an intravenous cannula was inserted into a forearm vein to facilitate arterialised venous blood sampling using a thermoregulated (55°C) box. A replacement cannula was inserted into the subcutaneous abdominal tissue for the variable administration of rapid acting insulin analogue (Humalog[®], Eli Lilly) by an insulin pump (D-Tron, Disetronic Medical Systems, Burgdorf, Switzerland). A double-lumen catheter was inserted into the subcutaneous adipose tissue on the opposite side of the abdominal wall to extract ISF by open-flow microperfusion. Local skin anaesthesia (Novanaest purum 2%, Gebro Broschek, Vienna, Austria) was used before the adipose

tissue was cannulated. Perfusion started immediately, but sampling of the perfusate began 60min after the insertion of the catheter (equilibration period) to allow the initial trauma to subside.

At the start of the study, the subjects ingested a standard meal (40g CHO) with a co-administration of an individually determined prandial bolus of insulin lispro. Only water was allowed for the rest of the study. In the case of a low plasma glucose concentration ($< 3.3 \text{ mmol L}^{-1}$) a 10-20g bolus of intravenous glucose (20% Dextrose solution, Fresenius Kabi, Graz, Austria) was administered.

Over 12 hours, the ISF was continuously collected and samples over 30min were subjected to the determination of IG. Arterialised venous blood samples were drawn every 15min for the determination of PG and every 30min for the determination of plasma insulin. The ISF samples and samples for the determination of plasma insulin were stored at -70°C instantly after sampling until they were analysed. Plasma glucose was determined on a bedside analyser.

6.2.2 Open-flow microperfusion

The OFM was employed to obtain samples of the ISF (68,69). The double-lumen catheter was prepared from a conventional intravenous cannula (24 gauge \times 19mm, 0.7mm OD; Neoflon, Becton-Dickinson, Helsingborg, Sweden) by perforating 30 holes (0.3mm diameter) with an Excimer Laser. The catheter was inserted into the adipose tissue of the anterior abdominal wall by a steel mandrin, which was subsequently removed and replaced by the inner cannula of the double-lumen catheter (steel tube, length 16mm, inner diameter 0.1mm, outer diameter 0.2mm, Goodfellow, Cambridge, UK). The inner cannula was connected to a plastic bag containing perfusate [isotonic, ion-free mannitol in aqueous solution (275mmol L^{-1} , 288mosmol L^{-1}); Leopold, Graz, Austria]. The perfusion fluid entered the catheter through the inner lumen and passed to the tip of the probe. Thereafter, it streamed back in the annular space between the inner cannula and the outer perforated

catheter, where partial equilibration between the ISF and the perfusate occurred. The outer lumen was connected to a peristaltic pump (Minipuls 3, Gilson, France) in push-pull mode, which transported the diluted ISF effluents through the tubing system to a collecting vial on ice. The vials were sealed with a film to prevent evaporation during sampling. The flow rate was set by the peristaltic pump. To verify appropriate average flow rate, each vial was weighed before and after sampling.

6.2.3 Assays and determination of interstitial glucose

Plasma glucose was measured in duplicate by a Beckman Glucose Analyser 2 (Beckman Instruments, Fullerton, CA) with a CV < 1.5% of the intra-assay measurement error. Plasma insulin was measured using the Iso-Insulin ELISA (Mercodia AB, Uppsala, Sweden) assay with an intra-assay CV < 6%. Sodium and potassium concentrations in the ISF were measured using a flame photometer (IL 943, Instrumentation Laboratory, Milano, Italy). The glucose concentration in ISF samples was measured enzymatically with glucose hexokinase programmed on a Cobas Integra analyser (Hoffman-La Roche, Basel, Switzerland). The interstitial glucose concentration was calculated by the ionic reference technique (68).

6.2.4 Data analysis

6.2.4.1 Modelling interstitial glucose kinetics

Compartment modelling described the PG-IG kinetics. PG was represented by one compartment, IG also by one compartment. The transfer of glucose between these two compartments represented diffusion across the capillary wall driven by the concentration gradient (4). The disposal from the IG compartment represented glucose transporters facilitated transport across the cell membrane (129).

Nine models were postulated to account for the temporal variations in the IG-PG ratio. In all models, PG was employed as the forcing function. The models

differed in the inclusion of physiologically motivated alterations of the three pathways entering/leaving the IG compartment. These effects included:

- (i) a saturable glucose disposal,
- (ii) a zero-order (constant) glucose disposal,
- (iii) a stimulatory effect of insulin on glucose transfer from plasma to ISF, and
- (iv) an effect of insulin on glucose removal from ISF.

Model 1 was the base model that assumed time invariant fractional transfer rates from and to the IG compartment.

Model 2 assumed a saturable glucose disposal from the IG compartment. To avoid posterior identifiability problems, the Michaelis-Menten form was not used and the transfer rate associated with the outflux decreased linearly with an increasing IG concentration. This is a reasonable approximation of the Michaelis-Menten form assuming that a narrow range of saturation levels is achieved during the experiment. Centring with an IG concentration of 4mmol L^{-1} (the "basal" IG value) was used to enable comparison of parameter estimates across models.

Model 3 implemented the stimulatory effect of insulin on glucose disposal from the IG compartment. To avoid expected posterior identifiability problems, the insulin effect did not involve a remote insulin compartment as the infrequent sampling of IG (sample every 30min) was not considered to be sufficient to determine the time delay of insulin action.

Model 4 combined Models 2 and 3, i.e. the saturability of glucose removal and the stimulatory effect of insulin on glucose disposal.

Model 5 extended Model 3 and employed the remote insulin compartment to assess the possibility of determining the delay in insulin action to test the assumption presented in Model 3.

Model 6 combined Models 2 and 5, i.e. the saturability of and the remote insulin action on glucose disposal.

Model 7 assumed that part of the glucose removed from the IG compartment is due to a zero-order disposal representing a constant flux independent of the IG concentration.

Model 8 implemented a stimulatory effect of insulin on the transfer of glucose from the plasma to the ISF (insulin effect on flux f_{21} in Figure 3.6). A remote insulin compartment was not used for posterior identifiability reasons.

Finally, Model 9 combined Models 7 and 8, i.e. the zero-order removal from the IG compartment and the stimulatory effect on the transfer of glucose from plasma to the ISF.

Formal definitions of models are shown in Table 6.1. The explanation of symbols is as follows: C_1 , C_2 represent PG and IG concentrations (mmol^{-1}), respectively; k_{12} , k_{21} , and k_{02} are transfer rate constants (min^{-1}); $k'_{02} = k_{02} + k_{12}$ is an aggregated constant (min^{-1}); k_s is the slope of a saturable component of the glucose disposal (min^{-1}); I is the plasma insulin concentration (mU L^{-1}); I_b is basal (pre-experimental) plasma insulin concentration (mU L^{-1}); X is the remote insulin action representing the delay in insulin action (min^{-1}); k_{30} and k_{03} represent the activation and the deactivation constants of the remote insulin, respectively (min^{-2} per mU L^{-1} and min^{-1}); S_I is the insulin sensitivity associated with glucose removal from IG (Model 3, 4, 5, and 6) or with plasma-to-interstitial-fluid transfer (Model 8 and 9) (min^{-1} per mmol L^{-1}); and F_{02} is the zero-order glucose disposal ($\text{mmol L}^{-1} \text{min}^{-1}$). All models are assumed to be *a priori* identifiable (23).

6.2.4.2 Parameter estimation

The parameters were estimated using an iterative two-stage technique (ITS) (27,110). In each iteration, model parameters were estimated employing a nonlinear, weighted, least-squares algorithm with an empirical Bayesian term.

Table 6.1 Nine proposed compartment models of interstitial glucose kinetics (see text for details).

Compartment structure	Model	Equations	Comments	Parameters
	1	$dC_2/dt = k_{21}C_1 - k'_{02}C_2$	Basic linear model	k_{21}, k'_{02}^*
	2	$dC_2/dt = k_{21}C_1 - [k'_{02} - k_s(C_2 - 4.0)]C_2$	Saturable glucose removal from ISF	k_{21}, k'_{02}, k_s
	3	$dC_2/dt = k_{21}C_1 - [k'_{02} + S_1(I - I_b)]C_2$	Glucose removal from ISF linearly dependent on plasma insulin concentration	k_{21}, k'_{02}, S_1
	4	$dC_2/dt = k_{21}C_1 - [k'_{02} + S_1(I - I_b) - k_s(C_2 - 4.0)]C_2$	Models 2 and 3 combined	$k_{21}, k'_{02}, k_s, S_1$
	5	$dC_2/dt = k_{21}C_1 - (X + k'_{02})C_2$ $dX/dt = k_{30}(I - I_b) - k_{03}X$ $S_1 = k_{30}/k_{03}$ [Eq.1]	Remote effect of insulin on glucose removal from ISF	$k_{21}, k'_{02}, S_1, k_{30}$
	6	$dC_2/dt = k_{21}C_1 - [k'_{02} + X - k_s(C_2 - 4.0)]C_2$	Models 2 and 5 combined and Equation 1	$k_{21}, k'_{02}, k_s, S_1, k_{03}$
	7	$dC_2/dt = k_{21}C_1 - k'_{02}C_2 - F_{02}$	Zero-order removal of glucose from ISF	k_{21}, k'_{02}, F_{02}
	8	$dC_2/dt = [k_{21} + S_1(I - I_b)]C_1 - k'_{02}C_2$	Insulin effect on glucose transfer from plasma to ISF	k_{21}, k'_{02}, S_1
	9	$dC_2/dt = [k_{21} + S_1(I - I_b)]C_1 - k'_{02}C_2 - F_{02}$	Models 7 and 8 combined	$k_{21}, k'_{02}, F_{02}, S_1$

* k'_{02} is an aggregated parameter, $k'_{02} = k_{02} + k_{12}$

Prior to the parameter estimation, parameters were log-transformed to assure non-negativity and to correct for skewed distributions of parameters with the exception of the parameter k_s , which was not transformed.

Model input was plasma glucose and plasma insulin (Models 3, 4, 5, 6, 8 and 9). Model output was the average interstitial glucose over a 30min period.

The relative weighting that assigns weights subject to a proportional constant, was adopted to reflect the fact that at the time of data analysis, we did not have information about the extent of the measurement error. The weight was defined as the reciprocal of the square of the nominal measurement error with a coefficient of variation of 5%. The model fit error (the difference between measurements and model predictions) was determined from the nominal measurement error and the variance parameter determined by the estimation procedure.

The accuracy of parameter estimates was obtained from the Fisher information matrix (23). The SAAM II Population Kinetics v 1.0b software package (SAAM Institute, Seattle, WA) was employed to carry out the calculations.

6.2.4.3 Model identification and validation

Parameter estimates were checked for physiological feasibility. Models with parameter estimates outside the physiological range were excluded from further analysis. Physiological ranges of parameters were determined from previously validated tracer studies.

To validate the models, three additional criteria were adopted. These were the goodness of fit, posterior identifiability, and the distribution of residuals (23). The goodness of fit was assessed on the basis of the model fit error, as discussed above. Posterior identifiability of each model was assessed on the basis of the accuracy of parameter estimates. A given parameter was

considered non-identifiable if the coefficient of variation of the parameter estimate $> 100\%$. The Runs test evaluated the randomness of the residuals.

6.2.4.4 Model selection

The best model, i.e. the model which best represented the experimental data, was selected by comparing the model fit error and by using the principle of parsimony as implemented by the Akaike criterion.

6.3 Results

6.3.1 Plasma glucose, interstitial glucose and interstitial-to-plasma glucose ratio

Figure 6.1 shows plasma glucose, interstitial glucose, and plasma insulin. PG and IG concentration ranged from 3.1 to 15.7mmol L⁻¹ and from 1.6 to 10.0mmol L⁻¹, respectively. The plot also shows the IG-PG ratio (0.6 ± 0.1 ; mean \pm SD), which significantly changed during the experiment ($P < 0.01$, two way ANOVA with effects due to the time instance and the subject).

6.3.2 Model identification and validation

The parameter estimate for k_{03} in Model 3 (data not shown) reached very low values prolonging the time delay for the remote insulin effect (equal to reciprocal of k_{03}) to over 350min. This is equivalent to a half time of 245min. Hence the insulin effect, as considered in Model 3, could not be responsible for the push-pull phenomenon. The parameters for Model 4, where the insulin effect was considered to be direct, could not be estimated, as the population model failed to converge. At that point the population mean of the insulin sensitivity parameter S_1 was low at $5 \times 10^{-5} \text{ min}^{-1} \text{ per mU L}^{-1}$ with a very small standard deviation of $\sim 10^{-8} \text{ min}^{-1} \text{ per mU L}^{-1}$. Similarly, population models 5 and 6 failed to achieve convergence and their parameters could not be estimated. As a result, models 3, 4, 5 and 6 were excluded from further analysis.

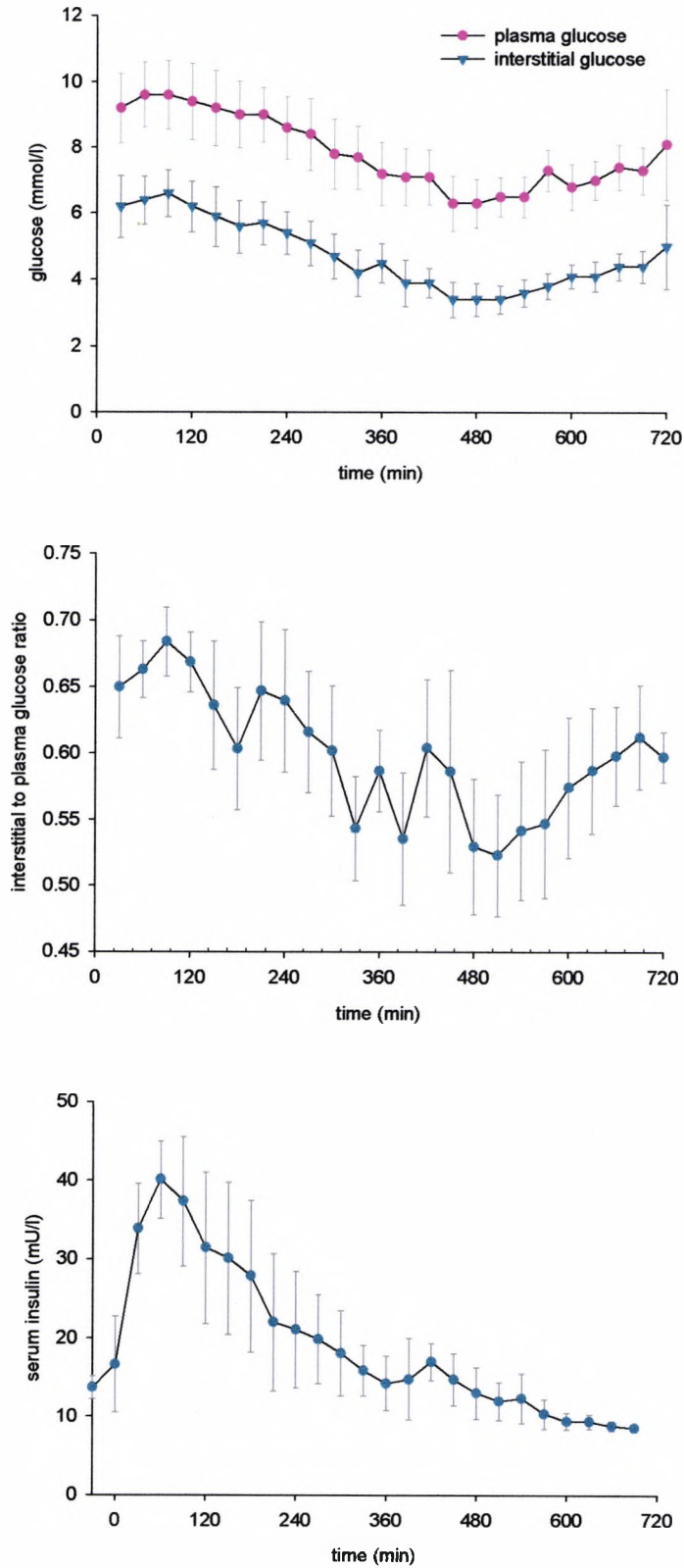


Figure 6.1 Plasma glucose and interstitial glucose (top panel), interstitial to plasma glucose ratio (middle panel), and plasma insulin concentration (bottom panel) (mean \pm SE; $n=9$).

Population parameter estimates, as determined by the iterative two-stage parameter estimation procedure, for the remaining models are shown in Table 6.2. In Models 1 and 2, individual estimates of k_{21} converged to an identical value indicating that the data did not contain sufficient information to discriminate this parameter individually.

Models 1, 2, 7, 8, and 9 demonstrated physiological feasibility of parameter estimates and a *posteriori* identifiability (see Table 6.3).

Figure 6.2 shows weighted residuals associated with these models. Table 6.3 shows the percentage of cases in each of the models, which passed the Runs test. The residuals are scaled assuming a “realistic” measurement error with a CV of 10%. This is an estimate of the true measurement error, which is not known. An upper bound of 16% has been determined from samples taken simultaneously from two interstitial probes (data not shown).

6.3.3 Model selection

The model fit error and the Akaike criterion for models 1, 2, 7, 8 and 9 are shown in Table 6.3. On the basis of these two criteria, Model 9 was selected as best representing the experimental data. This model is also characterised by the highest percentage of cases that passed the Runs test.

Individual parameter estimates for Model 9 are shown in Table 6.4. A sample model fit generated by Model 9 is shown in Figure 6.3. The ISF equilibration time constant (delay $\tau = 1/k'_{02}$) predicted by this model was 10.7 (4.8 - 23.9) min [mean (interquartile range)].

Table 6.2 Population analysis results for a posteriori identifiable models. Values are means (inter-quartile range) (n=9).

Model	k'_{02} ($10^{-2} \times \text{min}^{-1}$)	K_{21} ($10^{-2} \times \text{min}^{-1}$)	k_s ($10^{-3} \times \text{min}^{-1}$ per mmol L^{-1})	F_{02} ($10^{-2} \times \text{mmol L}^{-1}$ min^{-1})	S_i ($10^{-4} \times \text{min}^{-1}$ per mU L^{-1})
1	8.26*	4.44 (3.82 - 5.15)	--	--	--
2	7.25*	4.00 (3.51 - 4.57)	2.4 (-1.8 - 6.6)	--	--
7	4.76 (1.92 - 11.84)	3.48 (1.41 - 8.60)	--	4.04 (2.17 - 7.52)	--
8	11.33 (5.41 - 23.73)	5.78 (2.43 - 13.76)	--	--	3.57 (1.13 - 11.28)
9	9.33 (4.19 - 20.80)	5.73 (2.30 - 14.26)	--	4.66 (2.12 - 10.26)	2.34 (0.80 - 6.82)

*Individual values converged to an identical estimate

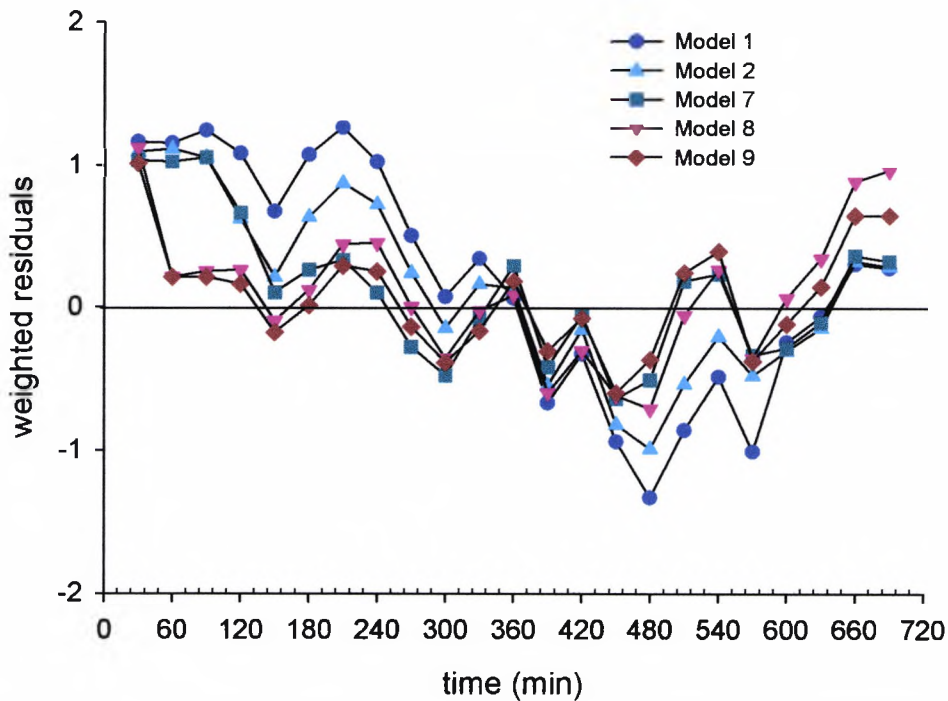


Figure 6.2 Weighted residuals for posteriorly identifiable models. Values are mean ($n=9$).

Table 6.3 Summary of validation and model selection results.

Model No	Physiological feasibility (Yes/No)	Acceptable accuracy (Yes/No)	Model fit error (Mean \pm SD)	Runs test (%) [*]	Akaike criterion (Mean \pm SD)
1	Yes	Yes	15 \pm 7 ^{**}	11	0.97 \pm 0.38
2	Yes	Yes	13 \pm 5	56	0.91 \pm 0.30
3	No	N/A	N/A	N/A	N/A
4	No	N/A	N/A	N/A	N/A
5	No	N/A	N/A	N/A	N/A
6	No	N/A	N/A	N/A	N/A
7	Yes	Yes	11 \pm 4	44	0.80 \pm 0.28
8	Yes	Yes	10 \pm 4	56	0.72 \pm 0.35
9	Yes	Yes	9 \pm 3	67	0.71 \pm 0.26

^{*} Percentage of cases satisfying the test

^{**} Expressed as fractional standard deviation (%)

Table 6.4 Parameter estimates for Model 9.

Subject	k'_{02} ($10^{-2} \times \text{min}^{-1}$)	k_{21} ($10^{-2} \times \text{min}^{-1}$)	F_{02} ($10^{-2} \times \text{mmol L}^{-1}$)	S_i ($10^{-4} \times \text{min}^{-1}$ per mU L^{-1})
1	21.15 (66)*	8.93 (61)	4.18 (111)	15.5 (70)
2	10.09 (49)	6.30 (48)	12.31 (55)	5.6 (58)
3	22.81 (58)	15.81 (57)	2.33 (113)	0.5 (146)
4	0.65 (31)	0.24 (16)	0.56 (71)	0.3 (45)
5	7.18 (30)	5.55 (29)	2.32 (67)	0.4 (138)
6	10.45 (48)	7.91 (49)	18.15 (53)	2.1 (141)
7	23.32 (39)	15.33 (39)	4.19 (77)	12.6 (53)
8	8.59 (23)	6.97 (22)	10.18 (25)	3.0 (33)
9	11.22 (55)	6.51 (52)	8.52 (75)	4.4 (72)

*Accuracy of parameter estimate expressed as a fractional standard deviation (%)

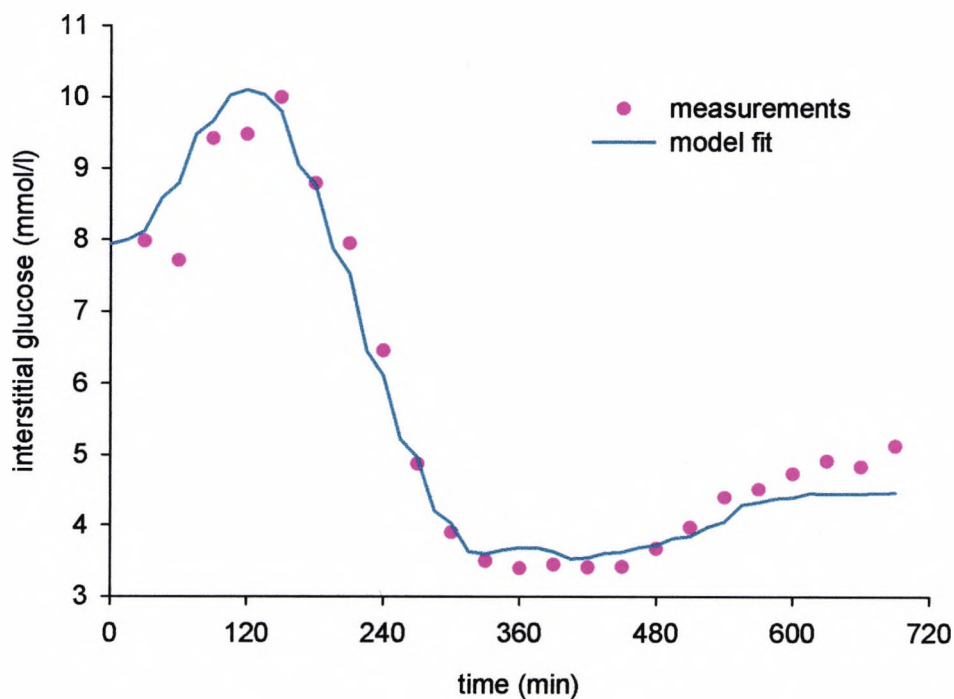


Figure 6.3 Example model fit generated by Model 9.

6.4 Discussion

Using compartment analysis, we identified and quantified possible physiological mechanisms related to the interstitial glucose kinetics during prandial, postprandial, and fasting conditions in subjects with type 1 diabetes.

Having postulated nine distinct models, we assessed their validity on the basis of four criteria: physiological feasibility, the goodness of fit, posterior identifiability, and the distribution of residuals. The selection process employed the principle of parsimony and was complemented by the assessment of the residual error.

Two mechanisms have been identified by the selected model (Model 9) to explain the temporal variation in the IG-PG ratio. These are the zero-order glucose disposal from the interstitial fluid and an insulin effect on glucose transfer from the plasma to the ISF. The former implies that a portion of the disposal is constant and independent of the glucose concentration. The remaining portion is concentration dependent. At normoglycaemia, the constant disposal contributes approximately 10% to the total outflux but this relative contribution increases at lower glucose concentrations. At a hypoglycaemia threshold of 3.3mmol L^{-1} , it is about 20% of the total outflux. Similarly, the IG-PG ratio is also glucose dependent. For example, a fall in plasma glucose from 9 to 3.3mmol L^{-1} will reduce the IG-PG ratio by 0.1. Extrapolating the results outside the range of our experimental data, a more pronounced fall from 9 to 2mmol L^{-1} would lower the IG-PG ratio even further by 0.2. This finding is consistent with observations made by others, who also found a drop in the IG-PG ratio in the hypoglycaemic range (17,130) and the finding may have important implications on the calibration of ISF glucose sensors.

Several authors have noted that recovery from hypoglycaemia takes longer in IG compared to PG (17,59,60,130). This is normally attributed to the push-pull phenomenon, i.e. the insulin-stimulated IG disposal. However, our data offer an alternative explanation. The zero-order disposal affects the time-to-

equilibrium in IG due to the kinetic properties of Model 9 (see model equations). A rise in glucose is associated with a prolonged time-to-equilibrium, whereas a drop in glucose is associated with a shorter equilibration time.

The constant, zero-order disposal can be explained by a portion of glucose transport across the adipose cell membrane being saturated even at low glucose concentrations as supported by Kozka *et al* (6) who found a low K_M value of 3.6mmol L^{-1} and low glucose transport activity in the human adipose tissue with a low GLUT-4 abundance, GLUT-4 being the principal glucose transporter isoform in human adipose cells (4).

The second mechanism identified by the present study is the stimulatory effect of insulin on glucose transfer from the plasma to the ISF. Contrary to current views, this suggests that the IG-PG ratio increases in parallel with plasma insulin within its physiological range. The effect is modest. The IG-PG ratio increases only by 0.03 per 10mU L^{-1} of plasma insulin with a considerable between-subject variability. One should emphasise here the failure of models 3 to 5, which were not compatible with the experimental data. The long time delay of insulin action estimated by model 3 (350min) shifted the insulin action from the early peak into a period of low plasma insulin concentrations making this model behave as Model 8.

Two possible explanations for this effect are at hand. Insulin has been found to induce vasodilatation (131,132) and also to mediate capillary recruitment in tissues (65). Both these effects potentially improve the micro-vascular perfusion and may be responsible for the insulin stimulated transfer of glucose from the plasma to the ISF.

Similarly to Rebrin *et al* (64), our study was not able to detect the stimulatory effect of insulin on glucose disposal, the so called push-pull phenomenon, which has been reported by others and widely discussed in the literature (17,59,66). The pull part of the push-pull phenomenon occurs when the (insulin-stimulated) enhanced uptake of interstitial glucose by the adipocytes

is not fully compensated for by increased delivery of glucose from the plasma. The phenomenon has been documented in studies using high physiological/supra-physiological insulin concentrations during a hyperinsulinaemic clamp, whereas plasma insulin concentrations in our study remained in the low physiological range potentially explaining the discrepancy and questioning the relevance of the push-pull phenomenon in physiological conditions. Furthermore, studies in humans showed that while glucose transport in the adipose tissue of healthy lean subjects is stimulated by insulin approximately two-fold, the transport in the adipose tissue of obese or overweight subjects is not responsive to insulin at all (133). This is also relevant to the present study, which included a few subjects on the borderline of obesity.

The IG-PG ratio estimated by Model 9 is 0.56 at plasma glucose of 9mmol L^{-1} . It is reduced to around 0.46 at the hypoglycaemic threshold of 3.3mmol L^{-1} . This is consistent with other studies. Monsod *et al* (17) documented the IG-PG ratio of 0.65 under basal glucose and insulin levels and also documented a drop in the IG-PG ratio by approximately 20% when moving from euglycaemia to hypoglycaemia. Schaupp *et al* (68) reported a ratio in the range 0.60 to 0.75 within the plasma glucose range from 5 to 10mmol L^{-1} . Both studies investigated healthy subjects.

The equilibration time constant reported in the literature varies considerably from 2min (66) to 25min (60), and even 45min (128), but most authors report a range from 5 to 10min (64,66,70,134), which is comparable to the equilibration time constant obtained in this study (11min). There are, however, difficulties in making direct comparisons as the differences may arise from the use of different sampling techniques, different glucose/insulin ranges, and different subject categories.

The identifiable models, Models 1, 2, 7, 8 and 9, provided consistent parameter estimates, see Table 6.2. The transfer rate constants k'_{02} and k_{21} compare well between the models. However, the individual parameter

estimates varied considerably between subjects, see Table 6.2. Other authors also reported high between-subject variability (63).

The selected Model 9 was only marginally better than Model 7 and Model 8 (see Table 6.3). It failed the Runs test in three out of nine cases suggesting the influence of additional unmodelled effects on the IG-PG ratio such as variable recovery or hormonal influences on model parameters. As hormones are cyclical in nature, a model was proposed, in which oscillations were superimposed on the k_{02} transfer rate constant. Preliminary results showed a marked improvement in model fit and a higher number of cases passing the Runs test. However, we excluded the model from detailed reporting as the nature of the oscillations is lacking explicit physiological interpretation.

We considered practical implications of our modelling study for ISF-based glucose sensing and applied a one-point calibration to the experimental data to determine PG from IG. Population parameter estimates were used as calibration constants. Models 1 and 7 were employed and the calibration results were compared. We chose Model 7 over the selected Model 9 for practical reasons. Model 7 does not require knowledge of plasma insulin concentrations and could, therefore, be used in real-time glucose monitoring.

Figure 6.4 shows the Clarke error grid analysis of a one-point calibration method for Models 1 and 7. The one-point calibration with Model 1 gave 56% points in the region A and 44% in the region B. Model 7 resulted in an increase in the number of points in the region A to 60% and a fall in the number of points in the region B to 40%. Hence, we documented a small advantage in the use of Model 7 for calibration, which could be extended assuming a higher proportion of low glucose readings.

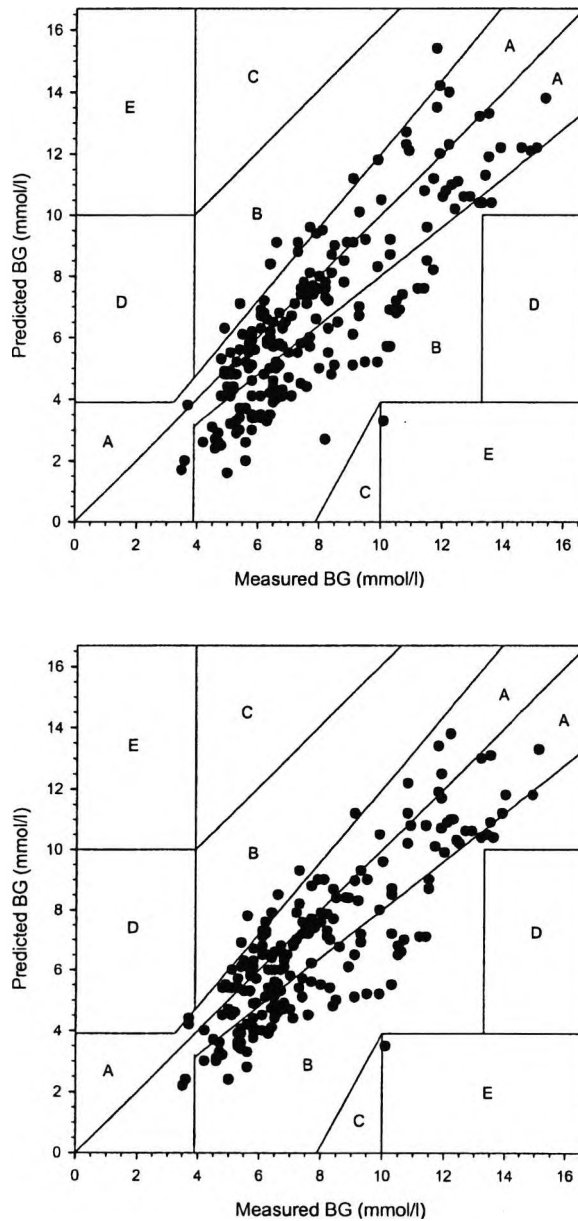


Figure 6.4. The Clarke error grid showing relationship between measured plasma glucose and glucose predicted from IG using Model 1 (top panel; 56% in zone A), and Model 7(bottom panel; 60% in zone A).

6.5 Conclusion

We identified and quantified a model of interstitial glucose kinetics applicable to physiological conditions in subjects with type 1 diabetes. The model implements two effects, which are responsible for temporal variations in the IG-PG ratio, the zero-order removal of glucose from the ISF and the insulin stimulated glucose transfer from the plasma to the ISF.

Chapter 7 Further Evaluation of the Model of Interstitial Glucose Kinetics

7.1 Introduction

A study of modelling interstitial glucose kinetics was described in the previous chapter. Out of the nine models analysed in this study, Model 9 provided the best representation of our experimental data and was, therefore, selected as the best model of interstitial glucose kinetics.

Since the completion of that study, a new richer data set collected over a longer period has become available. This data set was obtained from a clinical trial in twelve subjects with T1DM. The subjects participated in a thirty two hours long experiment.

Further evaluation of Model 9 is presented in this chapter with the aim to reassess the model validity and to compare the results with those obtained in Chapter 6.

7.2 Methods

7.2.1 Subjects and experimental protocol

The experimental protocol and the subjects are described in section 4.2.1. Subject 1 had to be omitted in this study due to an unacceptable high interstitial glucose measurement error. This section also describes the assays, the IG measurement method, and the OFM technique used for sampling the interstitial fluid.

Eleven subjects with type 1 diabetes treated with CSII participated in this study (7/4 M/F, age 41 ± 11 years, duration of diabetes 21 ± 9 years, BMI $24.2 \pm 2.2 \text{ kg/m}^2$, HbA_{1c} $7.4 \pm 0.9\%$, basal/prandial insulin requirements $20.9 \pm 5.6/21.4 \pm 6.0 \text{ U/day}$; mean \pm SD).

Basal insulin infusion profile was optimised prior to the study and the patients not using the short acting insulin analogue lispro were switched to this insulin. Subjects arrived at the clinic at 13:30 and remained there until 22:00 on the following day. They were given dinner at 18:00 on the first study day, breakfast at 8:00, lunch at 14:00 and dinner at 18:00 on the following day.

At the start of the study blood glucose was normalised to a level between 5.5 to 6.6mmol/L using intravenous insulin or glucose as appropriate. Blood samples for plasma insulin were collected every 30min from 14:00 and ISF sampling started at 18:00 using the OFM technique.

7.2.2 Data analysis

7.2.2.1 Model of interstitial glucose kinetics

Data analysis was done using Model 9 (see Chapter 6).

Two effects represented in this model are the zero-order removal of glucose from ISF and the stimulatory effect of insulin on glucose transfer from plasma to ISF. The Model of structure shown in Figure 7.1 is described by the following differential equation:

$$dC_2/dt=[k_{21}+S_I(I-I_b)]C_1-k'_{02}C_2-F_{02}$$

where $k'_{02}=k_{12}+k_{02}$, C_1 and C_2 represent PG and IG concentrations (mmol/L), k_{02} , k_{12} and k_{21} are transfer rate constants (min^{-1}), k'_{02} is the aggregate transfer rate constant (min^{-1}), S_I is insulin sensitivity associated with glucose transfer from plasma to the ISF (min^{-1} per mmol L^{-1}), and F_{02} is the zero-order glucose removal from the ISF ($\text{mmol L}^{-1} \text{min}^{-1}$).

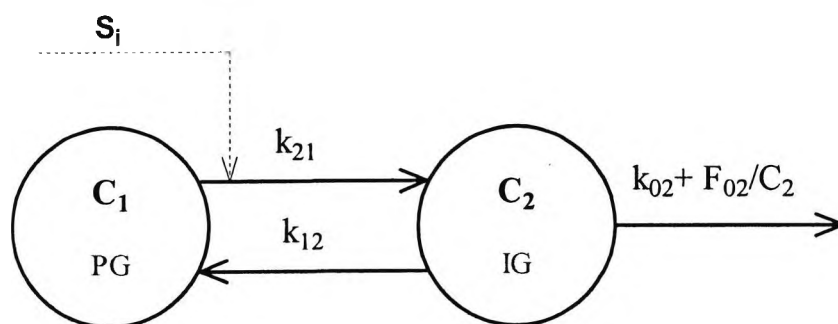


Figure 7.1 Structure of Model 9.

7.2.2.2 Parameter estimation

Model parameters were estimated using the iterative two-stage technique (ITS) implemented in SAAM II Population Kinetics v 1.01 (SAAM Institute, Seattle, WA, USA). In each iteration, the parameters were estimated employing a nonlinear, weighted, least-squares algorithm with an empirical Bayesian term. Prior to estimation the parameters were log-transformed. This was done to assure non-negativity and to correct for skewed distribution of the parameters.

Plasma glucose and plasma insulin were the driving functions. The interstitial glucose averaged over a 30min period was the model output.

As the extent of the measurement error was not known, the relative weighting method in SAAM II was adopted. The weight was defined as the reciprocal of the square of the nominal measurement error (ME) with a CV of 5%. The model fit error (MFE) was obtained from the nominal ME, and the variance parameter was determined by the estimation procedure.

7.2.2.3 Model identification and validation

Similarly to model validation described in Chapter 6, the validity of Model 9 was assessed on the basis of physiological feasibility of parameter estimates, posterior identifiability (CV < 100%), model fit error, and distribution of weighted residuals.

7.2.2.4 Statistical analysis

The significance of the change in the IG-PG ratio was established using a two-way analysis of variance (ANOVA) with effects due to time instance and subject.

The Runs test was used to test for the randomness of the weighted residuals. The Bonferroni correction was applied to the runs test results to correct for multiple comparisons.

In order to compare the two groups of results generated by Model 9, the nonparametric Mann-Whitney U test was applied.

7.3 Results

7.3.1 Plasma glucose, interstitial glucose, plasma insulin and interstitial to plasma glucose ratio

Figure 7.2 shows the mean plasma glucose, interstitial glucose, and plasma insulin. PG and IG concentration ranged from 3.1 to 18.0mmol/L and from 1.7 to 12.8mmol/L, respectively. The plot also shows the IG to PG ratio (0.64 ± 0.11 ; mean \pm SD), which changed significantly during the experiment ($p < 0.0001$).

7.3.2 Parameter estimates and model validation

All parameters demonstrated physiological feasibility. The parameter estimates with their accuracy expressed as CV are listed in Table 7.1.

The parameter k_{21} converged to a population mean in all subjects. The inter-subject variability of the parameter k'_{02} was small.

Table 7.1 Parameter estimates and their accuracy.

Subject	k'_{02} ($10^{-2} \times \text{min}^{-1}$)	k_{21} ($10^{-2} \times \text{min}^{-1}$)	F_{02} ($10^{-2} \times \text{mmol/L}$)	S_1 ($10^{-4} \times \text{min}^{-1}$ per mU L^{-1})
1	9.79 (4)*	8.13**	9.14 (19)	2.9 (63)
2	10.56 (3)	8.13**	4.64 (24)	1.1 (78)
3	12.47 (4)	8.13**	4.75 (40)	2.4 (46)
4	9.91 (4)	8.13**	8.12 (12)	3.5 (37)
5	9.63 (7)	8.13**	12.54 (19)	0.5 (64)
6	10.37 (3)	8.13**	8.76 (15)	1.5 (47)
7	12.42 (3)	8.13**	4.16 (41)	0.6 (84)
8	9.36 (7)	8.13**	21.83 (12)	0.7 (84)
9	10.70 (2)	8.13**	5.73 (17)	0.6 (71)
10	10.45 (4)	8.13**	5.79 (31)	5.9 (20)
11	11.44 (3)	8.13**	4.47 (30)	1.1 (71)

*Accuracy of parameter estimate expressed as a fractional standard deviation (%)

** Parameter value converged to the population mean

The model fit error was $9 \pm 3\%$ (mean \pm SD). The model fits for all eleven subjects are shown in Figure 7.3.

Figure 7.4 shows the distribution of weighted residuals associated with Model 9. The residuals are scaled assuming a 'realistic' measurement error with a CV of 10%. It was confirmed that 56% of cases passed the runs test.

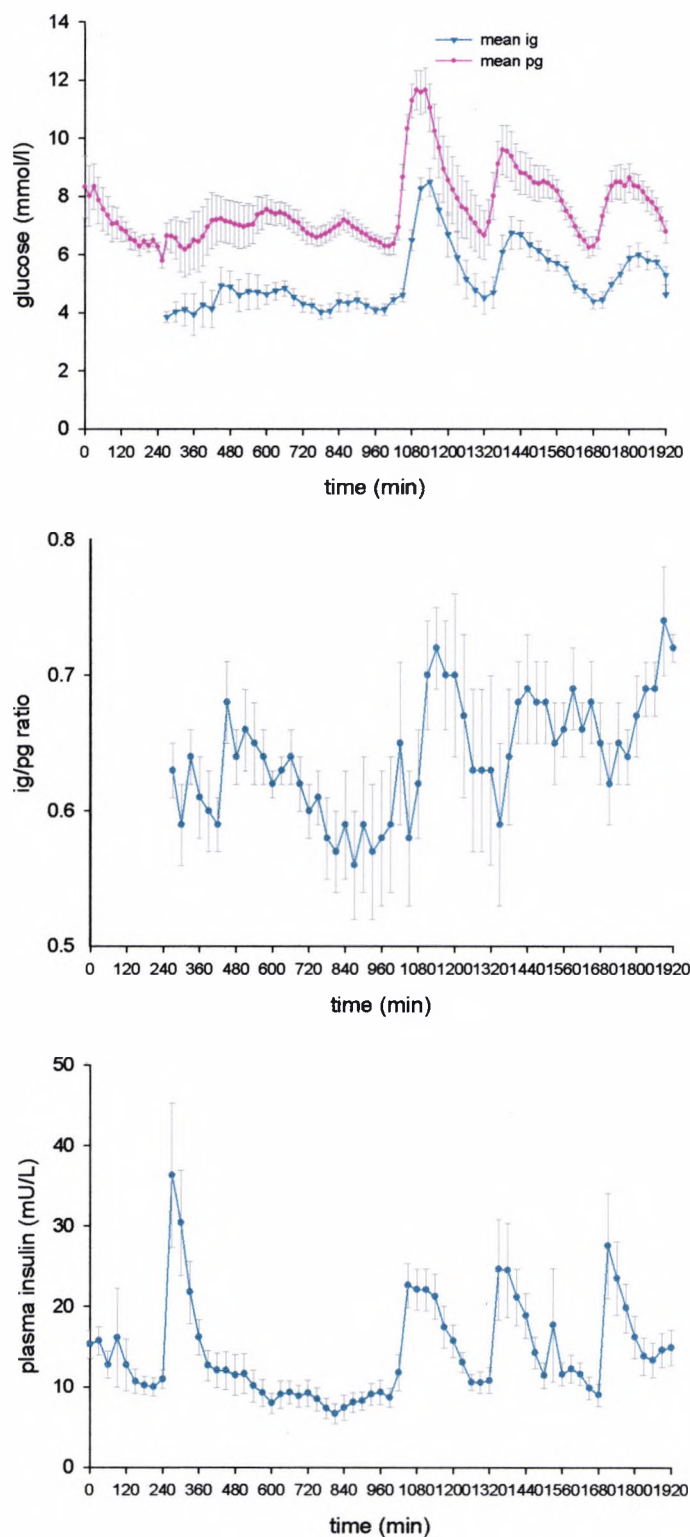


Figure 7.2 Plasma glucose, interstitial glucose (top panel), interstitial to plasma glucose ratio (middle panel), and plasma insulin (bottom panel). Values are mean \pm SE, $n=11$.

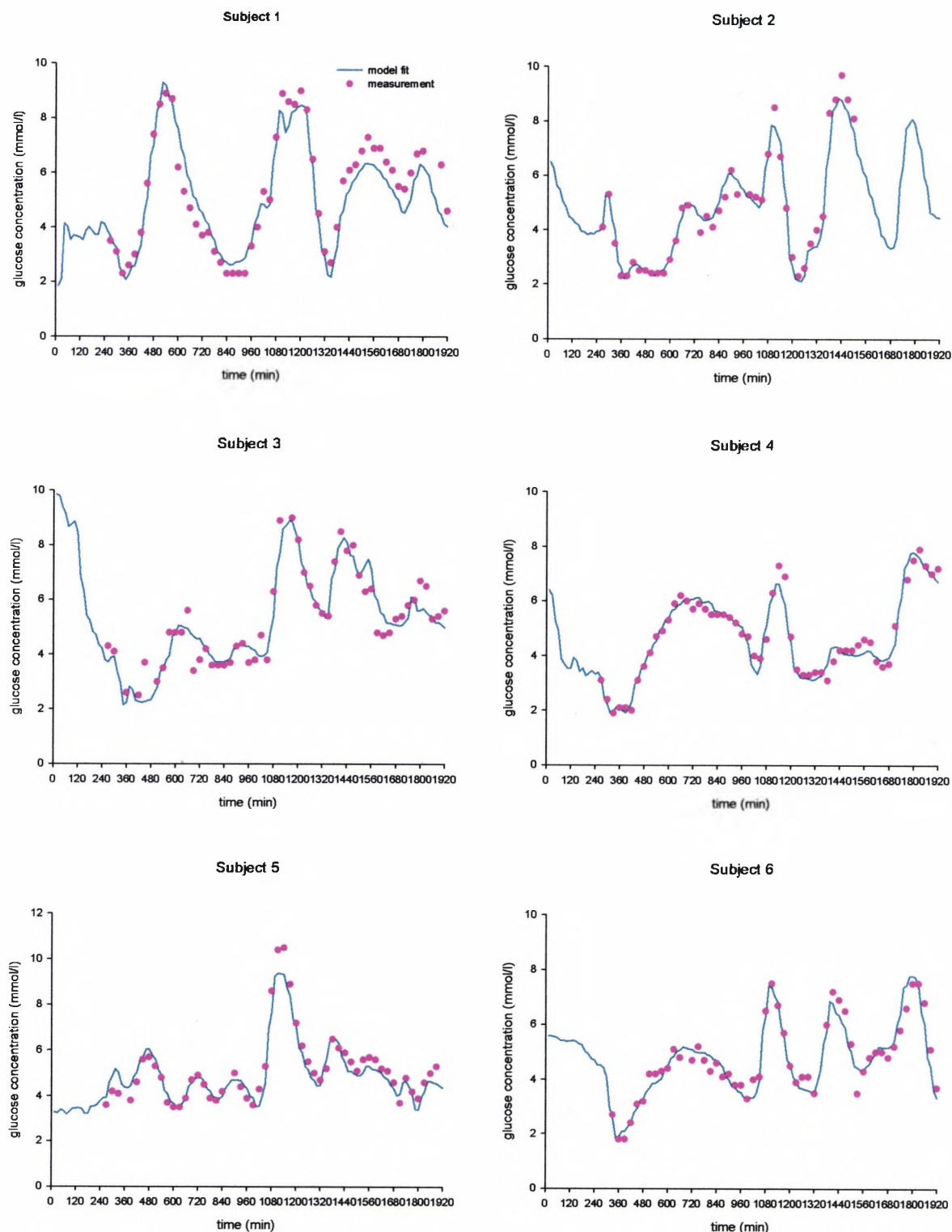


Figure 7.3 Individual model fits generated by Model 9. Pink dot (•) represents measurement and continuous line (—) represents the model fit.

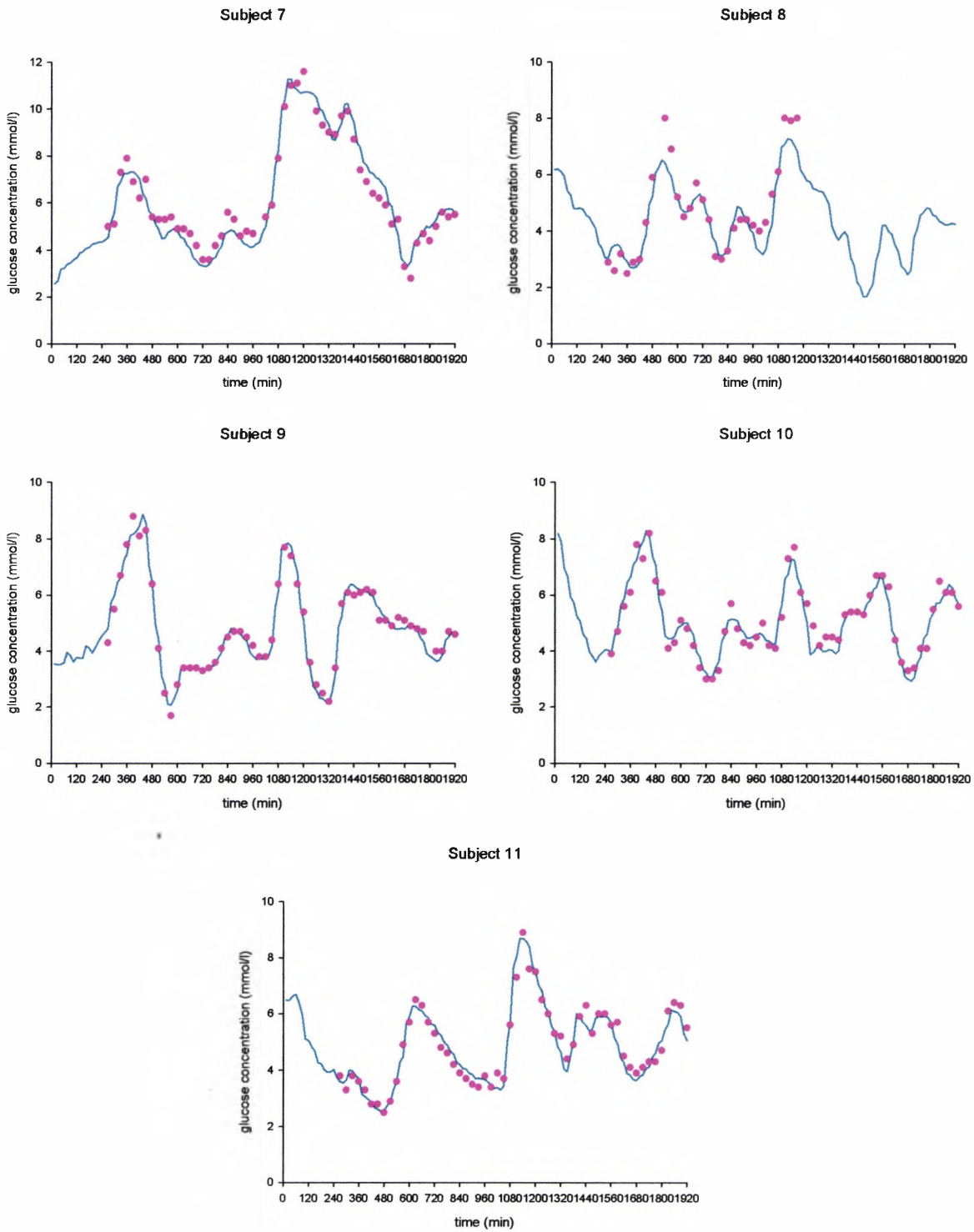


Figure 7.3 (cont.) Individual model fits generated by Model 9. Pink dot (•) represents measurement and continuous line (—) represents the model fit.

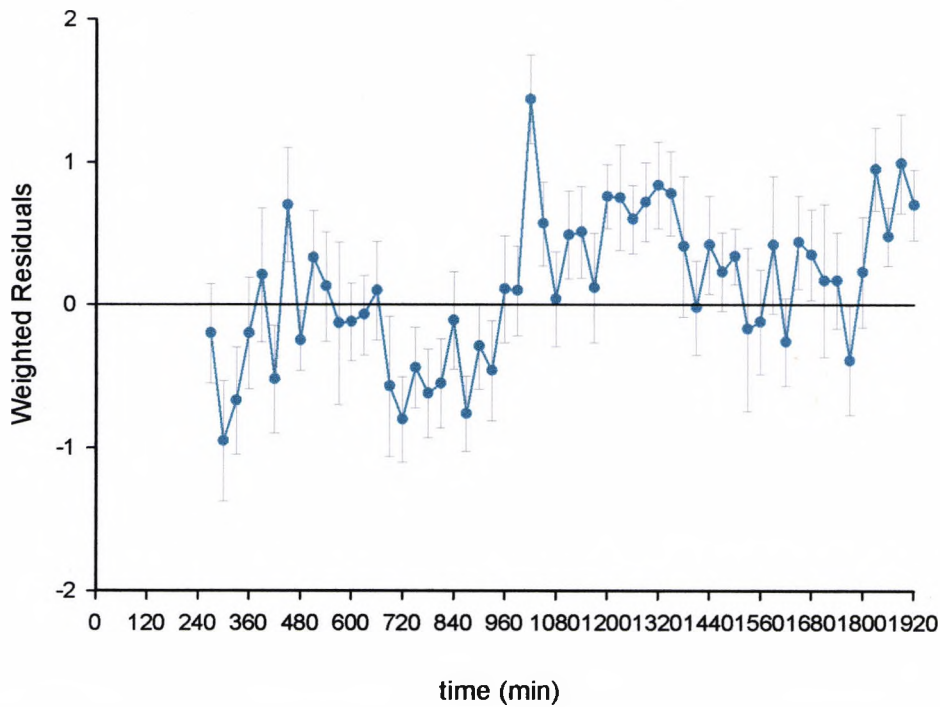


Figure 7.4 Weighted residuals assuming a nominal value for the ME at 10%. Values are mean \pm SE, $n = 11$.

7.3.3 Comparison with estimates obtained in Chapter 6

The population parameter estimates obtained by Model 9 in the present (32h long experiment) and the previous study (12h long experiment) are shown in Table 7.2.

Table 7.2 Population parameter estimates for the two data sets.

Parameter	Mean (IQR) 32h experiment (N=11)	Mean (IQR) 12h experiment (N=9)	p value
k'_{02} ($10^{-2} \times \text{min}^{-1}$)	10.60 (9.87 – 11.38)	9.33 (4.19 – 20.80)	0.94**
k_{21} ($10^{-2} \times \text{min}^{-1}$)	8.13*	5.73 (2.30 – 14.26)	N/A
F_{02} ($10^{-2} \times \text{mmol L}^{-1}$)	7.13 (4.89 – 10.40)	4.66 (2.12 – 10.26)	0.37
S_1 ($10^{-4} \times \text{min}^{-1}$ per mU L^{-1})	1.36 (0.73 – 2.51)	2.34 (0.80 – 6.82)	0.50

* Individual values converged to an identical estimate

** Mann-Whitney U test

7.4 Discussion

Model 9 of interstitial glucose kinetics was tested on an independent set of clinical data. The new data set was richer with four meals instead of one and was recorded over a longer period of time, i.e. 32 hours instead of 12 hours as in the previous study. The subjects differed in the quality of glycaemic control reflected in a lower HbA_{1c}. Reassessing validity of Model 9 and comparison of the results obtained for these two different data sets was an important task.

The obtained results support validity of Model 9. Parameter estimates were physiologically feasible and Model 9 demonstrated posterior identifiability with the range of CVs from 2 to 84% (see Table 7.1). Model 9 provided an acceptable fit to the data (see Figure 7.3) and the model fit error was similar to that reported in Chapter 6 (see Table 6.3).

The range of weighted residuals was acceptable with the exception of the time instant immediately following breakfast. At this particular time a clear underestimation is visible in several subjects (see Figure 7.3) suggesting the existence of unmodelled effects. The runs test was passed in 56% of cases, which is only slightly lower than 67% as obtained previously (see Table 6.3). Visual inspection of the weighted residuals suggests the presence of alternate positive and negative runs. This type of trend is indicative of an oscillatory pattern most likely associated with the possible parameter variation. This is consistent with diurnal changes in insulin sensitivity and carbohydrate metabolism (99,105,135).

The exact mechanisms responsible for these diurnal variations are not known. It is presumed that they could be hormonal, due to varying levels of growth hormone or cortisol, or neural caused by the rhythms in the autonomic nervous system where adrenergic stimulation has been shown to inhibit insulin action (136). The oscillations in carbohydrate metabolism could be linked to the cyclical nature of gastric motility occurring in man (137).

Van Cauter *et al* (105) demonstrated modulation of glucose responses to mixed meals by circadian rhythmicity and correlated these responses with cortisol concentrations. Their results also show that meal related increases in cortisol levels occur consistently in the morning and together with other hormonal or neural influences could be responsible for the particular difficulty of our model to provide a good fit to the data around the breakfast time.

Parameter estimates obtained in the new study were shown to be similar to those obtained in Chapter 6 (see Table 7.2).

An interesting characteristic of the new set of results is a smaller variability of parameters reflected in a narrower inter-quartile range (see Table 7.2). This finding is consistent with the fact that the subjects in 32h study were well controlled (a tight range of HbA_{1c}).

The convergence of parameter k_{21} to the population value appears to be associated with the property of ITS technique. Due to insufficient information included in the data individual estimates of this parameter could not be obtained. This, in turn, led to their convergence to the population mean.

The results of this study support the validity of Model 9 with an exception of nonrandom distribution of the weighted residuals in 44% of cases. This shortcoming of Model 9 suggests the presence of unmodelled effects, which were discussed earlier. The above effects were not included in our time invariant model. It might be, therefore, appropriate to consider a time varying model in the future investigations.

In summary, the current results support validity of Model 9, which provided a good explanation to our experimental data with a small model fit error and good precision of parameter estimates. Parameter estimates were physiologically feasible and were similar to those obtained in Chapter 6.

It is acknowledged, however, that certain effects, most probably associated with time varying parameters, may require further exploration.

Chapter 8 Discussion and Conclusion

8.1 Overall Discussion

The AP has been a research goal for over three decades. The first prototype (20) was designed for intravenous glucose sampling and intravenous insulin infusion. The present research has concentrated on the subcutaneous delivery of insulin and the subcutaneous glucose testing as these methods are less invasive and more suitable for routine use. However, the SC-SC approach, as it is called, poses problems to the efficient glucose control. Due to the lack of availability of a reliable SC glucose sensor, experimental set up for testing an AP algorithm often resorts to using a SC-IV approach, i.e. the subcutaneous insulin infusion and the intravenous glucose measurements.

The primary aim of this thesis was to explore the use of compartmental modelling techniques with in-built physiological constraints to facilitate the development of a wearable artificial pancreas. In particular, this study aimed to extend and evaluate an existing model of the glucoregulatory system on a set of data obtained in a clinical trial designed to test the AP algorithm.

Further objectives included support for the *in silico* testing of an artificial pancreas through investigating interstitial glucose and insulin lispro kinetics, and by generating sets of parameters to represent 'virtual' subjects with T1DM in the AP simulator.

Both the AP algorithm and the simulator were developed in the course of an EC-funded project ADICOL (Advanced Insulin Infusion using a Control Loop). The objective of this project was to develop a treatment system that continuously measures and controls glucose in subjects with type 1 diabetes, i.e. an artificial pancreas. The project activities included the development of glucose sensors, the development of glucose controllers encompassing the development of a glucose simulator, clinical testing, and system integration. After a series of successful clinical trials, the ADICOL project confirmed feasibility of glucose control with a wearable, modular AP comprising a SC

glucose sensor, a control algorithm running on a palmtop computer, and a SC delivery of lispro using insulin pump.

The availability of a rich set of clinical data obtained in clinical trials designed to test the AP control algorithm within the ADICOL project prompted the exploration of the possibility of modelling the input-output relationship between the subcutaneous insulin delivery and the intravenous glucose measurements. The study involved the extension of a previously validated model of the glucose-insulin system (55) in type 1 diabetes under new conditions. Apart from the model validation, the study had other potential benefits. Assuming that the model was valid, its parameters could be used in the AP simulator to represent a set of 'virtual' subjects with T1DM. This would constitute a major step towards enhancing the AP simulation environment and providing methods to create a 'virtual' but realistic population.

Unfortunately, the model validity could not be ascertained. A number of model parameters, such as the three insulin sensitivities and the glucose distribution volume, reached non-physiological values and displayed an excessively high inter-subject variability. Otherwise, the model provided a good fit to the data (see Figure 4.4 in Chapter 4).

Our study supported the presence of ultradian oscillations in the insulin sensitivities. The variation in response to different meals was shown to be on the borderline of statistical significance. Despite the fact that the model validity was not confirmed, the results are of importance and could serve as a benchmark for new models to be tested in the future.

The subcutaneous insulin delivery is associated with an additional delay and a high inter-subject variability in the absorption parameters. Although the new rapid acting insulin analogues produce a more predictable time action profile, certain issues around the absorption kinetics remain unresolved. The study described in Chapter 5 investigated the absorption kinetics of lispro insulin analogue during bolus and continuous infusion modes of delivery. Ten models, nine of which were compartmental, were proposed assuming various

putative physiological effects and re-using some of the previously published models (75,82). The assessment of model validity was based on four criteria discussed by Carson *et al* (23). Valid models were then compared using the principle of parsimony (23) and a model which best represented our experimental data was identified. The model best representing the experimental data was identified as Model 9 (see Chapter 5). This model assumed local insulin degradation at the injection site and two, slow and fast, absorption channels. Both effects are a little controversial. Local insulin degradation is considered significant by some authors (108,116) but disregarded by others (78,81). In Model 9 the local degradation, implemented as a Michaelis-Menten relation, was estimated as a small but significant proportion of the total insulin dose in the physiological range of insulin concentrations [$V_{MAX,LD}=1.93(0.62 - 6.03)\text{mU min}^{-1}$, $K_{M,LD}=62.6(62.6 - 62.6)\text{mU}$]. The idea of two insulin absorption channels, although reported in literature (87), does not have an immediate physiological interpretation. A possible explanation could be the existence of a dimer-monomer equilibrium, the two association states of insulin. The dimers have been shown to be absorbed slower than the monomers (78). Our model estimated that 67% of insulin passes through the slow absorption channel and the remaining 33% passes through the fast channel.

The greatest hurdle in the development of a wearable extracorporeal artificial pancreas is the availability of an accurate and reliable long-term subcutaneous glucose sensor. The accuracy of the current sensors has been questioned (17). One of the main problems related to the accuracy of subcutaneous sensors is the fact that they measure glucose concentration in the interstitial fluid and translate it into the plasma glucose reading using a simple multiplication factor. A significance test conducted in this study (see Chapter 6) demonstrated a time varying IG-PG ratio pointing to a more complex relationship between the two entities. To investigate the true relationship we postulated nine distinct compartmental models and quantified possible physiological mechanisms involved in this process. A similar process to that described in Chapter 5 was followed. The models were identified, validated, and the best model was selected using the principle of parsimony.

Two mechanisms explaining the temporal variation in the IG-PG ratio were identified by the selected model (Model 9 in Chapter 6). These were the zero-order glucose disposal and a positive effect of insulin on glucose transfer from the plasma to the ISF. The former is responsible for a reduction in the IG-PG ratio with a falling plasma glucose concentration (a fall in PG from 9 to 3.3mmol/L will reduce the IG-PG ratio by 0.1). The latter, a smaller effect, is responsible for an increase in the IG-PG ratio with a rising plasma insulin concentration (a 10mU/L rise in plasma insulin will increase the IG-PG ratio by 0.03).

The two mechanisms could explain observations made by other researchers. A lower IG-PG ratio was observed at low glucose concentrations (17,130). Several authors also observed a longer recovery from hypoglycaemia in the interstitial glucose (17,59,60,130). The effect, which is normally attributed to the push-pull phenomenon, can be explained by the kinetic properties of the model proposed in Chapter 6 (due to zero-order removal of glucose affecting the time-to-equilibrium). The stipulated push-pull phenomenon was not detected in this study.

Although Model 9 was shown to best represent our data, it was by no means an ideal representation. The Runs test was not passed in a number of cases suggesting the existence of unmodelled effects. Hence, as a new richer data set had become available we set out to re-evaluate this model on the new data set (see Chapter 7). The obtained results supported the validity of the model and the model parameters compared well with those obtained in Chapter 6. This was despite certain differences in the study population such as a tighter glycaemic control.

Model 9 describing the interstitial glucose kinetics was used successfully in the AP simulator to predict the results of clinical trials conducted as part of the ADICOL project.

As Claude Bernard said: "The application of mathematics to natural phenomena is the aim of all science" (*Bernard, 1895*). In this study the use of mathematical models in support of the development of an AP was explored.

Several models have been proposed and important results obtained. We acknowledge the fact that the proposed models are by no means the true representation of systems they are meant to represent. However, by definition, models only provide an approximate description of the real system. Thus, the assessment whether or not the given model is valid, i.e. adequate for its purpose, remains a difficult task. The models were subject to assumptions and simplifications, which are inevitable when dealing with a complex biological system. Certain effects could not be modelled due to an insufficient knowledge to describe them or due to the fact that they would affect the computational complexity to unacceptable levels.

In conclusion, this thesis provides an insight into the mechanisms involved in the insulin and interstitial glucose kinetics. The results should be expanded by a further research in this field.

8.2 Achievement of Objectives

This section deals with each of the objectives listed in Chapter 2 and describes the extent to which they were met.

A. Objectives in relation to modelling of the input-output relationship between subcutaneously administered insulin and intravenously measured plasma glucose:

- To extend and validate an existing model of the glucoregulatory system on a set of clinical data recorded over 28 hours in trials involving subjects with type 1 diabetes treated by CSII;
- To estimate model parameters for individual subjects with the aim to provide an AP simulator with a set of 'virtual' subjects with type 1 diabetes.

Of the two objectives in this category only the first one was met. The given model was extended and applied to the experimental data. Unfortunately, as the model validity was not confirmed, the parameter estimates are not reliable enough to be used to represent 'virtual' subjects in the AP simulator.

B. Objectives in relation to modelling of the subcutaneously administered insulin lispro kinetics:

- To develop and validate a model of subcutaneously administered insulin lispro kinetics in type 1 diabetes during the standard insulin pump treatment with bolus and CSII modes of delivery.

This objective was met in full. A model of insulin lispro kinetics in type 1 diabetes was identified and validated.

C. Objectives in relation to modelling of interstitial glucose kinetics:

- To investigate the relationship between plasma glucose and interstitial glucose;
- To develop and validate a model of interstitial glucose kinetics under physiological conditions in subjects with type 1 diabetes.

The objectives in relation to modelling of interstitial glucose kinetics were also met as planned. A model of interstitial glucose kinetics was developed and validated, and the relationship between plasma glucose and interstitial glucose was established.

8.3 Future Work

8.3.1 Generating 'virtual' subjects with type 1 diabetes

The objective of supplying the AP simulator with 'virtual' subjects with type 1 diabetes was not met in this study. In order to meet this objective, further attempts should be made to arrive at a valid model of the input-output relationship between subcutaneously administered insulin and plasma glucose concentration. Other models should be investigated. The most obvious suggestion would be to replace the simple two-compartment model of insulin kinetics with Model 9 described in Chapter 5. The gut absorption model also requires further research, in particular, the time of meal ingestion should be taken into account. Alternatively, to avoid the reported drawbacks of the ITS technique, other methods of population analysis should be explored.

8.3.2 Insulin lispro kinetics

Ten models were proposed in Chapter 5 to represent lispro absorption kinetics in subjects with type 1 diabetes treated by CSII. The list of possible models was not exhausted here. Other models could be explored and tested on the data. Similarly to the best model of interstitial glucose kinetics, Model 9 in Chapter 5 could also be re-evaluated on the set of independent data.

8.3.3 Interstitial glucose kinetics

The model of interstitial glucose kinetics proposed in Chapter 6 and re-evaluated in Chapter 7 provided a good representation to the experimental data. However, non-randomness of the weighted residuals in a number of cases also pointed to some unmodelled effects. These effects should be identified and modelled in future studies. In particular, time varying parameters may need to be considered. The oscillatory pattern observed in the insulin sensitivities in Chapter 4 may be responsible for the modulation of the relevant transfer rate constants.

References

1. Williams G, Pickup JC: *Handbook of Diabetes*. London, Blackwell Science, 1999
2. Diabetic Control and Complications Trial Research Group: The effect of intensive treatment of diabetes on the development and progression of long term complications in insulin-dependent diabetes mellitus. *N.Engl.J.Med.* 329:977-986, 1993
3. Tortora GH, Anagnostakos NP: *Principles of Anatomy and Physiology*. New York, Harper and Row Publishers, 1987
4. Zierler K: Whole body glucose metabolism. *Am.J.Physiol.* 276:E409-E426, 1999
5. Katzung BG: Basic Principles-Introduction. In Basic and Clinical Pharmacology. Katzung BG, Ed. Appleton-Lange, 1998, p. 5
6. Kozka IJ, Clark AE, Reckless JPD, Cushman SW, Gould GW, Holman GD: The effects of insulin on the level and activity of the GLUT4 present in human adipose-cells. *Diabetologia* 38:661-666, 1995
7. The Expert Committee on the Diagnosis and Classification of Diabetes Mellitus: Report of the Expert Committee on the Diagnosis and Classification of Diabetes Mellitus. *Diabetes Care* 26:S5-S20, 2003
8. WHO. Definition, Diagnosis and Classification of Diabetes Mellitus and its Complications. 1999. World Health Organization.
9. Bell GI, Polonsky KS: Diabetes mellitus and genetically programmed defects in beta- cell function. *Nature* 414:788-791, 2001
10. Douek IF, Gillespie KM, Bingley PJ, Gale EAM: Diabetes in the parents of children with Type I diabetes. *Diabetologia* 45:495-501, 2002
11. Van den Berghe G, Wouters P, Weekers F, Verwaest C, Bruyninckx F, Schetz M, Vlasselaers D, Ferdinande P, Lauwers P, Bouillon R: Intensive insulin therapy in the surgical intensive care unit. *N.Engl.J Med.* 345:1359-1367, 2001

References

12. Wild SH, Williams DRR: The Global Burden of Disease Study underestimates diabetes prevalence in the United Kingdom. *Diabetic Med.* 20:44, 2003
13. UK Prospective Diabetes Study Group. Intensive blood-glucose control with sulphonylureas or insulin compared with conventional treatment and risk of complications in patients with type 2 diabetes (UKPDS 33). *Lancet* 352:837-853, 1998
14. Kang S, Creagh FM, Peters JR, Brange J, Volund A, Owens DR: Comparison of subcutaneous soluble human insulin and insulin analogues (AspB9, GluB27; AspB10; AspB28) on meal-related plasma glucose excursions in type 1 diabetic subjects. *Diabetes Care* 14:571-577, 1991
15. Robinson MR, Eaton RP, Haaland DM, Koepp GW, Thomas EV, Stallard BR, Robinson PL: Noninvasive glucose monitoring in diabetic patients - A preliminary evaluation. *Clin.Chem.* 38:1618-1622, 1992
16. Heise HM: Non-invasive monitoring of metabolites using near infrared spectroscopy: State of the art. *Horm.Metab.Res.* 28:527-534, 1996
17. Monsod TP, Flanagan DE, Rife F, Saenz R, Caprio S, Sherwin R, Tamborlane W: Do sensor glucose levels accurately predict plasma glucose concentrations during hypoglycemia and hypoinsulinemia. *Diabetes Care* 25:889-893, 2002
18. Guerci B, Floriot M, Bohme P, Durain D, Benichou M, Jellimann S, Drouin P: Clinical performance of CGMS in type 1 diabetic patients treated by continuous subcutaneous insulin infusion using insulin analogs. *Diabetes Care* 26:582-589, 2003
19. Shichiri M: *Artificial Endocrine Pancreas. Development and Clinical Applications.* Kumamoto, Japan, Kamome Press Co., 2000
20. Albisser AM, Leibel BS, Ewart TG, Davidovac Z, Botz CK, Zingg W: An artificial endocrine pancreas. *Diabetes* 23:389-404, 1974
21. Renard E, Costalat G, Moran B, Shah R, Zhang YN, Villegas D, Kolopp M, Lebel R, Bringer J: First combined implantations of a long-term IV glucose sensor and an intra-peritoneal insulin pump in diabetic patients. *Diabetes* 50:A3, 2001

References

22. Cobelli C, Foster DM: Compartmental models: Theory and practice using the SAAM II software system. *Mathematical Modelling in Experimental Nutrition* 445:79-101, 1998
23. Carson ER, Cobelli C, Finkelstein L: *The Mathematical Modeling of Metabolic and Endocrine Systems*. New York, Wiley, 1983
24. Akaike H: A new look at the statistical model identification. *IEEE Trans. Automat. Contr.* AC-19:716-723, 1974
25. Schwartz G: Estimating the dimension of a model. *Annals Of Statistics* 5:461-464, 1978
26. Cobelli C, Foster D, Toffolo G: *Tracer Kinetics in Biomedical Research. From Data to Model*. New York, Kluwer Academic/Plenum Publishers, 2000
27. Hovorka R, Vicini P: Parameter estimation. In *Modelling Methodology for Physiology and Medicine*. Carson ER, Cobelli C, Eds. San Diego, Academic Press, 2001, p. 107-151
28. Vicini P, Cobelli C: The iterative two-stage population approach to IVGTT minimal modeling: improved precision with reduced sampling. Intravenous glucose tolerance test. *Am.J.Physiol.* 280:E179-E186, 2001
29. Cobelli C, Bier DM, Ferrannini E: Modeling glucose metabolism in man: Theory and practice. *Horm.Metab.Res.* 24:1-10, 1990
30. Bolie VW: Coefficients of normal blood glucose regulation. *J.Clin.Invest.* 39:783-788, 1960
31. Ackerman E, Gatewood LC, Rosevear JW, Molnar GD: Model studies of blood-glucose regulation. *Bull.Math.Biophys.* 27:21-37, 1965
32. Charrette, W. P., Kadish, A. H., and Sridhar, R. A nonlinear dynamic model of endocrine control of metabolic processes. 1967. Stockholm. *7th Int. Conf. on Med. and Biol. Eng.* 16-8-1967.
33. Cerasi E, Fick G, Rudemo M: A mathematical model for the glucose induced insulin release in man. *Eur.J.Clin.Invest.* 4:267-278, 1974

References

34. Insel PA, Liljenquist JE, Tobin JD, Sherwin RS, Watkins P, Andres R, Berman M: Insulin control of glucose metabolism in man. *J.Clin.Invest.* 55:1057-1066, 1975
35. Guyton JR, Foster RO, Soeldner JS, Tan MH, Kahn CB, Koncz L, Gleason RE: A model of glucose-insulin homeostasis in man that incorporates the heterogeneous fast pool theory of pancreatic insulin release. *Diabetes* 27:1027-1042, 1978
36. Sorensen, J. T.: A physiologic model of glucose metabolism in man and its use to design and assess improved insulin therapies for diabetes. PhD Thesis. Massachusetts Institute of Technology, 1985
37. Cramp DG, Carson ER: The dynamics of short-term blood glucose regulation. In *Carbohydrate Metabolism: Quantitative Physiology and Mathematical Modelling*. Cobelli C, Bergman RN, Eds. Chichester, Wiley, 1981, p. 349-367
38. Cobelli C, Federspil G, Pacini G, Salvan A, Scandellari C: An integrated mathematical model of the dynamics of blood glucose and its hormonal control. *Math.Biosc.* 58:27-60, 1982
39. Salzsieder E, Albrecht G, Fischer U, Freyse EJ: Kinetic modeling of the glucoregulatory system to improve insulin therapy. *IEEE Trans.Biomed.Eng.* 32:846-856, 1985
40. Berger M, Rodbard D: Computer-simulation of plasma-insulin and glucose dynamics after subcutaneous insulin injection. *Diabetes Care* 12:725-736, 1989
41. Bergman RN, Ider YZ, Bowden CR, Cobelli C: Quantitative estimation of insulin sensitivity. *Am.J.Physiol.* 236:E667-E677, 1979
42. Lehmann ED, Deutsch T: A physiological model of glucose interaction in Type 1 Diabetes Mellitus. *Journal of Biomedical Engineering* 14:235-242, 1992
43. Boroujerdi MA, Umpleby AM, Jones RH, Sonksen PH: A simulation-model for glucose kinetics and estimates of glucose- utilization rate in type-1 diabetic-patients. *Am.J.Physiol.* 31:E 766-E 774, 1995

References

44. Cobelli C, Toffolo G, Ferrannini E: A model of glucose kinetics and their control by insulin, compartmental and noncompartmental approaches. *Math.Biosc.* 72:291-315, 1984
45. Mari A: Mathematical modelling in glucose metabolism and insulin secretion. *Curr.Opin.Clin.Nutr.Metab.Care* 5:495-501, 2002
46. Matthews DR, Hosker JP, Rudenski AS, Naylor BA, Treacher DF, Turner RC: Homeostasis model assessment: insulin resistance and β -cell function from fasting plasma glucose and insulin concentrations in man. *Diabetologia* 28:412-419, 1985
47. Hosker JP, Matthews DR, Rudenski AS, Burnett MA, Darling P, Bown EG, Turner RC: Continuous infusion of glucose with model assessment: measurement of insulin resistance and β -cell function in man. *Diabetologia* 28:401-411, 1985
48. Cobelli C, Pacini G, Toffolo G, Sacca L: Estimation of insulin sensitivity and glucose clearance from minimal model: New insights from labeled IVGTT. *Am.J.Physiol.* 250:E591-E598, 1986
49. Regittnig W, Trajanoski Z, Leis HJ, Ellmerer M, Wutte A, Sendlhofer G, Schaupp L, Brunner GA, Wach P, Pieber TR: Plasma and interstitial glucose dynamics after intravenous glucose injection - Evaluation of the single-compartment glucose distribution assumption in the minimal models. *Diabetes* 48:1070-1081, 1999
50. Vicini P, Caumo A, Cobelli C: The hot IVGTT two-compartment minimal model: indexes of glucose effectiveness and insulin sensitivity. *Am.J.Physiol.* 273:E1024-E1032, 1997
51. Avogaro A, Bristow JD, Bier DM, Cobelli C, Toffolo G: Stable-label intravenous glucose tolerance test minimal model. *Diabetes* 38:1048-1055, 1989
52. Caumo A, Cobelli C: Hepatic glucose production during the labeled IVGTT: estimation by deconvolution with a new minimal model. *Am.J.Physiol.* 264:E829-E841, 1993
53. Cobelli C, Caumo A, Omenetto M: Minimal model S-G overestimation and S-I underestimation: improved accuracy by a Bayesian two-compartment model. *Am J Physiol* 277:E481-E488, 1999

References

54. Ferrannini E, Smith JD, Cobelli C, Toffolo G, Pilo A, DeFronzo RA: Effect of insulin on the distribution and disposition of glucose in man. *J.Clin.Invest.* 76:357-364, 1985
55. Hovorka R, Shojaee-Moradie F, Carroll PV, Chassin LJ, Gowrie IJ, Jackson NC, Tudor RS, Umpleby AM, Jones RH: Partitioning glucose distribution/transport, disposal, and endogenous production during IVGTT. *Am.J.Physiol.* 282:E992-E1007, 2002
56. Natali A, Gastaldelli A, Camastra S, Sironi AM, Toschi E, Masoni A, Ferrannini E, Mari A: Dose-response characteristics of insulin action on glucose metabolism: a non-steady-state approach. *Am.J.Physiol.* 278:E794-E801, 2000
57. Mari A, Stojanovska L, Proietto J, Thorburn AW: A circulatory model for calculating non-steady-state glucose fluxes. Validation and comparison with compartmental models. *Comput.Methods Programs Biomed.* 71:269-281, 2003
58. Zierler KL: Theory of the use of arteriovenous concentration differences for measuring metabolism in steady and non-steady-states. *J.Clin.Invest.* 40:2111-2125, 1961
59. Aussedat B, Dupire-Angel M, Gifford R, Klein JC, Wilson GS, Reach G: Interstitial glucose concentration and glycemia: implications for continuous subcutaneous glucose monitoring. *Am.J.Physiol.* 278:E716-E728, 2000
60. Moberg E, HagstromToft E, Arner P, Bolinder J: Protracted glucose fall in subcutaneous adipose tissue and skeletal muscle compared with blood during insulin-induced hypoglycaemia. *Diabetologia* 40:1320-1326, 1997
61. Schmidt FJ, Slatter WJ, Schooner AJM: Glucose concentration in subcutaneous extracellular space. *Diabetes Care* 16:695-700, 1993
62. Sternberg F, Meyerhoff C, Mennel FJ, Mayer H, Bischof F, Pfeiffer EF: Subcutaneous glucose concentration in humans: real estimation and continuous monitoring. *Diabetes Care* 18:1266-1269, 1995
63. Summers LKM, Clark ML, Humphreys SM, Bugler J, Frayn KN: The use of microdialysis to monitor rapid changes in glucose concentration. *Horm.Metab.Res.* 31:424-428, 1999

References

64. Rebrin K, Steil GM, Van Antwerp WP, Mastrototaro JJ: Subcutaneous glucose predicts plasma glucose independent of insulin: implications for continuous monitoring. *Am.J.Physiol.*E561-E571, 1999
65. Serne EH, IJzerman RG, Gans ROB, Nijveldt R, de Vries G, Evertz R, Donker AJM, Stehouwer CDA: Direct evidence for insulin-induced capillary recruitment in skin of healthy subjects during physiological hyperinsulinemia. *Diabetes* 51:1515-1522, 2002
66. Sternberg F, Meyerhoff C, Mennel FJ, Mayer H, Bischof F, Pfeiffer EF: Does fall in tissue glucose precede fall in blood glucose? *Diabetologia* 39:609-612, 1996
67. Thennadil SN, Rennert JL, Wenzel BJ, Hazen KH, Ruchti TL, Block MB: Comparison of glucose concentration in interstitial fluid, and capillary and venous blood during rapid changes in blood glucose levels. *Diabetes Technol. Ther.* 3:357-365, 2001
68. Schaupp L, Ellmerer M, Brunner GA, Wutte A, Sendlhofer G, Trajanoski Z, Skrabal F, Pieber TR, Wach P: Direct access to interstitial fluid in adipose tissue in humans by use of open-flow microperfusion. *Am.J.Physiol.* 39:E401-E408, 1999
69. Trajanoski Z, Brunner GA, Schaupp L, Ellmerer M, Wach P, Pieber TR, Kotanko P, Skrabal F: Open-flow microperfusion of subcutaneous adipose tissue for on-line continuous ex vivo measurement of glucose concentration. *Diabetes Care* 20:1114-1121, 1997
70. Bantle JP, Thomas W: Glucose measurement in patients with diabetes mellitus with dermal interstitial fluid. *Journal Lab Clin Med* 130:436-441, 1997
71. Lonroth P, Jansson PA, Smith U: A Microdialysis method allowing characterization of intercellular water space in humans. *Am.J.Physiol.* 253:E228-E231, 1987
72. Lonroth P, Jansson PA, Smith U: A microdialysis method allowing characterization of intercellular water space in humans. *Am.J.Physiol.* 253:E228-E231, 1987
73. Hoss U, Salgado M, Sternberg F, Rinne H, Pfeiffer EF: Insulin lispro improves glycemic control in iddm patients under continuous subcutaneous insulin infusion (CSII). *Diabetologia* 40:1320, 1997

References

74. Bolinder J, HagstromToft E, Ungerstedt U, Arner P: Self-monitoring of blood glucose in type 1 diabetic patients: Comparison with continuous microdialysis measurements of glucose in subcutaneous adipose tissue during ordinary life conditions. *Diabetes Care* 20:64-70, 1997
75. Berger M, Cuppers HJ, Hegner H, Jorgens V, Berchtold P: Absorption kinetics and biologic effects of subcutaneously injected insulin preparations. *Diabetes Care* 5:77-91, 1982
76. Binder C, Lauritzen T, Faber O, Pramming S: Insulin pharmacokinetics. *Diabetes* 7:188-199, 1984
77. Owens DR, Jones MK, Birtwell AJ, Burge CT, Jones IR, Heyburn PJ, Hayes TM, Heding LG: Pharmacokinetics of subcutaneously administered human, porcine and bovine neutral soluble insulin to normal man. *Horm.Metab.Res.* 16 Suppl 1:195-199, 1984
78. Kang S, Brange J, Burch A, Volund A, Owens DR: Subcutaneous insulin absorption explained by insulin's physicochemical properties. Evidence from absorption studies of soluble human insulin and insulin analogues in humans. *Diabetes Care* 14:942-948, 1991
79. Nucci G, Cobelli C: Models of subcutaneous insulin kinetics. A critical review. *Comput.Methods Programs Biomed.* 62:249-257, 2000
80. Kobayashi T, Sawano S, Itoh T, Kosaka K, Hirayama H, Kasuya Y: The pharmacokinetics of insulin after continuous subcutaneous infusion or bolus subcutaneous injection in diabetic patients. *Diabetes* 32:331-336, 1983
81. Kraegen EW, Chisholm DJ: Insulin responses to varying profiles of subcutaneous insulin infusion: kinetic modelling studies. *Diabetologia* 26:208-213, 1984
82. Puckett WR, Lightfoot M: A model for multiple subcutaneous insulin injections developed from individual diabetic patient data. *Am J Physiol* 269:E1115-E1124, 1995
83. Shimoda S, Nishida K, Sakakida M, Konno Y, Ichinose K, Uehara M, Nowak T, Shichiri M: Closed-loop subcutaneous insulin infusion algorithm with a short-acting insulin analog for long-term clinical application of a wearable artificial endocrine pancreas. *Front Med.Biol.Eng.* 8:197-211, 1997

84. Berger MP, Rodbard D: A pharmacodynamic approach to optimizing insulin therapy. *Comput.Methods Programs Biomed.* 34:241-253, 1991
85. Trajanoski Z, Wach P, Kotanko P, Ott A, Skraba F: Pharmacokinetic model for the absorption of subcutaneously injected soluble insulin and monomeric insulin analogs. *Biomedizinische Technik* 38:224-231, 1993
86. Berger MP, Rodbard D: Computer simulation of plasma insulin and glucose dynamics after subcutaneous insulin injection. *Diabetes Care* 12:725-736, 1989
87. Mosekilde E, Jensen KS, Binder C, Pramming S, Thorsteinsson B: Modeling absorption kinetics of subcutaneous injected soluble insulin. *J Pharmacokinet.Biopharm.* 17:67-87, 1989
88. Ferrannini E, Wahren J, Faber OK, Felig P, Binder C, DeFronzo RA: Splanchnic and renal metabolism of insulin in human subjects: A dose-response study. *Am.J.Physiol.* 244:E517-E527, 1983
89. Brange J, Owens DR, Kang S, Volund A: Monomeric insulins and their experimental and clinical implications. *Diabetes Care* 13:923-954, 1990
90. Worthington DR: Minimal model of food absorption in the gut. *Med.Inform.(Lond)* 22:35-45, 1997
91. Hovorka R, Powrie JK, Smith GD, Sonksen PH, Carson ER, Jones RH: Five-compartment model of insulin kinetics and its use to investigate action of chloroquine in NIDDM. *Am.J.Physiol.* 265:E162-E175, 1993
92. Regittnig W, Trajanoski Z, Leis HJ, Ellmerer M, Wutte A, Sendlhofer G, Schaupp L, Brunner GA, Wach P, Pieber TR: Plasma and interstitial glucose dynamics after intravenous glucose injection - evaluation of the single-compartment glucose distribution assumption in the minimal models. *Diabetes* 48:1070-1081, 1999
93. Hovorka R, Bannister P, Eckland DJA, Halliday D, Murley DN, Rees SE, Young MA: Reproducibility and comparability of insulin sensitivity indices measured by stable-label intravenous glucose tolerance test. *Diabetic Med.* 15:234-246, 1998
94. Mari A: Assessment of insulin sensitivity and secretion with the labelled intravenous glucose tolerance test: improved modelling analysis. *Diabetologia* 41:1029-1039, 1998

References

95. Hansen K: Oscillations in the blood sugar in fasting normal persons. *Acta Med.Scand. Suppl.* 4:27-58, 1923
96. Marsh BD, Marsh DJ, Bergman RN: Oscillations enhance the efficiency and stability of glucose disposal. *Am.J.Physiol.* 250:E576-E582, 1986
97. Kraegen EW, Young JD, George EP, Lazarus L: Oscillations in blood glucose and insulin after oral glucose. *Horm.Metab.Res.* 4:409-413, 1972
98. Van Cauter E, Desir D, Decoster C, Fery F, Balasse EO: Nocturnal decrease in glucose tolerance during constant glucose infusion. *J.Clin.Endocrinol.Metab.* 69:604-611, 1989
99. Simon C, Weibel L, Brandenberger G: Twenty-four-hour rhythms of plasma glucose and insulin secretion rate in regular night workers. *Am J Physiol Endocrinol Metab* 278:E413-E420, 2000
100. Simon C, Brandenberger G: Ultradian oscillations of insulin secretion in humans. *Diabetes* 51:S258-S261, 2002
101. Boden G, Ruiz J, Urbain JL, Chen XH: Evidence for a circadian-rhythm of insulin-secretion. *Am.J.Physiol.* 34:E 246-E 252, 1996
102. Van Cauter EV, Polonsky KS, Scheen AJ: Roles of circadian rhythmicity and sleep in human glucose regulation. *Endocr.Rev.* 18:716-738, 1997
103. Plat L, Byrne MM, Sturis J, Polonsky KS, Mockel J, Fery F, Van Cauter EV: Effects of morning cortisol elevation on insulin secretion and glucose regulation in humans. *Am.J.Physiol.* 33:E36-E42, 1996
104. Sturis J, Polonsky KS, Mosekilde E, Van Cauter E: Computer model for mechanism underlying ultradian oscillations of insulin and glucose. *Am.J.Physiol.* 260:E801-E809, 1991
105. Van Cauter E, Shapiro ET, Tillil H, Polonsky KS: Circadian modulation of glucose and insulin responses to meals: relationship to cortisol rhythm. *Am.J.Physiol.* 262:E467-E475, 1992
106. Benn JJ, Bozzard SJ, Kelley D, Mitrakou A, Aoki T, Sorensen J, Gerich JE, Sonksen PH: Persistent abnormalities of the metabolism of an oral

- glucose load in insulin-treated Type 1 diabetics. *Metabolism* 38:1047-1055, 1989
107. Jameson JL: Update: Insulin Lispro: A new, rapidly acting analogue. In Harrison's Principles of Internal Medicine. Braunwald E, Fauci AS, Isselbacher KJ, Kasper DL, Hauser SL, Longo DL, Jameson JL, Eds. London, McGraw-Hill, 1999,
108. Berger M, Halban PA, Girardier L, Seydoux J, Offord RE, Renold RE: Absorption kinetics of subcutaneously injected insulin. Evidence for degradation at the injection site. *Diabetologia* 17:97-99, 1979
109. Owens DR: *Clinical Pharmacological Studies in Normal Man*. MA, MTP, Hingham, 1986
110. Steimer JL, Mallet A, Golmard JL, Boisvieux JF: Alternative approaches to estimation of population pharmacokinetic parameters: Comparison with the nonlinear mixed-effect model. *Drug Metab.Rev.* 15:265-292, 1984
111. Murat A, Slama G: Influence of concentration on the kinetics of sc-infused insulin. Comparison between square-wave sc infusion and bolus sc injection. *Metabolism* 34:120-123, 1985
112. Binder C: Absorption of injected insulin. A clinical-pharmacological study. *Acta Pharmacol.Toxicol.* 2:1-84, 1969
113. Sonksen PH, Tompkins CV, Srivastava MC, Nabarro JDN: A comparative study on the metabolism of human insulin and porcine proinsulin in man. *Clin.Sci.Mol.Med.* 45:633-654, 1973
114. Tranberg KG: Hepatic uptake of insulin in man. *Am.J.Physiol.* 237:E509-E518, 1979
115. Frost DP, Srivastava MC, Jones RH, Nabarro JDN, Sonksen PH: The kinetics of insulin metabolism in diabetes mellitus. *Postgrad.Med.J.* 49:949-954, 1973
116. Kitabchi AE, Stentz FB, Cole C, Duckworth WC: Accelerated insulin degradation: an alternate mechanism for insulin resistance. *Diabetes Care* 2:414-417, 1979

References

117. Kang S, Brange J, Burch A, Volund A, Owens DR: Absorption kinetics and action profiles of subcutaneously administered insulin analogues (AspB9GluB27, AspB10, AspB28) in healthy subjects. *Diabetes Care* 14:1057-1065, 1991
118. Lauritzen T, Faber OK, Binder C: Variation in ¹²⁵I-insulin absorption and blood glucose concentration. *Diabetologia* 17:291-295, 1979
119. Koivisto VA, Felig P: Alterations in insulin absorption and in blood glucose control associated with varying insulin injection sites in diabetic patients. *Ann.Intern.Med.* 92:59-61, 1980
120. Hildebrandt P, Sejrsen P, Nielsen SL, Birch K, Sestoft L: Diffusion and polymerisation determines the insulin absorption from subcutaneous tissue in diabetic patients. *Scand.J.Clin.Lab Invest* 45:685-690, 1985
121. Kolendorf K, Bojsen J, Deckert T: Clinical factors influencing the absorption of ¹²⁵I-NPH insulin in diabetic patients. *Horm.Metab.Res.* 15:274-278, 1983
122. Gough DA, Armour JC: Development of the implantable glucose sensor - what are the prospects and why is it taking so long. *Diabetes* 44:1005-1009, 1995
123. Fischer U, Ertle R, Rebrin K, Freyse EJ: The wick technique - a reference method for implanted glucose sensors. *Artif.Organs* 11:314, 1987
124. Bolinder J, Ungerstedt U, Arner P: Long-term continuous glucose monitoring with microdialysis in ambulatory insulin-dependent diabetic patients. *Lancet* 342:1080-1085, 1993
125. Tamada JA, Bohannon NJV, Potts RO: Measurement of glucose in diabetic subjects using noninvasive transdermal extraction. *Nat.Med.* 1:1198-1201, 1995
126. Schaupp L, Brunner GA, Schaller H, Bodelenz M, Wutte A, Wach P, Pieber TR: Glucose monitoring in the adipose tissue of type 1 diabetic patients using open-flow microperfusion and microdialysis. *Diabetologia* 44:A46, 2001

References

127. Claremont DJ, Sambrook IE, Penton C, Pickup JC: Subcutaneous implantation of a ferrocene-mediated glucose sensor in pigs. *Diabetologia* 29:817-821, 1986
128. Pfeiffer EF, Meyerhoff C, Bischof F, Keck FS, Kerner W: On line continuous monitoring of subcutaneous tissue glucose is feasible by combining portable glucosensor with microdialysis. *Horm. Metab. Res.* 25:121-124, 1993
129. Mueckler M: Facilitative glucose transporters. *Eur.J.Biochem.* 219:713-725, 1994
130. Kerr D, Cheyne EH, Weiss M, Ryder J, Cavan DA: Accuracy of Minimed continuous glucose monitoring system during hypoglycaemia. *Diabetologia* 44:A239, 2001
131. Scherrer U, Randin D, Vollenweider P, Vollenweider L, Nicod P: Nitric-oxide release accounts for insulins vascular effects in humans. *J.Clin. Invest.* 94:2511-2515, 1994
132. Steinberg HO, Brechtel G, Johnson A, Fineberg N, Baron AD: Insulin-mediated skeletal muscle vasodilation is nitric oxide dependent. A novel action of insulin to increase nitric oxide release. *J.Clin. Invest.* 94:1172-1179, 1994
133. Stolic M, Russell A, Hutley L, Fielding G, Hay J, MacDonald G, Whitehead J, Prins J: Glucose uptake and insulin action in human adipose tissue - influence of BMI, anatomical depot and body fat distribution. *Int.J. Obesity* 26:17-23, 2002
134. Rebec MV, Neal DW, Farmer B, Scott M, Smous J, Melle B, Burson P, Cherrington AD: Comparison of plasma and interstitial fluid glucose obtained by microperforation. *Diabetes* 51:A11, 2002
135. Lee A, Ader M, Bray GA, Bergman RN: Diurnal-variation in glucose-tolerance - cyclic suppression of insulin action and insulin-secretion in normal-weight, but not obese, subjects. *Diabetes* 41:750-759, 1992
136. Martin IK, Weber KM, Boston RC, Alford FP, Best JD: Effects of epinephrine infusion on determinants of intravenous glucose tolerance in dogs. *Am.J.Physiol.* 255:E668-E673, 1988

References

137. Hiatt JF, Kripke DF: Ultradian rhythms in waking gastric activity.
Psychosomat Med 37:320, 1975

Personal Bibliography

Journal Papers

1. Chassin LJ, **Wilinska ME**, Hovorka R: Evaluation of glucose controllers in virtual environment: Methodology and sample application. *Artif.Intell.Med.* (accepted)
2. **Wilinska ME**, Chassin LJ, Schaller HC, Schaupp L, Pieber D, Hovorka R: Modelling insulin lispro kinetics during CSII in type 1 diabetes. *IEEE Trans.Biomed.Eng* (in revision)
3. **Wilinska ME**, Bodenlenz M, Chassin LJ, Schaller HC, Schaupp L, Pieber TR, Hovorka R: Interstitial glucose kinetics in subjects with type 1 diabetes under physiological conditions. *Metabolism* (submitted)

Abstracts

4. Canonico V, Orsini-Federici M, Ferolla P, Celleno R, Akwe J, Timi A, Chassin L, **Wilinska M**, Vering T, Hovorka R, Massi-Benedetti M: Evaluation of a feed back model based on simulated interstitial glucose for continuous insulin infusion. *Diabetologia* 45 (Suppl. 2):A322, 2002
5. Chassin, L, **Wilinska, ME**, and Hovorka, R Virtual type 1 'diabetic' treated by CSII: Model description. In: *Proceedings of World Congress on Medical Physics and Biomedical Engineering*, edited by Allen, B. and Lowell, N., Sydney, 2003
6. Chassin LJ, Haueter U, Hovorka R, Massi-Benedetti M, Orsini-Federici M, Pieber T, Schaller HC, Schaupp L, Vering T, **Wilinska M**: Closed-loop glucose control algorithm: Evaluation methodology by simulation. *Diabetes Technol. Ther.* 4:212, 2002
7. Chassin LJ, Haueter U, Hovorka R, Massi-Benedetti M, Orsini-Federici M, Pieber TR, Schaller H, Schaupp L, Vering T, and **Wilinska M**: Closed-loop glucose control algorithm: Evaluation methodology by simulation. In: *First Diabetes Technology Meeting*, San Francisco, 2001, A9

8. Chassin LJ, Haueter U, Hovorka R, Massi-Benedetti M, Orsini-Federici M, Pieber T R, Schaller H, Schaupp L, Vering T, and **Wilinska M**: Simulating control of glucose concentration in subjects with type 1 diabetes: example of control system with inter- and intra-individual variations. In: *Adaptive Systems and Hybrid Computational Intelligence in Medicine. Special Session Proceedings of the EUNITE-2001 Symposium*, edited by Dounias GD and Linkens DA, Chios: University of Aegean. 2001, p. 68
9. Chassin LJ, **Wilinska M**, and Hovorka R: The effect of temporary loss of glucose readings on closed-loop glucose monitor: An evaluation study using simulations. In: *Third Annual Diabetes Technology Meeting*, San Francisco, 2003, A145
10. Chassin LJ, **Wilinska ME**, Hovorka R: Assessing the effect of delay in glucose sampling on closed-loop glucose control: A simulation study. *Diabet.Med.* 19 (Suppl. 2):69, 2002
11. Chassin LJ, **Wilinska ME**, Hovorka R: Simulating closed-loop glucose control: Effect of delay in glucose measurement. *Diabetes* 51 (Suppl. 2):1606, 2002
12. Chassin LJ, **Wilinska ME**, Hovorka R: In silico methodology to test closed loop control system in type 1 diabetes. *Int.J.Artif.Organs* 26:658, 2003
13. Hovorka R, Canonico V, Chassin LJ, Massi-Benedetti M, Orsini-Federici M, Pieber TR, Schaller HC, Schaupp L, Vering T, and **Wilinska, M**: Control of glucose in type 1 diabetes with subcutaneous insulin infusion: Non-linear model predictive control with Bayesian parameter estimation. In: *Proceedings of World Congress on Medical Physics and Biomedical Engineering*, edited by Allen B and Lowell N, Sydney, 2003
14. Hovorka R, Chassin LJ, Haueter U, Massi-Benedetti M, Orsini-Federici M, Pieber, TR, Schaller H, Schaupp L, Vering T, and **Wilinska M**: Model predictive control algorithm for artificial pancreas. In: *First Diabetes Technology Meeting*, San Francisco, 2001, A26
15. Hovorka R, Chassin LJ, Haueter U, Massi-Benedetti M, Orsini-Federici M, Pieber TR, Schaller H, Schaupp L, Vering T, and **Wilinska M** Model predictive control algorithm: using nonlinear model to control glucose excursions in subjects with type 1 diabetes. In: *Adaptive Systems and Hybrid Computational Intelligence in Medicine. Special Session Proceedings of the EUNITE-2001 Symposium*, edited by Dounias, G. D. and Linkens, D. A., Chios: University of Aegean. 2001, p. 44

16. Hovorka R, Chassin LJ, Haueter U, Massi-Benedetti M, Orsini-Federici M, Pieber TR, Schaller HC, Schaupp L, Vering T, **Wilinska M**: Model predictive control algorithm for artificial pancreas. *Diabetes Technol. Ther.* 4:221, 2002
17. Schaller H, Bodenlenz M, Schaupp L, Plank J, Wach P, Pieber TR, Chassin LJ, **Wilinska M**, Hovorka R, Haueter U, Vering T, Orsini-Federici M, Celleno R, Canonico V, Akwe J, and Massi-Benedetti M: MPC algorithm controls blood glucose in patients with Type 1 diabetes mellitus under fasting conditions using IV-SC route. In: *First Diabetes Technology Meeting*, San Francisco, 2001, A48
18. Schaller HC, Bodenlenz M, Schaupp L, Plank J, Wach P, Pieber TR, Chassin LJ, **Wilinska M**, Hovorka R, Haueter U, Vering T, Orsini-Federici M, Celleno R, Akwe J, Canonico V, Massi-Benedetti M: MPC algorithm controls blood glucose in patients with type 1 diabetes mellitus under fasting conditions using the IV-SC route. *Diabetes Technol. Ther.* 4:234, 2002
19. Schaller HC, Bodenlenz M, Schaupp L, Wutte A, Wach P, Pieber TR, Chassin LJ, **Wilinska M**, Hovorka R, Haueter U, Vering T, Orsini-Federici M, Celleno R, Canonico V, Akwe J, Massi-Benedetti M: Regelung des Blutzuckerspiegels von Patienten mit Typ-1-Diabetes mellitus mit Hilfe des MPC-Algorithmus. *Acta Med. Austriaca* (Suppl. 55):19, 2001
20. Schaller HC, Schaupp L, Bodenlenz M, Wutte A, Plank J, Sommer R, Zapotoczky H, Semlitsch B, Chassin LJ, **Wilinska ME**, Hovorka R, Vering T, Wach P, Pieber TR: Avoidance of hypo- and hyperglycaemia with a control loop system in patients with type 1 DM under daily life conditions. *Diabetes Metab* 29:A2225, 2003
21. Schaller HC, Schaupp LA, Bodenlenz M, Sommer R, Wutte A, Semlitsch B, Chassin LJ, **Wilinska M**, Hovorka R, Wach P, Pieber TR: Feasibility of the SC-SC route for an extracorporeal artificial pancreas. *Diabetes* 51:462, 2002
22. Vering T, Beyer U, Both M, Heiniger H, Hutzli I, Kalt L, Kaufman H, Patte C, Trosh M, Zaugg C, Hovorka R, Chassin, LJ, **Wilinska M E**, Kohler H, Schaupp L, Schaller HC, and Pieber, TR: Minimally invasive control loop system for SC-SC control on patients with type 1 diabetes. In: *Third Annual Diabetes Technology Meeting*, San Francisco, 2003, A21
24. **Wilinska ME**, Chassin LJ, Schaller HC, Schaupp L, Pieber TR, and Hovorka R: Modeling insulin lispro kinetics during physiological

conditions in subjects with type 1 diabetes treated by CSII. In: *Proceedings of World Congress on Medical Physics and Biomedical Engineering*, edited by Allen B and Lowell N, Sydney, 2003

25. **Wilinska ME**, Schaller H, Schaupp L, Pieber TR, Chassin LJ, Hovorka R: Hypoglycaemia reduces and insulin increases interstitial to plasma glucose ratio during physiological conditions in subjects with Type 1 diabetes. *Diabetologia* 45:960, 2002
26. **Wilinska ME**, Schaller HC, Schaupp L, Pieber TR, Chassin LJ, and Hovorka, R: Modelling interstitial glucose kinetics in subjects with type 1 diabetes during physiological conditions. In: *Proceedings of the Second Joint IEEE EMBS-BMES Conference, Houston Texas, October 2002*, edited by Ghorbel FH, Piscataway, NJ: IEEE, 2002, p. 228-229
27. **Wilinska ME**, Schaller HC, Schaupp L, Pieber TR, Chassin LJ, Hovorka R: Relationship between interstitial glucose and plasma glucose during physiological conditions. *Diabet.Med.* 19 (Suppl. 2):71, 2002

Appendix

This Appendix contains the menu groups for 32h study reported in Chapter 4.
The top table specifies how the subjects were allocated to these menu groups

Menu group allocation

Subject No.	1	2	3	4	5	6	7	8	9	10	11	12
Menu group [BE*/day]	14	10	14	14	10	14	14	20	10	14	17	14

* 1 BE = 12g Carbohydrates

10 BE-Menu group

Meal	CHO [%] ([g])	Fat [%] ([g])	Proteins [%] ([g])
Dinner 1	39(38)	29(12)	34(33)
Breakfast	71(48)	12(4)	19(13)
Lunch	41(39)	30(13)	30(29)
Dinner 2	53(40)	35(12)	13(10)

14 BE-Menu group

Meal	CHO [%] ([g])	Fat [%] ([g])	Proteins [%] ([g])
Dinner 1	43(48)	26(13)	32(35)
Breakfast	73(61)	11(4)	18(15)
Lunch	48(62)	25(15)	28(37)
Dinner 2	40(52)	46(27)	15(20)

17 BE-Menu group

Meal	CHO [%] ([g])	Fat [%] ([g])	Proteins [%] ([g])
Dinner 1	47(59)	24(13)	30(37)
Breakfast	63(73)	25(13)	14(17)
Lunch	49(75)	23(16)	29(44)
Dinner 2	43(64)	44(29)	16(23)

20 BE-Menu group

Meal	CHO [%] ([g])	Fat [%] ([g])	Proteins [%] ([g])
Dinner 1	51(73)	23(14)	26(37)
Breakfast	67(86)	23(13)	13(17)
Lunch	52(88)	22(16)	28(47)
Dinner 2	38(71)	46(38)	17(32)